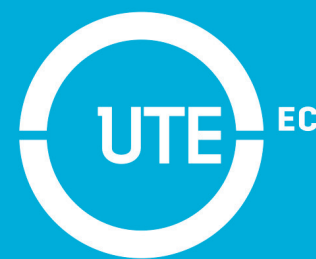


# ENFOQUE

UTE  
REVISTA

Facultad Ciencias de la Ingeniería e Industrias  
eISSN:13906542



Volumen 15 • N°4 • Octubre 2024

# Sumario

|   |    |
|---|----|
| ARTIFICIAL NEURAL NETWORKS FOR CLASSIFICATION TASKS: A SYSTEMATIC LITERATURE REVIEW<br><i>Eduardo Molina Menéndez and Jorge Parraga-Alava</i> .....   | 1  |
| AIRCRAFT STRUCTURAL ASSESSMENTS IN DATA-LIMITED ENVIRONMENTS: A VALIDATED FE METHOD<br><i>Aun Haider</i> .....  | 11 |
| MODEL FOR ESTIMATING SOIL CHEMICAL PROPERTIES WITH RGB DRONE IMAGES<br><i>Manuel Álava Bermeo, Antony García Solórzano, Henry Pacheco Gil, Cristhian Delgado Marcillo</i> .....   | 19 |
| EFFECT OF CUTTING AGE ON THE PRODUCTIVE INDICATORS AND NUTRITIONAL QUALITY<br>OF <i>BRACHIARIA HYBRID</i> VC. <i>MULATO I</i><br><i>Jonathan B. López-Bósquez, Juan P. Salazar-Arias, Danis M. Verdecia-Acosta,</i><br><i>Luis G. Hernández-Montiel, Edilberto Chacón-Marcheco, Jorge L. Ramírez-de la Ribera</i> .....               | 27 |
| ASSESSMENT OF ANIMAL DRINKING WATER QUALITY IN LIVESTOCK FARMS IN GALAPAGOS ISLANDS<br><i>Andrea Belén Casanova Intriago, María Emilia Zambrano Loor, María Fernanda Pincay Cantos</i><br><i>and José Manuel Calderón Pincay</i> .....  | 35 |
| THE BIOACCUMULATIVE POTENTIAL OF HEAVY METALS IN FIVE FOREST SPECIES<br>LIVING IN MINING ENVIRONMENTS IN THE ECUADORIAN AMAZON REGION<br><i>Yudel García-Quintana, Dixon Domingo Andi-Grefa, Luis Ramón Bravo-Sánchez,</i><br><i>Samantha García-Decoro, Sonia Vega-Rosete, Sting Brayan Luna-Fox and Yasiel Arteaga-Crespo</i> ..... | 41 |

It is a pleasure to present Volume 15, Issue 4 of Enfoque UTE journal, which features a selection of high-quality research articles. It is important to mention that the articles included in this edition have undergone a rigorous peer review process by national and international experts. After this thorough process, we have selected six articles that are presented in the current issue.

The first article, led by Eduardo Molina Menéndez and his team from the Faculty of Computer Science at Universidad Técnica de Manabí, Ecuador, offers a systematic literature review on artificial neural networks (ANNs) for classification tasks. This study examines various architectures, such as Convolutional Neural Networks (CNNs) and Multilayer Perceptron (MLP) and highlights that Feed Forward Neural Networks (FFNN) achieved the highest average accuracy of 97.12%. This review emphasizes the broad application of ANNs in fields like medical diagnostics and remote sensing.

In the second article, Aun Haider and collaborators from the Institute of Aeronautics and Avionics (IAA) at Air University in Islamabad, Pakistan, present a method for finite element analysis (FEA) of aircraft structures when detailed design data is not available. Their case study, which focuses on an aircraft wing, validates the practicality of using geometric simplifications in structural assessments, helping extend the service life of modified aircraft.

The third article, authored by Manuel Álava Bermeo and his team from Universidad Técnica de Manabí, Ecuador, discusses the application of precision agriculture through the use of drone-captured RGB images to estimate soil chemical properties such as pH, electrical conductivity, and organic matter. Their findings reveal strong correlations between these properties and spectral indices, contributing valuable information for optimizing crop management and sustainability.

Dr. Oscar Martínez Mozos  
Universidad Politécnica de Madrid  
Editor-in-Chief

Jonathan B. López-Bósquez and his co-authors from Universidad Técnica de Cotopaxi, Ecuador, lead the fourth article, which investigates the productive components, chemical composition, and digestibility of the *Brachiaria hybrid* vs *Mulato I* grass at different growth stages and during both the rainy and dry seasons. Their results demonstrate that the age of regrowth significantly affects nutritional quality and yield, with higher productivity observed during the rainy period.

The fifth article, by Andrea Belén Casanova Intriago and collaborators from Escuela Superior Politécnica Agropecuaria de Manabí Manuel Félix López, Ecuador, examines the water quality for bovine consumption on livestock farms in the Galapagos Islands. The study finds that while some farms have good water quality, others only reach a medium classification. These findings stress the importance of regular water source monitoring and better management practices to ensure safe water for livestock.

Finally, the sixth article, led by Yudel García-Quintana and co-authors from Universidad Estatal Amazónica, Ecuador, evaluates the bioaccumulation potential of heavy metals in five forest species from mining environments in the Ecuadorian Amazon. Their work highlights certain species' ability to absorb metals such as lead, cadmium, and iron, providing insights into the potential use of these species for phytoremediation in contaminated areas.

We invite readers to explore these six contributions, each of which reflects the dedication of their respective authors to advancing scientific knowledge across a diverse range of fields. These studies not only deepen our understanding of key topics but also offer practical solutions to pressing global challenges.

Dr. Diego Guffanti Martínez  
Universidad UTE  
Editor-in-Chief

Es un placer presentar el Volumen 15, Número 4 de la revista Enfoque UTE, que presenta una selección de artículos de investigación de alta calidad. Cabe mencionar que los artículos incluidos en esta edición han pasado por un riguroso proceso de revisión por pares, a cargo de expertos nacionales e internacionales. Tras este minucioso proceso, hemos seleccionado seis artículos que conforman el número actual.

El primer artículo, dirigido por Eduardo Molina Menéndez y su equipo de la Facultad de Ciencias Informáticas de la Universidad Técnica de Manabí, Ecuador, ofrece una revisión sistemática de la literatura sobre redes neuronales artificiales (ANN) aplicadas a tareas de clasificación. Este estudio examina diversas arquitecturas, como las Redes Neuronales Convolucionales (CNN) y las Redes Perceptrón Multicapa (MLP), y destaca que las Redes Neuronales de Retroalimentación (FFNN) alcanzaron la mayor precisión promedio del 97.12%. Esta revisión enfatiza la amplia aplicación de las ANN en campos como el diagnóstico médico y la teledetección.

En el segundo artículo, Aun Haider y colaboradores del Instituto de Aeronáutica y Aviónica (IAA) de la Universidad del Aire en Islamabad, Pakistán, presentan un método para el análisis de elementos finitos (FEA) de estructuras aeronáuticas cuando no se dispone de datos detallados de diseño. Su estudio de caso, que se centra en el análisis estructural de un ala de avión, valida la practicidad de utilizar simplificaciones geométricas en las evaluaciones estructurales, ayudando a extender la vida útil de aviones modificados.

El tercer artículo, autoría de Manuel Álava Bermeo y su equipo de la Universidad Técnica de Manabí, Ecuador, discute la aplicación de la agricultura de precisión mediante el uso de imágenes RGB capturadas por drones para estimar propiedades químicas del suelo, como el pH, la conductividad eléctrica y la materia orgánica. Sus hallazgos revelan fuertes correlaciones entre estas propiedades y los índices espectrales, aportando infor-

mación valiosa para optimizar la gestión agrícola y la sostenibilidad.

Jonathan B. López-Bósquez y sus coautores de la Universidad Técnica de Cotopaxi, Ecuador, lideran el cuarto artículo, que investiga los componentes productivos, la composición química y la digestibilidad del pasto Brachiaria híbrido vc Mulato I en diferentes etapas de crecimiento y durante las estaciones de lluvia y sequía. Sus resultados demuestran que la edad del rebrote afecta significativamente la calidad nutricional y el rendimiento, observándose una mayor productividad durante la temporada de lluvias.

El quinto artículo, de Andrea Belén Casanova Intriago y colaboradores de la Escuela Superior Politécnica Agropecuaria de Manabí Manuel Félix López, Ecuador, examina la calidad del agua para el consumo bovino en fincas ganaderas de las Islas Galápagos. El estudio revela que, mientras algunas fincas tienen agua de buena calidad, otras solo alcanzan una clasificación media. Estos hallazgos subrayan la importancia de monitorear regularmente las fuentes de agua y mejorar las prácticas de manejo para garantizar agua segura para el ganado.

Finalmente, el sexto artículo, dirigido por Yudel García-Quintana y coautores de la Universidad Estatal Amazónica, Ecuador, evalúa el potencial de bioacumulación de metales pesados en cinco especies forestales de entornos mineros en la Amazonía ecuatoriana. Su trabajo destaca la capacidad de ciertas especies para absorber metales como plomo, cadmio y hierro, proporcionando información valiosa sobre el uso potencial de estas especies para la fitorremediación en áreas contaminadas.

Invitamos a los lectores a explorar estos seis aportes, cada uno de los cuales refleja la dedicación de sus respectivos autores para avanzar en el conocimiento científico en una variedad de campos. Estos estudios no solo profundizan nuestra comprensión de temas clave, sino que también ofrecen soluciones prácticas a desafíos globales urgentes.

Dr. Oscar Martínez Mozos  
Universidad Politécnica de Madrid  
Editor en Jefe

Dr. Diego Guffanti Martínez  
Universidad UTE  
Editor en Jefe

# Artificial Neural Networks for Classification Tasks: A Systematic Literature Review

Eduardo Molina Menéndez<sup>1</sup>, and Jorge Parraga-Alava<sup>2</sup>

**Abstract** — Artificial neural networks (ANNs) have become indispensable tools for solving classification tasks across various domains. This systematic literature review explores the landscape of ANN utilization in classification, addressing three key research questions: the types of architectures employed, their accuracy, and the data utilized. The review encompasses 30 studies published between 2019 and 2024, revealing Convolutional Neural Networks (CNNs) as the predominant architecture in image-related tasks, followed by Multilayer Perceptron (MLP) architectures for general classification tasks. Feed Forward Neural Networks (FFNN) exhibited the highest average accuracy with a 97.12%, with specific studies achieving exceptional results across diverse classification tasks. Moreover, the review identifies digitized images as a commonly utilized data source, reflecting the broad applicability of ANNs in tasks such as medical diagnosis and remote sensing. The findings underscore the importance of machine learning approaches, highlight the robustness of ANNs in achieving high accuracy, and suggest avenues for future research to enhance interpretability, efficiency, and generalization capabilities, as well as address challenges related to data quality.

**Keyword:** artificial neural networks; classification; machine learning, neural networks architecture, data mining.

**Resumen** — Las redes neuronales artificiales (ANNs) se han convertido en herramientas indispensables para resolver tareas de clasificación en diversos dominios. Esta revisión sistemática de la literatura explora el panorama de la utilización de ANN en la clasificación, abordando tres preguntas clave de investigación: los tipos de arquitecturas empleadas, su precisión y los datos utilizados. La revisión abarca 30 estudios publicados entre 2019 y 2024, revelando las Redes Neuronales Convolucionales (CNNs) como la arquitectura predominante en tareas relacionadas con imágenes, seguidas por las arquitecturas de Perceptrón Multicapa (MLP) para tareas de clasificación en general. Las Redes Neuronales de Propagación Hacia Adelante (FFNN) exhibieron la mayor precisión promedio con un 97.12 %, con estudios específicos logrando resultados excepcionales en diversas tareas de clasificación. Además, la revisión identifica las imágenes digitalizadas como una fuente de datos comúnmente utilizada, reflejando la amplia aplicabilidad de las ANN en tareas como el diagnóstico médico y la teledetección. Los hallazgos subrayan la importancia de los enfoques de aprendizaje automático, destacan la robustez de las

ANN en lograr una alta precisión y sugieren caminos para investigaciones futuras para mejorar la interpretabilidad, eficiencia y capacidades de generalización, así como abordar desafíos relacionados con la calidad de los datos.

**Palabras Clave:** redes neuronales artificiales, clasificación, aprendizaje automático, arquitectura redes neuronales, minería de datos.

## I. INTRODUCTION

THE fourth industrial revolution has reestablished every aspect of daily life across the globe, through the integration of new digital technologies such as Artificial Intelligence(AI) and Internet of Things (IoT) [1].

The emerge of this technologies have facilitated the generation of vast volumes of data known as Big Data, which presents challenges in extracting knowledge from it, needing to be processed and classified [2].

Classification is a technique for determining the class of a new observation using training data with a known class label [3], it is a common technique used in data mining to identify patterns and relationships in data [4]. It serves diverse purposes, from diagnosing diseases to predicting future events and identifying data patterns [5]. This technique encompasses two primary types: binary and multiclass classification. In binary classification, the task is to predict one of two possible outcomes, whereas multiclass classification involves predicting from several possible outcomes [6]. There are several alternatives to solve classification tasks.

Some of the commonly used methods are Machine Learning based models including Decision Trees, Random Forest, Support Vector Machines and like Artificial Neural Networks [7].

Machine learning (ML) is a field of artificial intelligence that focuses on the development of computer programs that can change when exposed to new data. It uses computer models and information obtained from past and previous data to aid classification, prediction, and detection processes [8]. Within ML Artificial Neural networks (ANN) are computational models that mimic the human brain and its information processing capabilities. They are composed of highly interconnected processing elements called neurons, which are capable of self-organization and acquisition of information [9]. There are various types of ANNs, including feed-forward-based architectures such as Convolutional Neural Networks (CNN), Autoencoder and Recurrent

Neural Networks (RNN) [10]. These networks are used for various applications such as pattern recognition, data mining, bioinformatics data classification, and medical diagnosis [11].

1. Eduardo Molina Menéndez. Facultad de Ciencias Informáticas, Universidad Técnica de Manabí, Portoviejo 130104, Ecuador, (e-mail: [wmolina5666@utm.edu.ec](mailto:wmolina5666@utm.edu.ec)). ORCID <https://orcid.org/0009-0000-7147-2599>.

2. Jorge Parraga Alava. Ph.D. Facultad de Ciencias Informáticas, Universidad Técnica de Manabí, Portoviejo 130104, Ecuador, (e-mail: [jorge.parraga@utm.edu.ec](mailto:jorge.parraga@utm.edu.ec)). ORCID <https://orcid.org/0000-0001-8558-9122>.

Manuscript Received: 29/05/2024

Revised: 30/07/2024

Accepted: 15/08/2024

DOI: <https://doi.org/10.29019/enfoqueute.1058>

The choice of which ANN architecture to use for a specific classification task will depend on the characteristics of the data being classified, such as the number of features, the complexity of the relationships between the features and the target variable, and the amount of available training data [12]. It is important to note that the effectiveness of an ANN also depends on the training, validation, and generalization process, as well as the choice of hyperparameters such as the number of nodes in the hidden layer and the learning rate [13].

Some literature reviews have examined the utilization of ANNs in classification tasks. The study in [14] conducted a review specifically focused on classification techniques in Breast Cancer diagnosis, including SVM, Decision Trees, and of course ANN. Another review study in Breast Cancer diagnosis compares the use of different ANN architectures like CNN, SNN, DBN [15]. The work in [16] highlights Machine Learning supervised algorithms to Gene classification tasks. Another review focused on Machine learning and Deep Learning methods for skin lesion classification [17]. A review discussed the opportunities and challenges of AI and ML addressing different problems, classification included [18].

While literature reviews on ML methods in classification tasks do exist, they often lack comprehensive comparisons of different ANN architectures. This omission restricts understanding and decision-making processes when selecting a specific neural network model. Absolutely, conducting a literature review is crucial to supplement the actual science knowledge in this topic.

This paper follows the subsequent structure: Section Introduction furnishes a review of the theoretical foundations and pertinent literature. Section Materials and Methods delineates the methodology utilized in this study. The findings are presented in Section Results, where the outcomes of the review process, inclusive of the analysis of the ANN architectures,

their accuracies, and the dataset, are scrutinized and deliberated upon. Section Discussion provides an exhaustive discussion of the results, contextualizing the findings and drawing comparisons with existing research. Finally, Section Conclusions summarizes the main findings and their implications, while offering recommendations for future research aimed at further exploring the applications of ANN for resolving classification tasks.

## II. MATERIALS AND METHODS

This study employed the PRISMA (Preferred Reporting Items for Systematic Reviews and Meta-Analyses) methodology to conduct a systematic literature review, ensuring a structured and transparent approach to minimize bias and enhance the reproducibility of results [19].

The choice of a systematic literature review as the study design was motivated by its rigorous and objective methodology, allowing for the comprehensive synthesis of all pertinent evidence regarding a particular topic. Specifically, this approach is well-suited for discerning and analyzing trends in the applications of artificial neural networks (ANNs) in classification problems. By adopting this methodology, the study aims to uncover current trends in ANNs, offering insights into the solutions applied to these problems. Moreover, it anticipates identifying potential gaps in existing knowledge and areas warranting further research within this domain.

The PRISMA process was conducted in three phases:

1. Identification: Initial search in databases and other sources.
2. Screening: Review of titles and abstracts for initial eligibility assessment which implies full-text evaluation of selected articles.
3. Inclusion: Final selection of studies to be included in the review.

Fig.1 diagram illustrates the process of the systematic literature review conducted in this research:

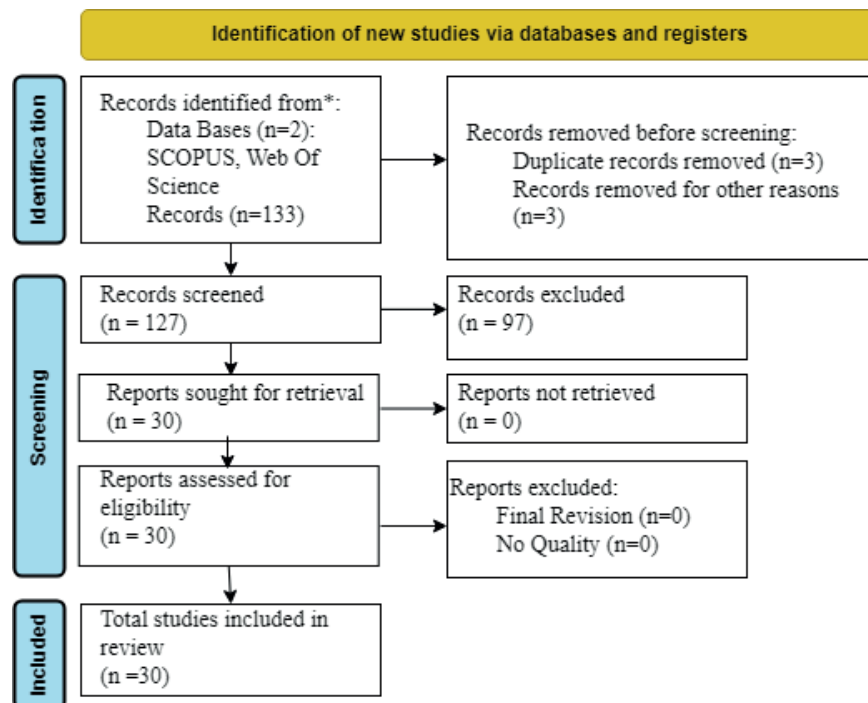


Fig. 1. Study Flow Chart.

The PARSIFAL tool was utilized to aid in organizing and selecting pertinent studies [20] and Zotero for bibliographic management [21].

The purpose of this study is to conduct a thorough and organized examination of artificial neural networks used to classify data. Moreover, the study proposes the following three research questions:

RQ1: What are the most commonly artificial neural networks employed in classification tasks?

RQ2: What is the accuracy of the architectures utilized in the conducted studies?

RQ3: What are the most frequently used data in classification tasks?

#### A. Identification

For the information search, keywords related to the research topic were used. These keywords were selected based on the importance of the respective study topic, according to a preliminary review of the literature and were refined as the search progressed.

Keywords related to the research topic were carefully selected based on a preliminary literature review and refined as the search progressed. The primary keywords used were:

- “Classification”
- “Machine Learning”
- “Artificial Neural Network”
- “Neural Network”
- “Prediction”

These keywords were combined using Boolean operators (AND, OR) and truncation (\*) to expand or restrict the search according to the inclusion and exclusion criteria. The search strings were tailored for each database to ensure optimal results.

To conduct the literature search, two databases deemed pertinent to the study’s subject matter were chosen: Scopus and Web of Science. These databases were selected due to their extensive coverage of computer science and emerging technologies literature, robust search functionalities, and capacity to identify influential publications. The use of multiple databases ensured a comprehensive search and minimized the risk of missing relevant studies.

To establish the search criteria, limitations were set on publication dates and languages. Specifically, articles published between January 2019 and February 2024 in English were included, by this means concentrating the review on the latest and most pertinent literature pertaining to the topic. Furthermore, only articles obtained from the chosen databases were taken into account. It’s important to highlight that numerous preliminary search iterations were performed to precisely define the criteria and guarantee a comprehensive and precise search. The search criteria and keywords were customized for each database, and the outcomes were meticulously assessed for relevance and consistency.

Table 1 provides a detailed breakdown of the search strings utilized during the search process

TABLE I  
SEARCH STRATEGY AND INFORMATION SOURCE

| Database       | Search String   |
|----------------|---|
| Scopus         | (“Artificial Neural Networks” OR “Neural Networks” OR “Machine Learning”) AND (“Classification “)                 |
| Web of Science | (“Artificial Neural Networks” OR “Neural Networks” OR “Machine Learning”) AND (“Classification “ OR “prediction”) |

#### B. Screening

To obtain screened records in this phase, both inclusion and exclusion criteria were established to ensure the systematic review’s relevance and quality. Inclusion criteria focus on machine learning for classification, particularly ANNs, published in peer-reviewed sources from January 2019 to February 2024, ensuring the review covers current, credible, and detailed studies. Exclusion criteria remove studies without detailed methods/results, non-English publications, pre-2019 studies, review articles, theoretical papers, non-classification ANN tasks, and non-peer-reviewed works, to maintain quality, avoid language bias, focus on recent advancements, and concentrate on empirical applications. These criteria ensure that included studies directly address the research questions on ANN accuracy and applications in classification tasks. Table 2 outlines some of the relevant selection criteria that were included in the review, which led to the exclusion of certain records.

TABLE II  
SELECTION CRITERIA

| Inclusion Criteria   | Exclusion Criteria   |
|--|--|
| <ul style="list-style-type: none"> <li>• Documents where classification tasks use machine learning techniques.</li> <li>• Documents related to Artificial Neural Networks (ANN)</li> <li>• Document related to Classification Tasks</li> </ul> | <ul style="list-style-type: none"> <li>• Articles that do not include the methods used or detailed results.</li> <li>• Articles in a different language than English.</li> <li>• Research below 2019.</li> </ul> |

The full text of the articles that passed the filter of the selection criteria was assessed by two independent reviewers using a standardized. The checklist included items such as:

- Relevance to the research questions
- Clarity of methodology
- Quality of data analysis
- Significance of findings

#### C. Included

Articles that met all eligibility criteria were included in the final review. Relevant information was extracted from these articles using a standardized data extraction form, which included fields such as:

- Type of artificial neural network used
- Specific classification task
- Dataset used
- Performance metrics
- Experimental setup and parameters
- Key findings and conclusions

### III. RESULTS

#### A. Identification

During this phase, a total of 133 articles were obtained from the databases searched. Afterward, duplicate entries were eliminated, leading to the removal of 3 records. Additionally, 3 records were excluded as they had been withdrawn from their respective journals.

#### B. Screening

Following the previous phase, a total of 127 records underwent screening, leading to the exclusion of 97 records. Consequently, 30 articles were deemed eligible for retrieval and further assessment. A graphical representation of this process is illustrated in Fig. 2.

#### C. Included

In the final phase, 30 new studies were included in the review. Fig. 2 provides a graphical representation of the article selection process.

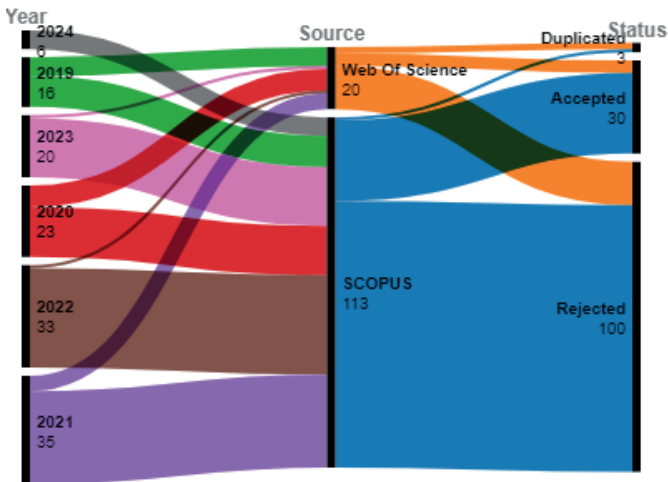


Fig. 2. Results of Article Analysis.

Fig. 2 illustrates the publication year of the studies on the left side, while the middle section displays the source repository of the articles. The number of selected articles is depicted on the right side of the diagram.

Fig. 3 emphasizes the most common words found in the selected studies, notably featuring terms like neural network, model, data, train, accuracy and machine learning. On the other hand, less prevalent terms include predict, analysis and processing.

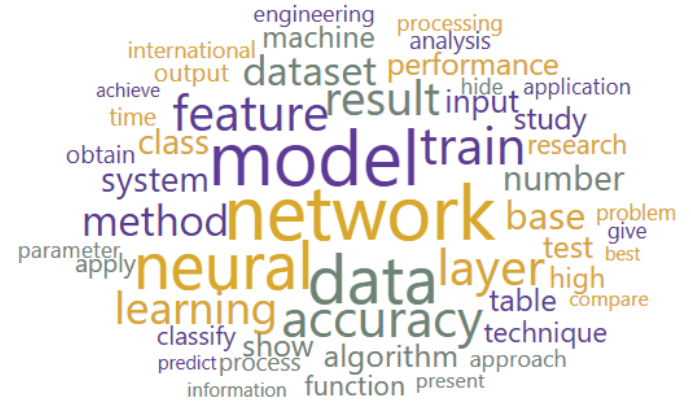


Fig. 3. Word count of the 30 selected studies

Table 3 displays the eligible records, providing details such as the year of publication, authors, study title and responses to RQ1(ANN Architecture), RQ2(ANN Accuracy) and RQ3(Data).

After ensuring that each selected study pertained to the proposed topic and addressed the research questions, the eligible documents underwent meticulous review. The information extracted from these documents was systematically organized and categorized to address the research questions, as outlined below:

RQ1: What are the most commonly artificial neural networks employed in classification tasks?

In examining the literature, it becomes evident that various types of ANNs are favored for classification tasks. We observed a prevalent use of Convolutional Neural Networks (CNNs) across various classification tasks. CNNs are particularly popular in tasks involving image data due to their ability to effectively capture spatial dependencies. Among the reviewed studies, CNNs were utilized in 14 out of 30 cases (46.66%), indicating their dominance in the field of image classification and analysis. Multilayer Perceptron (MLP) architectures were also frequently employed, appearing in 5 out of 30 studies. MLPs are versatile and well-suited for general classification tasks. Their widespread usage suggests their effectiveness in a broad range of classification scenarios. Backpropagation Neural Networks (BPNN) and their variations, such as Bayesian regularized artificial neural networks (BRANN) and Backpropagation Neural Networks (BPNN), were employed in fewer studies compared to CNNs and MLPs. However, they still played a significant role in specific tasks, such as EEG signal analysis and wood classification.



TABLE III  
RESULTS OF RESEARCH

| Year | Authors   | Study   | ANN Architecture (RQ1)   | Model Accuracy (RQ2) | Data used (RQ3)  |
|------|---|---|--|----------------------|--|
| 2019 | Omondiagbe, David A. and Veeramani, Shanmugam and Sidhu, Amandeep S.  | Machine Learning Classification Techniques for Breast Cancer Diagnosis [22]   | Multilayer Feed Forward Neural Network (MFFNN)                     | 97.06 %              | Digitized images of fine needle aspirates (FNA)  |
|      | Rivera Sánchez, F A and González Cervera, J A   | ECG Classification Using Artificial Neural Networks [23]  | Convolutional Neural Network (CNN)                                 | 97.6 %               | ECG signals  |
|      | Haider Bin Abu Yazid, Mohamad and Shukor Talib, Mohamad and Haikal Satria, Muhammad                                 | Flower Pollination Neural Network For Heart Disease Classification [24]   | Flower Pollination Neural Network                                  | 91.42 %              | Patient Records  |
|      | E. Rehn, A. Rehnc, A.Possemlers   | Fossil charcoal particle identification and classification by two convolutional neural networks [25]  | Convolutional neural network (CNN)                                 | 85.6 %               | Sediment Samples Images  |
| 2020 | Iqbal, Mudasser and Ali, Syed and Abid, Muhammad and Majeed, Furqan and Ali, Ans                                    | Artificial Neural Network based Emotion Classification and Recognition from Speech [26]   | Bayesian Regularized Artificial Neural Network (BRANN)             | 95 %                 | Speech Samples   |
|      | Li, Ying and Di, Jianglei and Wang, Kaiqiang and Wang, Sufang and Zhao, Jianlin                                     | Classification of cell morphology with quantitative phase microscopy and machine learning [27]  | Convolutional Neural Network (CNN)                                 | 93.5 %               | Cell morphology  |
|      | Mohammad Vahedi Torshizi, Ali Asghari, Farhad Tabarsa, Payam Danesh, Ali Akbarzadeh                                 | Classification by artificial neural network for mushroom color changing under effect uv-a irradiation [28]  | Multilayer Perceptron (MLP)  | 100%                 | Mushroom Color   |
|      | Zaloga, Alexander N. and Stanovov, Vladimir V. and Bezrukova, Oksana E. and Dubinin, Petr S. and Yakimov, Igor S.   | Crystal symmetry classification from powder X-ray diffraction patterns using a convolutional neural network [29]  | Convolutional Neural Network (CNN)                                 | 90.02 %              | Crystal structures   |
| 2021 | Berto, Tamires Messias and Santos, Mônica Cardoso and Pereira, Fabíola Manhas Verbi and Filletti, Érica Regina      | Artificial neural networks applied to the classification of hair samples according to pigment and sex using non-invasive analytical techniques [13]                   | Multilayer Perceptron (MLP)  | 92.1 %               | wavelength dispersive X-ray fluorescence (WDXRF) laser-induced breakdown spectroscopy (LIBS) |
|      | Hu, Xudong and Zhang, Penglin and Zhang, Qi and Wang, Junqiang  | Improving wetland cover classification using artificial neural networks with ensemble techniques [30]   | Rotation Artificial Neural Network (RANN)                          | 96.1 %               | Landsat 8 OLI images.  |
|      | Koklu, Murat and Cinar, Ilkay and Taspinar, Yavuz Selim   | Classification of rice varieties with deep learning methods [31]  | Convolutional Neural Network (CNN)                                 | 100 %                | Rice Images  |
|      | Hartpence, Bruce and Kwasinski, Andres  | CNN and MLP neural network ensembles for packet classification and adversary defense [32]   | Multilayer Perceptron (MLP) and Convolutional neural network (CNN) | 99 %                 | Network Packet   |
| 2021 | Vives-Boix, Víctor and Ruiz-Fernández, Daniel   | Fundamentals of artificial metaplasticity in radial basis function networks for breast cancer classification [33]   | Artificial Metaplasticity Radial Basis Function Network (AMRBFN)   | 98.82 %              | Digitized images of fine needle aspirates (FNA)  |
|      | Majidzadeh Gorjani, Ojan and Byrtus, Radek and Dohnal, Jakub and Bilik, Petr and Koziorek, Jiri and Martinek, Radek | Human Activity Classification Using Multilayer Perceptron [34]  | Multilayer Perceptron (MLP)  | 98 %                 | Environmental parameters and Mechanical quantities   |
|      | Rwigema, James and Mfitumukiza, Joseph and Tae-Yong, Kim  | A hybrid approach of neural networks for age and gender classification through decision fusion [35]   | Convolutional Neural Network (CNN)                                 | 80.5 %               | Facial Images Samples  |
|      | Totakura, Varun and Madhusudhana Reddy, E. and Vuribindi, Bhargava Reddy  | Symptomatically Brain Tumor Detection Using Convolutional Neural Networks [36]  | Convolutional Neural Network (CNN)                                 | 99.89 %              | Magnetic Resonance Images (MRI)  |
| 2022 | Maria Camila Guerrero, Juan Sebastián Parada, Helbert Eduardo Espitia   | EEG signal analysis using classification techniques: Logistic regression, artificial neural networks, support vector machines, and convolutional neural networks [37] | Convolutional neural network (CNN)                                 | 59.90 %              | Electroencephalogram (EEG) signals   |
|      | Anupama, Bollampally and Narayana, Somayajulu Laxmi and Rao, K S  | Artificial neural network model for detection and classification of alcoholic patterns in EEG [38]  | Back propagation neural network (BPNN)                             | 92 %                 | Electroencephalogram (EEG) signals   |
|      | Das, Subrata and Wahi, Amitabh and Kumar, S. Madhan and Mishra, Ravi Shankar and Sundaramurthy, S.                  | Moment-Based Features of Knitted Cotton Fabric Defect Classification by Artificial Neural Networks [39]   | Back propagation neural network (BPNN)                             | 77.78 %              | Cotton Fabric Images   |
|      | Kostrzewa, Łukasz and Nowak, Robert   | Polish Court Ruling Classification Using Deep Neural Networks [40]  | Convolutional Neural Networks (CNNs)                               | 98.8 %               | Court Ruling   |

| Year | Authors   | Study   | ANN Architecture (RQ1)   | Model Accuracy (RQ2) | Data used (RQ3)                                 |
|------|---|---|--|----------------------|---|
| 2023 | Nasien, Dewi and Enjeslina, Veren and Hasmil Adiya, M. and Baharum, Zirawani                            | Breast Cancer Prediction Using Artificial Neural Networks Back Propagation Method [41]  | Back propagation neural network (BPNN)                                       | 96.929 %             | Digitized images of fine needle aspirates (FNA) |
|      | Alkhamees, Bader Fahad  | An Optimized Single Layer Perceptron-based Approach for Cardiotocography Data Classification [42]   | Single Layer Perceptron (SLP)  | 99.20 %              | Cardiotocography (CTG) patterns                 |
|      | Cao, Shubo and Zhou, Shiyu and Liu, Jiying and Liu, Xiaoping and Zhou, Yucheng                          | Wood Classification Study based on Thermal Physical Parameters with Intelligent Method of Artificial Neural Networks [43]                                       | Back Propagation Neural Network (BPNN)                                       | 98.95 %              | Wood samples                                    |
|      | Leško, Jakub and Andoga, Rudolf and Bréda, Róbert and Hlinková, Miriam and Fözö, Ladislav               | Flight Phase Classification For Small Unmanned Aerial Vehicles [44]   | Feedforward Neural Network (FFNN)  | 97.18 %              | Fuzzy inference                                 |
|      | Ahmed, Mumtaz and Afreen, Neda and Ahmed, Muneeb and Sameer, Mustafa and Ahamed, Jameel                 | An inception V3 approach for malware classification using machine learning and transfer learning [45]   | Convolutional Neural Network (CNN)   | 98.76 %              | Malware Samples                                 |
|      | Nurulain Nusrat Mohd Azam, Mohd Arfian Ismail, Mohd Saberi Mohamad, Ashraf Osman Ibrahim, Shermina Jeba | Classification of COVID-19 Symptoms Using Multilayer Perceptron [46]  | Multilayer Perceptron (MLP)  | 77.10 %              | Patient symptom                                 |
|      | Tran-Thi-Kim, Tuan Pham-Viet, Insoo Koo, Vladimir Mariano, Tuan Do-Hong                                 | Enhancing the Classification Accuracy of Rice Varieties by Using Convolutional Neural Networks [47]   | Convolutional neural network (CNN)   | 97.88 %              | Rice Images and Features                        |
|      | Muhammad Hasanat, Waleed Khan, Nasru Minallah, Najam Aziz, Awab-Ur-Rashid Durrani                       | Performance evaluation of transfer learning based deep convolutional neural network with limited fused spectrottemporal data for land cover classification [48] | Deep Convolutional Neural Network (DCNN)                                     | 93 %                 | Land Cover Images                               |
|      | Chavan, Rupali and Pete, Dnyandeo   | Automatic multi-disease classification on retinal images using multilevel glowworm swarm convolutional neural network [49]                                      | Multilevel Glowworm Swarm Optimization Convolutional Neural network (MGSCNN) | 95.09 %              | Retinal Images                                  |
|      | Susanto, Susanto and Nanda, Deri Sis  | Predicting the classification of high vowel sound by using artificial neural network: a study in forensic linguistics [50]                                      | Backpropagation Artificial Neural Network (BPNN)                             | 92.26 %              | Vowel Sounds                                    |

Table 4 provides an overview of the prevalence of different artificial neural network (ANN) architectures used in the studies reviewed, first column lists the types of ANN architectures used in the reviewed studies, next column indicates the number of studies that utilized each type of ANN, last column shows the percentage of the total 30 studies that employed each ANN architecture

TABLE IV  
ANN ARCHITECTURES EMPLOYED

| Architecture | Number of Studies | Percentage |
|--------------|-------------------|------------|
| CNN          | 14                | 46.66 %    |
| MLP          | 5                 | 16.67 %    |
| BPNN         | 5                 | 16.67 %    |
| FFNN         | 2                 | 6.67 %     |
| Others       | 4                 | 13.33 %    |

RQ2: What is the accuracy of the architectures utilized in the conducted studies?

Analyzing the accuracy of the architectures utilized in the reviewed studies provides insights into their performance across different classification tasks. FFNNs demonstrated the highest average accuracy among the architectures, with an average accuracy of 97.12%. CNNs exhibited a great accuracy of 90.7%. This high accuracy can be attributed to CNNs' ability to automatically learn hierarchical features from raw input data, making them particularly effective in tasks such as image classification and pattern recognition. MLPs also showcased strong performance, with an average accuracy of 93.87%. MLPs are known for their simplicity and flexibility, making them suitable for a wide range of classification tasks. Specific studies reported exceptional accuracies, such as Multilevel Perceptron achieving 100 % accuracy in mushroom color classification [28] and CNNs achieving 100 % accuracy in symptomatically brain tumor detection [36]. While BPNNs and their variations exhibited slightly lower average accuracies compared to MLPs, they still demonstrated great performance. These architectures are often employed in tasks requiring sequential processing, such as time series analysis or signal processing.

Table 5 showcases the averages and highest accuracies obtained by the different ANN architectures.

TABLE V  
ANN ARCHITECTURES ACCURACY

| Architecture | Average Accuracy | Highest Reported Accuracy |
|--------------|------------------|---------------------------|
| FFNN         | 97.12%           | 97.18%                    |
| CNN          | 90.7%            | 100.00%                   |
| MLP          | 93.87%           | 100.00%                   |
| BPNN         | 91.58%           | 98.95%                    |
| Others       | 88.45%           | 99.20%                    |

RQ3: What are the most frequently used data in classification tasks?

Examining the data sources utilized in classification tasks sheds light on the types of input data that ANNs are commonly applied to. Digitized images emerged as the most frequently utilized data type, appearing in 14 out of 30 studies (46.66 %). These images encompassed various domains, including medical imaging (MRI scans [36], ECG signals [23], retinal images [49]), microscopy (cell morphology [27]), and remote sensing (land cover [30], [48]).

Patient records, symptoms and patterns were also commonly used, appearing in 3 out of 30 studies (10 %). These records typically include demographic information, medical history, and diagnostic test results, making them valuable for tasks such as disease prediction and risk assessment, and reveals the importance of ANN models in the medicine campus.

Other data types, such as environmental parameters, mechanical quantities, and sound samples [26], [50], were utilized in a smaller proportion of studies. These data sources reflect the diverse range of applications for ANNs, spanning domains such as environmental science, engineering, and forensic linguistics.

The differences in accuracy among various ANN architectures can be attributed to the nature of the data and the specific requirements of the classification tasks. CNNs, for instance, excel in tasks involving image data due to their ability to capture spatial hierarchies through convolutional layers. This explains their dominance and high accuracy in image-related studies. FFNNs, MLPs, and BPNNs, while versatile and effective for general classification tasks, may not perform as well as CNNs in image-intensive tasks but excel in handling structured and sequential data. The high accuracy of FFNNs and BPNNs in certain studies indicates their robustness in tasks with less complex spatial relationships. BPNNs, in particular, have shown significant performance in tasks requiring sequential processing, such as sample analysis and prediction.

#### IV. DISCUSSION

A comprehensive analysis of 30 studies was conducted to investigate Artificial neural networks (ANNs) for solving classification tasks across diverse domains. In this systematic literature review, we addressed three research questions pertaining to the types of architectures employed, their accuracy, and the data sources utilized.

Our findings reveal a prevalent use of Convolutional Neural Networks (CNNs) in classification tasks, particularly those involving image data [25], [31], [35], [36], [47], [48]. CNNs have revolutionized the field of computer vision due to their ability to automatically learn hierarchical features from raw input data, making them highly effective in tasks such as object detection, image recognition, and medical imaging [23], [36], [37], [38]. Additionally, Multilayer Perceptron (MLP) architectures were frequently employed, showcasing their versatility and effectiveness in handling different tasks, such as sex classification from hair samples [13]. While other architectures, such as Backpropagation Neural Networks (BPNN), were employed in fewer studies, they still played significant roles in specific tasks requiring sequential processing.

Analyzing the accuracy of the architectures utilized in the reviewed studies provides insights into their performance across different classification tasks. The FFNNs demonstrated the highest average accuracy in our study, achieving a remarkable 97.12 %. This superior performance can be attributed to several factors. FFNNs are highly effective at capturing complex, non-linear relationships within the data, which is critical for accurate classification tasks. Their architecture, which consists of multiple layers of interconnected neurons, allows for the automatic learning of features without manual intervention. This adaptability makes FFNNs particularly robust in various applications [51], such as medical diagnosis [22], followed closely by MLPs, these networks are versatile and well-suited for a broad range of classification tasks. Their simplicity and ease of implementation make them a popular choice for general classification problems [52]. These findings are consistent with existing literature highlighting the superior performance of CNNs in image classification tasks. Notably, specific studies reported exceptional accuracies, underscoring the effectiveness of ANNs in achieving high accuracy across a broad spectrum of classification tasks, according to the work related in [14], high accuracy is one of the strengths of machine learning methods.

Examining the data sources utilized in classification tasks revealed a diverse range of inputs employed across the studies. Digitized images emerged as the most frequently utilized data type, reflecting the widespread application of ANNs in image-based tasks such as medical diagnosis [22], [23], [24], [33], [36], [37], [38], [41], [42], [46], matching with the review conducted in [53] that exhibits image classification as one of the most common application purposes for ANN in the maritime industry. Remote sensing, and object recognition. Patient records were also commonly used, highlighting the utility of ANNs in healthcare applications for disease prediction, risk assessment, and patient management. Other data types, such as environmental parameters and sound samples, were utilized in a smaller proportion of studies, demonstrating the versatility of ANNs in handling various types of input data for classification tasks.

The findings of this systematic literature review have several implications for both researchers and practitioners in the field of artificial intelligence and machine learning. Firstly, the prevalence of CNNs in classification tasks underscores the importance of machine learning approaches, particularly in domains where image data are prevalent, the same review mentioned before [53], reveals FFNNs and CNNs as the most commonly employed

yed ANNs architectures in the maritime industry. Secondly, the high accuracy achieved by ANNs across a broad range of tasks highlights their effectiveness as robust and reliable classification tools. Lastly, the diverse range of data sources utilized in classification tasks suggests the potential for further exploration and integration of multimodal data in ANN-based approaches.

The present study showcases several strengths in the application of artificial neural networks (ANN) to classification problems. Firstly, the utilization of a robust dataset and advanced preprocessing techniques has ensured high-quality input data, which is critical for the accurate training of ANN models [54]. This high-quality data can serve as a benchmark for future research, enabling other studies to compare their results against a standardized dataset and ensuring consistency in the evaluation of ANN models. The implementation of various architectures and the systematic evaluation of their performance has provided a comprehensive understanding of the capabilities and limitations of different ANN configurations. This detailed evaluation is invaluable for guiding future research in selecting the most appropriate ANN architectures for specific types of classification tasks. For instance, our findings on the strengths of Convolutional Neural Networks (CNNs) in image data tasks can inform future studies focusing on medical imaging or remote sensing, while the versatility of Multilayer Perceptrons (MLPs) and Feedforward Neural Networks (FFNNs) can be leveraged for tasks involving structured data.

However, there are inherent limitations to this research that must be acknowledged. One significant limitation is the computational complexity associated with deep training neural networks [55], which may not be feasible for all research environments due to resource constraints. Addressing this issue in future research could involve developing more efficient algorithms or leveraging cloud computing resources to make deep learning more accessible. Additionally, the variability in performance metrics across different datasets suggests that further research is needed to confirm the robustness of these models in diverse real-world scenarios. Future studies could focus on testing ANN models across a wider range of datasets to enhance their generalizability and reliability. Another limitation is the potential for hyperparameter selection bias, which, despite efforts to mitigate it through systematic tuning, could still influence the outcomes. Future research should aim to develop more automated and unbiased methods for hyperparameter optimization to ensure that the performance improvements are genuine and not artifacts of overfitting.

The precision of the models is another critical aspect of this study. High precision in ANN models indicates their reliability and accuracy in making predictions [56], which is essential for applications in fields like healthcare, finance, and autonomous systems. Future research should continue to focus on improving the precision of these models through better training techniques, more diverse datasets, and advancements in ANN architectures. By addressing these strengths and limitations, this study lays the groundwork for future research to build upon, aiming to develop more robust, efficient, and precise ANN models for a variety of classification tasks.

Future research should focus on enhancing the interpretability, efficiency, and generalization capabilities of ANNs. One approach to improving interpretability is the development of visualization tools that can provide insights into the decision-making process of neural networks. Techniques such as Layer-wise Relevance Propagation (LRP) and Gradient-weighted Class Activation Mapping (Grad-CAM) can help researchers and practitioners understand which features are most influential in a model's predictions.

To improve efficiency, research can explore the optimization of neural network architectures and the use of advanced training techniques such as transfer learning and fine-tuning. These methods can reduce the computational burden and make ANN applications more accessible in various domains.

Enhancing generalization capabilities requires addressing issues related to data quality and diversity. One strategy is to employ data augmentation techniques to create more representative training datasets. Additionally, the development of hybrid models that combine different neural network architectures could leverage the strengths of each, leading to more robust and generalizable solutions.

## V. CONCLUSION

Through our systematic literature review, we have provided a comprehensive analysis of the utilization of ANNs in classification tasks, addressing three key research questions pertaining to the types of architectures employed, their accuracy, and the data sources utilized.

The most commonly used ANN architectures identified in this review are Convolutional Neural Networks (CNNs), Multilayer Perceptrons (MLPs), Feedforward Neural Networks (FFNNs), and Backpropagation Neural Networks (BPNNs). CNNs dominate in image-related tasks due to their ability to capture spatial hierarchies, while MLPs and FFNNs are versatile and effective for general classification tasks involving structured and sequential data. BPNNs, although less common, have shown significant performance in tasks requiring sequential processing.

The accuracy of ANN architectures varies depending on the nature of the data and the specific requirements of the classification tasks. FFNNs demonstrated the highest average accuracy in this review, achieving a remarkable 97.12%. CNNs also exhibited high accuracy, particularly in image classification tasks, with some studies reporting accuracies as high as 100%. MLPs and BPNNs showed strong performance across various classification scenarios, indicating their robustness and reliability in handling diverse types of data.

For Convolutional Neural Networks (CNNs), the most frequently used data type is digitized images. Multilayer Perceptrons (MLPs) commonly use structured data. Feedforward Neural Networks (FFNNs) are often used with tabular data and images. Backpropagation Neural Networks (BPNNs) frequently use data that require sequential processing, such as sample analysis and prediction.

## REFERENCES

- [1] I. H. Sarker, "Machine Learning: Algorithms, Real-World Applications and Research Directions," *SN Comput. Sci.*, vol. 2, no. 3, p. 160, May 2021. <https://doi.org/10.1007/s42979-021-00592-x>.
- [2] J. Tanha, Y. Abdi, N. Samadi, N. Razzaghi and M. Asadpour, "Boosting methods for multi-class imbalanced data classification: an experimental review," *J. Big Data*, vol. 7, no. 1, p. 70, Dec. 2020. <https://doi.org/10.1186/s40537-020-00349-y>.
- [3] S. N. Bardab, T. M. Ahmed and T. A. A. Mohammed, "Data mining classification algorithms: An overview," *Int. J. Adv. Appl. Sci.*, vol. 8, no. 2, pp. 1-5, Feb. 2021, doi: 10.21833/ijaas.2021.02.001.
- [4] I. Tougui, A. Jilbab, and J. El Mhamdi, "Heart disease classification using data mining tools and machine learning techniques," *Health Technol.*, vol. 10, no. 5, pp. 1137–1144, Sep. 2020. <https://doi.org/10.1007/s12553-020-00438-1>.
- [5] B. Charbuty and A. Abdulazeez, "Classification Based on Decision Tree Algorithm for Machine Learning," *J. Appl. Sci. Technol. Trends*, vol. 2, no. 01, pp. 20-28, Mar. 2021. <https://doi.org/10.38094/jastt20165>.
- [6] M. Grandini, E. Bagli, and G. Visani, "Metrics for Multi-Class Classification: an Overview," Aug. 13, 2020, *arXiv: arXiv:2008.05756*. <https://doi.org/10.48550/arXiv.2008.05756>
- [7] A. Dogan and D. Birant, "Machine learning and data mining in manufacturing," *Expert Syst. Appl.*, vol. 166, p. 114060, Mar. 2021. <https://doi.org/10.1016/j.eswa.2020.114060>.
- [8] D. Mustafa Abdullah and A. Mohsin Abdulazeez, "Machine Learning Applications based on SVM Classification A Review," *Qubahan Acad. J.*, vol. 1, no. 2, pp. 81-90, Apr. 2021. <https://doi.org/10.48161/qaj.v1n2a50>
- [9] M. A. Rahman and R. C. Muniyandi, "An Enhancement in Cancer Classification Accuracy Using a Two-Step Feature Selection Method Based on Artificial Neural Networks with 15 Neurons," *Symmetry*, vol. 12, no. 2, p. 271, Feb. 2020. <https://doi.org/10.3390/sym12020271>
- [10] S. S., J. I. Zong Chen, and S. Shakya, "Survey on Neural Network Architectures with Deep Learning," *J. Soft Comput. Paradigm*, vol. 2, no. 3, pp. 186-194, Jul. 2020. <https://doi.org/10.36548/jscp.2020.3.007>
- [11] M. Tanveer, A. H. Rashid, R. Kumar and R. Balasubramanian, "Parkinson's disease diagnosis using neural networks: Survey and comprehensive evaluation," *Inf. Process. Manag.*, vol. 59, no. 3, p. 102909, May 2022. <https://doi.org/10.1016/j.ipm.2022.102909>
- [12] M. A. M. Sadeeq and A. M. Abdulazeez, "Neural Networks Architectures Design, and Applications: A Review," in *2020 International Conference on Advanced Science and Engineering (ICOASE)*, Duhok, Iraq: IEEE, Dec. 2020, pp. 199-204. <https://doi.org/10.1109/ICOASE51841.2020.9436582>
- [13] T. M. Berto, M. C. Santos, F. M. V. Pereira, and É. R. Filletti, "Artificial neural networks applied to the classification of hair samples according to pigment and sex using non-invasive analytical techniques," *X-Ray Spectrom.*, vol. 49, no. 6, pp. 632-641, Nov. 2020. <https://doi.org/10.1002/xrs.3163>
- [14] B. ElOuassif, A. Idri, M. Hosni and A. Abran, "Classification techniques in breast cancer diagnosis: A systematic literature review," *Comput. Methods Biomech. Biomed. Eng. Imaging Vis.*, vol. 9, no. 1, pp. 50-77, Jan. 2021. <https://doi.org/10.1080/21681163.2020.1811159>
- [15] S. Bharati, P. Podder, and M. R. H. Mondal, "Artificial Neural Network Based Breast Cancer Screening: A Comprehensive Review," 2020. <https://doi.org/10.48550/arXiv.2006.01767>
- [16] D. M. Abdulqader, A. M. Abdulazeez, and D. Q. Zeebaree, "Machine Learning Supervised Algorithms of Gene Selection: A Review," vol. 62, no. 03, 2020. ISSN: 04532198. Available: <https://bit.ly/3X2O3w6>
- [17] M. A. Kassem, K. M. Hosny, R. Damaševičius and M. M. Eltouky, "Machine Learning and Deep Learning Methods for Skin Lesion Classification and Diagnosis: A Systematic Review," *Diagnostics*, vol. 11, no. 8, p. 1390, Jul. 2021. <https://doi.org/10.3390/diagnostics11081390>
- [18] R. I. Mukhamediev *et al.*, "Review of Artificial Intelligence and Machine Learning Technologies: Classification, Restrictions, Opportunities and Challenges," *Mathematics*, vol. 10, no. 15, p. 2552, Jul. 2022. <https://doi.org/10.3390/math10152552>
- [19] L. A. Kahale *et al.*, "Extension of the PRISMA 2020 statement for living systematic reviews (LSRs): protocol [version 2; peer review: 1 approved]," 2022. Available: <https://f1000research.com/articles/11-109>
- [20] "Perform Systematic Literature Reviews," Parsifal. Accessed: May 22, 2024. [Online]. Available: <https://parsifal.ai/>
- [21] "Zotero | Your personal research assistant." Accessed: May 22, 2024. [Online]. Available: <https://www.zotero.org/>
- [22] D. A. Omondiagbe, S. Veeramani and A. S. Sidhu, "Machine Learning Classification Techniques for Breast Cancer Diagnosis," *IOP Conf. Ser. Mater. Sci. Eng.*, vol. 495, p. 012033, Jun. 2019. <https://doi.org/10.1088/1757-899X/495/1/012033>
- [23] F. A. Rivera Sánchez and J. A. González Cervera, "ECG Classification Using Artificial Neural Networks," *J. Phys. Conf. Ser.*, vol. 1221, no. 1, p. 012062, Jun. 2019. <https://doi.org/10.1088/1742-6596/1221/1/012062>
- [24] M. Haider Bin Abu Yazid, M. Shukor Talib and M. Haikal Satria, "Flower Pollination Neural Network for Heart Disease Classification," *IOP Conf. Ser. Mater. Sci. Eng.*, vol. 551, no. 1, p. 012072, Aug. 2019. <https://doi.org/10.1088/1757-899X/551/1/012072>
- [25] E. Rehn, A. Rehn, and A. Possemiers, "Fossil charcoal particle identification and classification by two convolutional neural networks," *Quat. Sci. Rev.*, vol. 226, p. 106038, Dec. 2019. <https://doi.org/10.1016/j.quascirev.2019.106038>
- [26] M. Iqbal, S. Ali, M. Abid, F. Majeed and A. Ali, "Artificial Neural Network based Emotion Classification and Recognition from Speech," *Int. J. Adv. Comput. Sci. Appl.*, vol. 11, no. 12, 2020. <https://doi.org/10.14569/IJACSA.2020.0111253>
- [27] Y. Li, J. Di, K. Wang, S. Wang, and J. Zhao, "Classification of cell morphology with quantitative phase microscopy and machine learning," *Opt. Express*, vol. 28, no. 16, p. 23916, Aug. 2020. <https://doi.org/10.1364/OE.397029>
- [28] "Classification by artificial neural network for mushroom color changing under effect UV-A irradiation," *Carpathian J. Food Sci. Technol.*, pp. 152-162, Jun. 2020. <https://doi.org/10.34302/crpfst/2020.12.2.16>
- [29] A. N. Zaloga, V. V. Stanovov, O. E. Bezrukova, P. S. Dubinin and I. S. Yakimov, "Crystal symmetry classification from powder X-ray diffraction patterns using a convolutional neural network," *Mater. Today Commun.*, vol. 25, p. 101662, Dec. 2020. <https://doi.org/10.1016/j.mtcomm.2020.101662>
- [30] X. Hu, P. Zhang, Q. Zhang and J. Wang, "Improving wetland cover classification using artificial neural networks with ensemble techniques," *GIScience Remote Sens.*, vol. 58, no. 4, pp. 603–623, May 2021. <https://doi.org/10.1080/15481603.2021.1932126>
- [31] M. Koklu, I. Cinar and Y. S. Taspınar, "Classification of rice varieties with deep learning methods," *Comput. Electron. Agric.*, vol. 187, p. 106285, Aug. 2021. <https://doi.org/10.1016/j.compag.2021.106285>
- [32] B. Hartpence and A. Kwasinski, "CNN and MLP neural network ensembles for packet classification and adversary defense," *Intell. Conver. Netw.*, vol. 2, no. 1, pp. 66-82, Mar. 2021. <https://doi.org/10.23919/ICN.2020.0023>
- [33] V. Vives-Boix and D. Ruiz-Fernández, "Fundamentals of artificial metaplasticity in radial basis function networks for breast cancer classification," *Neural Comput. Appl.*, vol. 33, no. 19, pp. 12869-12880, Oct. 2021. <https://doi.org/10.1007/s00521-021-05938-3>.
- [34] O. Majidzadeh Gorjani, R. Byrtus, J. Dohnal, P. Bilik, J. Koziorek and R. Martinek, "Human Activity Classification Using Multilayer Perceptron," *Sensors*, vol. 21, no. 18, p. 6207, Sep. 2021. <https://doi.org/10.3390/s21186207>
- [35] J. Rwigema, J. Mfitumukiza and K. Tae-Yong, "A hybrid approach of neural networks for age and gender classification through decision fusion," *Biomed. Signal Process. Control*, vol. 66, p. 102459, Apr. 2021. <https://doi.org/10.1016/j.bspc.2021.102459>
- [36] V. Totakura, E. Madhusudhana Reddy, and B. R. Vuribindi, "Symptomatically Brain Tumor Detection Using Convolutional Neural Networks," *IOP Conf. Ser. Mater. Sci. Eng.*, vol. 1022, no. 1, p. 012078, Jan. 2021, doi: 10.1088/1757-899X/1022/1/012078.
- [37] M. C. Guerrero, J. S. Parada, and H. E. Espitia, "EEG signal analysis using classification techniques: Logistic regression, artificial neural networks, support vector machines, and convolutional neural networks," *Heliyon*, vol. 7, no. 6, p. e07258, Jun. 2021. <https://doi.org/10.1016/j.heliyon.2021.e07258>
- [38] B. Anupama, S. L. Narayana and K. S. Rao, "Artificial neural network model for detection and classification of alcoholic patterns in EEG," 2022. <https://doi.org/10.1504/IJBRA.2022.121764>

- [39] S. Das, A. Wahi, S. M. Kumar, R. S. Mishra and S. Sundaramurthy, "Moment-Based Features of Knitted Cotton Fabric Defect Classification by Artificial Neural Networks," *J. Nat. Fibers*, vol. 19, no. 4, pp. 1498-1506, Apr. 2022. <https://doi.org/10.1080/15440478.2020.1779900>
- [40] Ł. Kostrzewa and R. Nowak, "Polish Court Ruling Classification Using Deep Neural Networks," *Sensors*, vol. 22, no. 6, p. 2137, Mar. 2022. <https://doi.org/10.3390/s22062137>
- [41] D. Nasien, V. Enjeslina, M. Hasmil Adiya and Z. Baharum, "Breast Cancer Prediction Using Artificial Neural Networks Back Propagation Method," *J. Phys. Conf. Ser.*, vol. 2319, no. 1, p. 012025, Aug. 2022. <https://doi.org/10.1088/1742-6596/2319/1/012025>
- [42] B. F. Alkhamees, "An Optimized Single Layer Perceptron-based Approach for Cardiotocography Data Classification," *Int. J. Adv. Comput. Sci. Appl.*, vol. 13, no. 10, 2022. <https://doi.org/10.14569/IJACSA.2022.0131030>
- [43] S. Cao, S. Zhou, J. Liu, X. Liu, and Y. Zhou, "Wood classification study based on thermal physical parameters with intelligent method of artificial neural networks," *BioResources*, vol. 17, no. 1, pp. 1187-1204, Jan. 2022. <https://doi.org/10.15376/biores.17.1.1187-1204>
- [44] J. Leško, R. Andoga, R. Bréda, M. Hlinková and L. Fözö, "Flight phase classification for small unmanned aerial vehicles," *Aviation*, vol. 27, no. 2, pp. 75-85, May 2023. <https://doi.org/10.3846/aviation.2023.18909>
- [45] M. Ahmed, N. Afreen, M. Ahmed, M. Sameer, and J. Ahamed, "An inception V3 approach for malware classification using machine learning and transfer learning," *Int. J. Intell. Netw.*, vol. 4, pp. 11-18, 2023, <https://doi.org/10.1016/j.ijin.2022.11.005>
- [46] N. N. M. Azam, M. A. Ismail, M. S. Mohamad, A. O. Ibrahim, and S. Jeba, "Classification of COVID-19 Symptoms Using Multilayer Perceptron," *Iraqi J. Comput. Sci. Math.*, pp. 100-110, Oct. 2023. <https://doi.org/10.52866/ijcsm.2023.04.04.009>
- [47] Faculty of Electrical and Electronics Engineering, Ho Chi Minh City University of Technology (HCMUT), Ho Chi Minh City, Vietnam, N. Tran-Thi-Kim, T. Pham-Viet, I. Koo, V. Mariano and T. Do-Hong, "Enhancing the Classification Accuracy of Rice Varieties by Using Convolutional Neural Networks," *Int. J. Electr. Electron. Eng. Telecommun.*, pp. 150-160, 2023. <https://doi.org/10.18178/ijeetc.12.2.150-160>
- [48] M. Hasanat, W. Khan, N. Minallah, N. Aziz, and A.-U.-R. Durrani, "Performance evaluation of transfer learning based deep convolutional neural network with limited fused spectro-temporal data for land cover classification," *Int. J. Electr. Comput. Eng. IJECE*, vol. 13, no. 6, p. 6882, Dec. 2023. <https://doi.org/10.11591/ijece.v13i6.pp6882-6890>
- [49] R. Chavan and D. Pete, "Automatic multi-disease classification on retinal images using multilevel glowworm swarm convolutional neural network," *J. Eng. Appl. Sci.*, vol. 71, no. 1, p. 26, Dec. 2024. <https://doi.org/10.1186/s44147-023-00335-0>
- [50] S. Susanto and D. S. Nanda, "Predicting the classification of high vowel sound by using artificial neural network: a study in forensic linguistics," *IAES Int. J. Artif. Intell. IJ-AI*, vol. 13, no. 1, p. 195, Mar. 2024. <https://doi.org/10.11591/ijai.v13.i1.pp195-200>
- [51] K.-L. Du and M. N. S. Swamy, *Neural Networks and Statistical Learning*. London: Springer London, 2019. <https://doi.org/10.1007/978-1-4471-7452-3>
- [52] A. Mohammadzadeh, M. H. Sabzalian, O. Castillo, R. Sakthivel, F. F. M. El-Sousy and S. Mobayen, *Neural Networks and Learning Algorithms in MATLAB*. in Synthesis Lectures on Intelligent Technologies. Cham: Springer International Publishing, 2022. <https://doi.org/10.1007/978-3-031-14571-1>
- [53] N. Assani, P. Matic, N. Kaštelan and I. R. Čavka, "A Review of Artificial Neural Networks Applications in Maritime Industry," *IEEE Access*, vol. 11, pp. 139823-139848, 2023. <https://doi.org/10.1109/ACCESS.2023.3341690>
- [54] X. Wang, W. Tian, and Z. Liao, "Framework for Hyperparameter Impact Analysis and Selection for Water Resources Feedforward Neural Network," *Water Resour. Manag.*, vol. 36, no. 11, pp. 4201-4217, Sep. 2022. <https://doi.org/10.1007/s11269-022-03248-4>
- [55] I. Fostiropoulos, B. Brown, and L. Itti, "Trustworthy model evaluation on a budget," 2023.
- [56] H. Ali *et al.*, "Machine Learning-Enabled NIR Spectroscopy. Part 3: Hyperparameter by Design (HyD) Based ANN-MLP Optimization, Model Generalizability, and Model Transferability," *AAPS PharmSci-Tech*, vol. 24, no. 8, p. 254, Dec. 2023. <https://doi.org/10.1208/s12249-023-02697-3>

# Aircraft Structural Assessments in Data-limited Environments: a Validated fe Method

Aun Haider<sup>1</sup>

**Abstract** — Aircraft operators often modify aircraft configurations, install new equipment, and alter airframes to accommodate this equipment, leading to operations in flight envelopes different from original design profile. These modifications necessitate airframe structural assessments, which typically require comprehensive aircraft design data, often unavailable to operators. This study aims to develop and validate a practical method for finite element analysis (FEA) of aircraft structures in the absence of this detailed design data. Focusing on a case study involving structural analysis of an aircraft wing, this study presents assumptions and idealizations used to develop 2.5D finite element (FE) model of the wing. Fidelity of this model is established by comparing FE analysis results with experimental data. Key validation metrics include reaction forces, load distribution at wing-fuselage attachments, and deformation at reference points on the wing under design load. Comparison between FE analysis and experimental results is carried out to substantiate accuracy of these geometric simplifications and idealizations of load-carrying behaviour of structural members. Therefore, practicality of these idealizations in absence of design data is demonstrated. This study offers a novel approach for structural assessments of aircraft without relying on proprietary design data. The validated method enhances capability of aircraft operators to perform effective structural analyses, thereby extending service life of aircraft with continued airworthiness.

**Keywords:** Finite element analysis, Structural integrity, Reduced scale model, Structural idealization, Experimental validation

**Resumen** — Los operadores de aeronaves a menudo modifican las configuraciones de las aeronaves, instalan nuevos equipos y modifican las estructuras de los aviones para acomodar estos equipos, lo que lleva a operaciones en envolventes de vuelo diferentes al perfil de diseño original. Estas modificaciones requieren evaluaciones estructurales de la estructura del avión, que normalmente requieren datos completos de diseño de la aeronave, que a menudo no están disponibles para los operadores. Este estudio tiene como objetivo desarrollar y validar un método práctico para el análisis de elementos finitos (FEA) de estructuras de aeronaves en ausencia de estos datos de diseño detallados. Centrándose en un estudio de caso que involucra el análisis estructural del ala de un avión, este estudio presenta suposiciones e idealizaciones utilizadas para desarrollar un modelo de elementos finitos (FE) 2.5D del ala. La fidelidad de este modelo se establece comparando

los resultados del análisis FE con datos experimentales. Las métricas clave de validación incluyen fuerzas de reacción, distribución de carga en las uniones ala-fuselaje y deformación en puntos de referencia en el ala bajo carga de diseño. Se lleva a cabo una comparación entre el análisis EF y los resultados experimentales para corroborar la precisión de estas simplificaciones geométricas e idealizaciones del comportamiento de carga de los miembros estructurales. Por lo tanto, se demuestra la practicidad de estas idealizaciones en ausencia de datos de diseño. Este estudio ofrece un enfoque novedoso para evaluaciones estructurales de aeronaves sin depender de datos de diseño patentados. El método validado mejora la capacidad de los operadores de aeronaves para realizar análisis estructurales efectivos, extendiendo así la vida útil de las aeronaves con aeronavegabilidad continua.

**Palabras clave:** Análisis de elementos finitos, integridad estructural, modelo a escala reducida, idealización estructural, validación experimental.

## I. INTRODUCTION

### A. Research Problem

**S**TRUCTURAL integrity analysis is paramount for safety, maintenance, and operational readiness of aircraft [1]. Structural integrity of aircraft is essential to prevent catastrophic failures that could lead to loss of life and equipment [2]. Moreover, structural integrity directly influences the frequency and cost of maintenance operations, as well as overall readiness of aircraft for their intended missions [3].

One of most significant hurdles in maintaining and assessing structural integrity of aging aircraft is the lack of access to comprehensive design data. This issue is exacerbated when either original equipment manufacturer (OEM) is no longer in business or has shifted focus to newer products [4]. For aircraft procured from foreign countries, the situation is often worse, with operators finding it virtually impossible to obtain necessary design data when technology transfer restrictions are in place [5].

The need for structural assessments arises from modifications made by operators to accommodate new equipment or to meet changing mission profiles [6]. These modifications can alter flight envelope and resultant structural loads, necessitating detailed analysis to ensure continued airworthiness [7]. However, unavailability of design data including CAD models, finite element (FE) models, material properties, and external loads, poses a significant challenge [8].

1. Aun Haider. Email: [aunbhutta@gmail.com](mailto:aunbhutta@gmail.com), ORCID: <https://orcid.org/0009-0000-5279-2829>, Institute of Aeronautics and Avionics (IAA) Air University Islamabad, Pakistan.

Manuscript Received: 13/07/2024

Revised: 22/08/2024

Accepted: 31/08/2024

DOI:<https://doi.org/10.29019/enfoqueute.1080>

Therefore, operators often rely on CAD models as templates for creating FE models [9]. This process is labour-intensive, requiring extensive geometric cleaning and discretization to produce a model suitable for analysis. FE model must be detailed enough to allow for comparison with actual deformation results, while coarse enough to ensure a quick turnaround of numerical results [10].

Moreover, as mission profiles often deviate from design profiles, and aircraft capabilities remain under-utilized or over-exploited [11]. This situation is further complicated when OEMs withdraw customer support at the end of contractual agreements, focusing instead on newer products [12]. Operators may also be forced to keep aircraft operational beyond design life due to procurement restrictions. Consequently, most operators of aging aircraft lack technical support from OEMs, making it challenging to keep them airworthy beyond design service life [13]. Therefore, to ensure the continued airworthiness of aging aircraft, structural assessments must be conducted [14]. These assessments require access to comprehensive design data, which directly impacts fidelity of the analysis. Access to accurate and detailed design data is crucial for developing reliable FE models, conducting thorough structural assessments, and ultimately ensuring safety of the aircraft [15].

### B. Research Hypothesis

In the absence of detailed aircraft design data, it is hypothesized that a reduced-scale finite element model developed using appropriate material properties, structural idealizations, and computationally inexpensive finite element assumptions, can accurately represent structural behaviour of the aircraft.

### C. Research Objectives

The objective of this research is to establish validity of these finite element (FE) idealizations invoked for analysis of an aircraft wing. These idealizations are intended to be highly practical, particularly when detailed aircraft design data is unavailable. This study presents a practical method for finite element analysis (FEA) of aircraft in absence of design data with reduced computational costs.

### D. Section wise Organization of Document

In this research, FE model of a wing isolated from the fuselage is presented. This model is developed using idealizations proposed in this paper. The structural behaviour of FE model is validated through comparison with experimental data. A positive correlation between FE results and experimental data validates the proposed assumptions. Significance of these assumptions lays in correct structural behaviour predicted by underlying FE model.

## II. LITERATURE REVIEW

### A. Existing Relevant Literature

An aircraft wing is a semi-monocoque structure designed to resist and transmit aerodynamic forces to the airframe [16].

The wing is statically indeterminate due to redundant structural members. Therefore, resulting structural response of each member depend on the stiffness of adjacent members [17].

Outer skin of the wing encloses three different types of structural members [18]. Beam-type structural members running along the wing span are called spars. Longitudinal structural members, which are considerably thinner compared to spars, are referred to as stringers. The third type of structural member, called ribs, is positioned along transverse chord direction [19]. Transverse ribs and longitudinal stringers are made from stamped sheet metal, while spars are machined. These structural members work together to support external aerodynamic and inertial loads and transfer them to the airframe [20].

The skin transmits aerodynamic forces to both longitudinal members (spars and stringers) and transverse members (ribs) through plate and membrane action [21]. Along with longitudinal members, the skin reacts to applied bending and axial loads. In conjunction with transverse ribs, the skin reacts to hoop or circumferential loads due to internal pressurization. The skin also develops shear stress that reacts to applied torsional moments [22].

Longitudinal members, including spars and stringers, primarily resist bending and axial loads. They segment the skin into smaller patches, which increases the buckling and compressive failure stresses. They also help arrest crack growth in the skin [23].

Transverse ribs maintain cross-sectional wing shape, distribute concentrated loads and redistribute stresses around structural discontinuities [24]. Ribs also establish column length for longitudinal members by providing end restraint, thereby increasing buckling strength of these members.

### B. Gaps in Existing Knowledge

Behaviour of wing and its structural members have been explained in detail in existing literature. However, no general guideline is available to FE analyst for developing wing models for structural analysis [25]. Therefore, FE analyst tends to use a variety of techniques ranging from simple beam model to full scale 3D model with all installed components. Fidelity and computational cost, thus, vary enormously between these extremes [26].

### C. Justification for New Research

In absence of comprehensive aircraft design data, a reduced-scale finite element (FE) model is required that can deliver high-fidelity results with quick turnaround time [27]. A reduced-scale FE model is a simplified version of full-scale finite element model, based on idealization of structural members. This model is designed to accurately capture aircraft's structural performance while reducing complexity. This approach facilitates timely decision-making and ensures that structural assessments are both accurate and efficient.

## III. METHODOLOGY

Idealization of load-bearing behaviour of an aircraft wing is presented for developing a reduced-scale finite element (FE)



model [28]. It involves simplifying geometry, using shell and beam elements for thin-walled structures, applying averaged material properties and focusing on representative load cases. MSC Patran® and Nastran® are used for FE analysis of wing model [29]. Validation of reduced-scale FE model against available experimental data or benchmark case is carried out to substantiate accuracy of these idealizations.

#### IV. FE ANALYSIS OF WING

##### A. Idealization of Wing

The wing of an aircraft is attached to fuselage at four different locations through spars, designated as Front Wall (FW), Front Spar (FS), Main Spar (MS), and Rear Spar (RS) [30]. Only the placement and limited geometric details of these structural members are available in maintenance manuals (MM). This information is utilized to develop 2.5 D FE model. Several assumptions regarding the load-carrying capacity of the wing's structural members have been made [31]:

1. Longitudinal stiffeners and spar flanges carry only axial stresses.
2. Rib web, skin, and spar web carry only shear stresses.
3. Axial stress is assumed to be constant along cross-section of each longitudinal stiffener (spars and stringers).
4. Shear stress is assumed to be uniform throughout the web of ribs and spars.
5. Transverse frames (ribs) are considered rigid within their own planes and have no rigidity normal to their planes.

The structural members of wing have geometric details, including lightening holes [32], variations in thickness, cross-sectional warp, and manufacturing artifacts like fillets, chamfers, and radii. These features are not included in the reduced-scale FE model. Following geometric simplifications have also been carried out:

1. Using average thickness for structural members.
2. Assuming no warp in the cross-sectional shape.
3. Omitting fasteners such as bolts and rivets, with load transfer between adjoining members ensured through coincident nodes [33].

Various components installed inside the wing, such as fuel transfer valves, hydraulic actuators, landing gear attachments, and electrical ancillaries contribute to 30 % mass and internal volume of the aircraft wing [34]. These components do not contribute to structural stiffness of the wing. Additionally, flight control surfaces attached to the wing, including airspeed brakes, leading edge flaps (LEF), trailing edge flaps (TEF), and ailerons, are required for aeroelastic analysis. The present study deals with static structural analysis whereby these ancillary component and control surfaces do not add structural stiffness and hence, are not included in the model [35].

The purpose of this reduced-scale FE model is to calculate internal load distribution, load paths, structural deformation, and free-body loads [36]. The model uses 0D mass and spring elements, 1D beam elements, and 2D shell elements [37] arranged in 3D space to mimic the wing structure. Fig. 1 presents the illustration of wing and placement of internal members in wing.

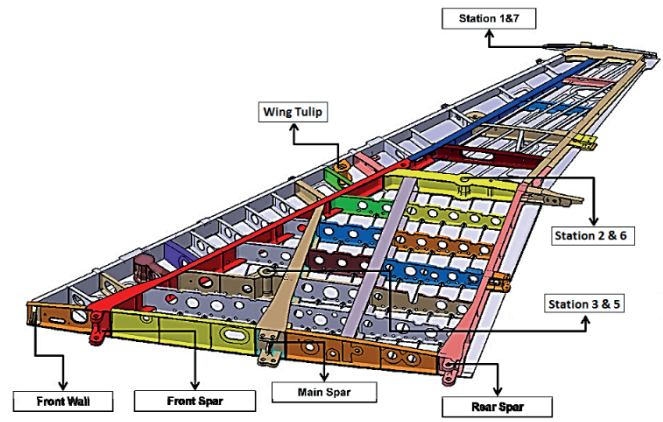


Fig. 1. Wing Model

##### B. Finite Elements Selection

3D solid elements are often unsuitable for modelling thin-walled aircraft structures due to the phenomenon of shear locking [38]. This issue can be mitigated by selecting first order 2D elements with appropriate mesh density (element size). Nastran Element Library recommends using shell elements (CQUAD4) and beam elements (CBEAM) for plate and beam-like structures, respectively [39]. For structures where cross-section remains constant along the length, lower-order CROD element can also be used as an alternative to beam elements.

CQUAD4 (linear 2D shell) elements is used to model aircraft skin and webs of ribs / spars. Each node in a shell element has 5 degrees of freedom (DOFs), while each node in a beam element has 6 DOFs. Flanges of ribs and spars, which carry axial loads, are modelled using beam elements. Stiffeners in skin panels and stringers in aircraft wing are modelled using 1D rod element CROD. This modelling approach balances computational efficiency with the need for accurate representation of the aircraft's structural behaviour under various loads [40]. Fig. 2 shows the finite element model of the wing with outer skin removed.

##### C. Material Properties

In aircraft maintenance manuals, except for nomenclature, material properties are often not provided. Due to lack of specific material details, properties available from open resources, as listed in Table 1, have been considered for the analysis.

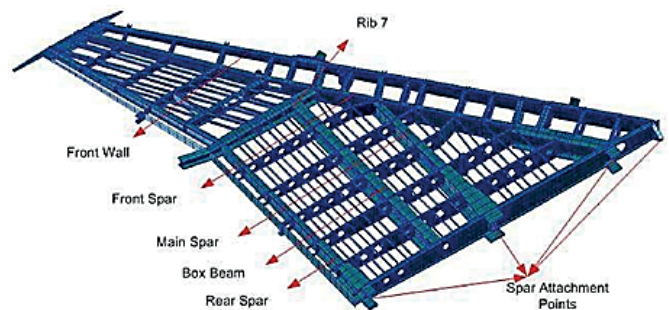


Fig. 2. Internal Members in FE Model

TABLE I  
MATERIAL PROPERTIES FOR WING

| Component  | Material       | E (GPa) | Poisson Ratio( $\mu$ ) |
|------------|----------------|---------|------------------------|
| Front Wall |                |         |                        |
| Front Spar |                |         |                        |
| Box Beam   | Al 2000 series | 73.1    | 0.33                   |
| Rear Spar  |                |         |                        |
| Ribs       |                |         |                        |
| Stingers   |                |         |                        |
| Main Spar  | Steel          | 196     | 0.3                    |
| Skin       | Al 7000 series | 70      | 0.3                    |

D. Systems of Units

MSC Patran Nastran is independent of unit system and therefore, consistency of units is the responsibility of FE analyst. For current analysis, mm, kg, s unit system is used. So, deformation output is mm and stress output is MPa.

E. Boundary Conditions

The wing is connected to a root beam which is attached to four transverse bulkheads of the fuselage. These bulkheads are modelled using beam elements (CBEAM) with a very high stiffness of 1 GN/m which are fixed at aircraft centreline (CL). Fig. 3 illustrates these boundary conditions applied on the wing.

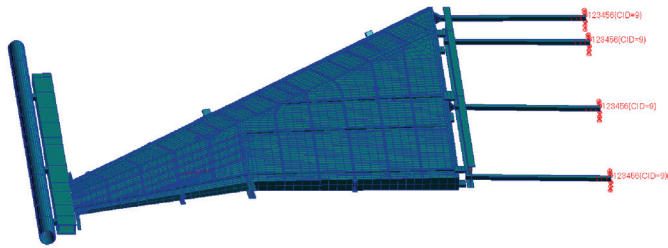


Fig. 3. Applied Boundary Conditions on Wing

Use of very stiff beam elements to represent wing-fuselage attachment offers two main benefits. [41] First, it ensures that the deflection of the wing spar attachments remains minimal, allowing the wing deformation from numerical results to closely match experimental data. Second, by applying the fixed boundary condition away from the spar attachments, it helps to avoid stress singularities at these attachment points.

F. Loads

Available experimental results were obtained by applying discrete forces to the wing through hydraulic actuators, with applied load set equal to design limit load for the wing. This load is simulated in finite element (FE) model by applying nodal forces at the locations corresponding to the actuators. Fig. 4 illustrates the application of these nodal forces on FE model of the wing.

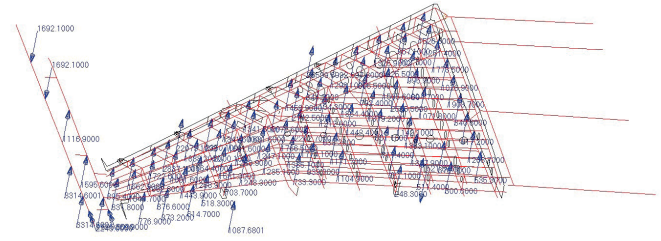


Fig. 4. Applied Load on Wing

G. Verification of FE Model

To ensure adequacy of finite element (FE) model, following steps have been implemented [42]:

1. A mapped mesh approach is used for development of FE model of the wing.
2. More than 95 percent of shell elements are quadrilateral. Triangular shell elements are employed only in mesh transition regions to maintain model consistency.
3. Edge length for shell elements is set to 50 mm. Mesh density is adjusted to ensure at least four shell elements along beam cross-sections of ribs and spars.
4. Coincidence of nodes between adjoining structural members is enforced to ensure effective load transfer throughout the model.
5. Using default settings in MSC Patran, mesh quality checks (including taper ratio, skewness and warp) are conducted and confirm no errors.
6. Shell normal and beam orientations are verified to ensure consistency within FE model.
7. No duplicate elements or free edges are present in FE model.

These measures collectively ensure that FE model accurately represents wing structure to produce reliable simulation results.

H. Static Structural Analysis

Finite Element analysis has been performed at design load. Pre- & Post processing is performed in MSC Patran while MSC Nastran is used as solver. Deformation field of wing under applied load is given in Fig. 5. Von-Mises equivalent stress in wing at design load is given in Fig. 6.

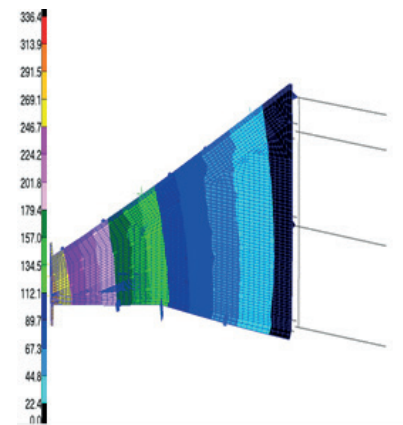


Fig. 5. Wing Deformation Field

I. Validation of FE Results

Validation of the finite element (FE) results has been performed using experimental data to substantiate the proposed assumptions and idealizations for the FE analysis of the wing. The available experimental data includes:

1. Reactions (Forces and moments) measured at the wing attachments.
2. Measurements of wing deformation at various locations along the span under design load.

By comparing these experimental data points with the results obtained from FE analysis, accuracy and reliability of underlying assumptions and idealizations of the model are assessed.

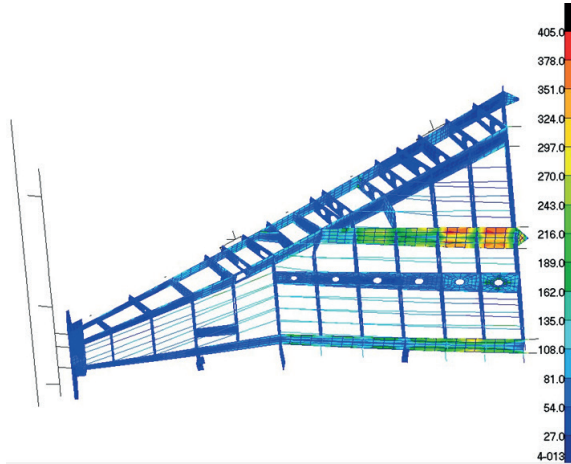


Fig. 6. Wing Stress Field (Outer Skin Removed)

V. DISCUSSION

A. Interpretation of Results

Table 2 presents comparison of reaction (forces and moments) at wing attachment for FE and experimental results. Both experimental and FE results correlate because maximum percentage difference between these results is less than 6 %.

TABLE II  
COMPARISON OF REACTION FORCES

| Attachment | FE Results |              | Experimental Results |              | %Age Difference |        |
|------------|------------|--------------|----------------------|--------------|-----------------|--------|
|            | Force (N)  | Moment (N.m) | Force (N)            | Moment (N.m) | Force           | Moment |
| Main Spar  | 79354      | 124704       | 83520                | 129950       | 4.99            | 4.04   |
| Front Spar | 37578      | 58431        | 39810                | 61120        | 5.61            | 4.4    |
| Rear Spar  | 33643      | 52334        | 35350                | 54870        | 4.83            | 4.62   |
| Front Wall | 2791       | 4263         | 2915                 | 4435         | 4.25            | 3.88   |
| Total      | 153366     | 239732       | 161595               | 250375       | --              | --     |

Table 3 gives load distribution among wing spars from FE and experimental results. Both methods predict that main spar takes 52 % load, front spar takes 24 % load, rear spar takes 22 % and front wall takes 2 % load, approximately.

Comparison of deflection field of wing for FE and experimental results have been carried out. Front wall, front spar and rear spar run from wing root to wing tip. Fig. 7 shows the monitor points for which experimental deformation of wing under design load is available.

TABLE III  
LOAD DISTRIBUTION

| Attachment | FE Results |          | Experimental Results |          |
|------------|------------|----------|----------------------|----------|
|            | Force %    | Moment % | Force %              | Moment % |
| Main Spar  | 51.74      | 52.02    | 51.68                | 51.9     |
| Front Spar | 24.5       | 24.37    | 24.64                | 24.41    |
| Rear Spar  | 21.94      | 21.83    | 21.88                | 21.92    |
| Front Wall | 1.82       | 1.78     | 1.8                  | 1.77     |
| Total      | 100        | 100      | 100                  | 100      |

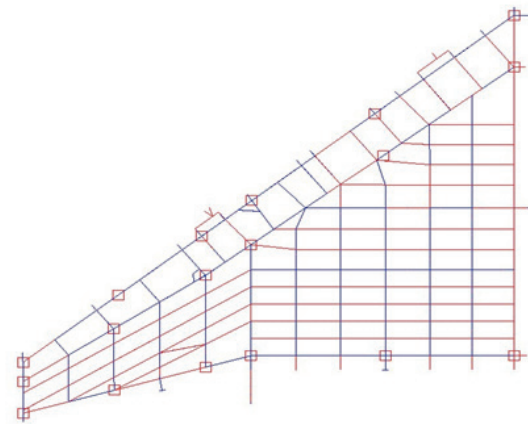


Fig. 7. Monitor Points on Wing

Fig. 8 shows the comparison of deformation of along Front Wall, Front Spar and rear spar for FE analysis and experimental results. Deformation field of wing available from both studies correlate with each other.

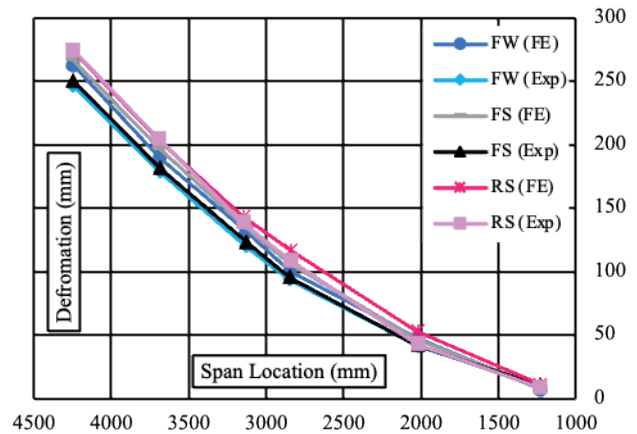


Fig. 8. Comparison of Deformation along Wing Spars

### B. Research Questions and Hypothesis

Validation of FE results confirms that the idealized behaviour of wing structure can be accurately assumed. It has been demonstrated that geometric simplifications do not significantly impact the deformation field of the aircraft structure. Additionally, it has been validated that the fasteners can be excluded from FE model, with load transfer effectively facilitated through coincident nodes. Effects of surface and heat treatments on the mechanical behaviour of structural members can be disregarded in FE model without compromising accuracy. Use of candidate material properties, rather than exact material specifications, is acceptable for modelling structural members in FE model. These findings provide comprehensive answers to key research questions, substantiating the initial hypothesis that such assumptions are valid for aircraft structural analysis. The study demonstrates that idealized behaviour and simplifications can be reliably used in FE modelling without adversely affecting accuracy of results.

### C. Placement of Results with Existing Literature

These findings are unique within existing literature, addressing the limitations of both low-fidelity analysis and computationally expensive methods. It has been demonstrated that useful and accurate results can be achieved by implementing these idealizations and assumptions with minimal computational cost. This approach provides a practical solution for analyzing aircraft structures, especially when detailed design data is unavailable.

## VI. CONCLUSION AND RECOMMENDATIONS

Comparison of reaction forces, load distribution, and deformation field of the wing with experimental results validates the methodology for development of FE model. This validation confirms that the following idealizations are useful for FE analysis:

1. *Idealized behaviour of structural members in the wing can be assumed for static structural analysis. Longitudinal stiffeners and spar flanges carry only axial stresses. Rib web, skin, and spar web carry only shear stresses.*
2. *Geometric simplifications can be made in FE model, omitting manufacturing features like fillets, chamfers, and small cut-outs.*
3. *In absence of specific material nomenclature, reasonable material properties can be used for components, and effect of surface treatments on mechanical behaviour of structural members can be ignored.*
4. *Fasteners can be excluded from FE model, with load transfer effectively handled through coincident nodes.*
5. *Far-field boundary conditions can be applied to isolate structural members from the global assembly. This boundary condition can provide an accurate approximation of their structural behaviour.*

These validated assumptions streamline modelling process and ensure accuracy of FE model without requiring exhaustive detail, thus facilitating efficient and reliable structural analysis.

### A. Contributions of Present Research

This research offers a methodology for developing a reduced-scale FE model of aircraft structures. The reduced-scale model can be developed using information accessible to aircraft operators, without relying on detailed design data. This model is particularly advantageous for achieving a quick turnaround of results during design iterations and modification phases. This approach enables effective structural analysis and decision-making, even the absence of proprietary design details, thereby supporting maintenance and modification efforts.

### B. Benefits and Limitations of Proposed Solution

The proposed solution offers accurate predictions of deformation and load transfer paths within the aircraft wing. Extension of this methodology for the development of FE model of aircraft fuselage is also required to establish its robustness. Further studies are also necessary to verify the stress results obtained from the reduced-scale finite element model. These additional investigations will help ensure the reliability and accuracy of stress distributions, providing a more comprehensive validation of the methodology.

### C. Potential Applications

This research holds significant potential in the field of aerospace engineering. By employing proposed idealizations, a reduced-scale finite element model can be developed, which effectively captures the structural behaviour of the aircraft. In absence of design data, this model offers high-fidelity results at minimal computational cost, making it a valuable tool for structural analysis, design optimization, and modifications in aerospace applications.

### D. Future Lines of Research

It is recommended that a strain gauge survey of the complete wing under design load be conducted to verify the fidelity of 2.5D FE model for stress calculation. This experimental validation would ensure that the model accurately represents the stress distributions within the wing structure, providing a more comprehensive assessment of its reliability and accuracy.

## ACKNOWLEDGMENTS

The author acknowledges the facilitation of his department at Air University for providing all the resources for this publication.

## REFERENCES

- [1] S. M. Tavares, J. A. Ribeiro, B. A. Ribeiro and P. M. de Castro, "Aircraft Structural Design and Life-Cycle Assessment through Digital Twins," *Designs*, vol. 8, no. 2, p. 29, 2024. <https://doi.org/10.3390/designs8020029>
- [2] B. Main, L. Molent, R. Singh and S. Barter, "Fatigue Crack Growth Lessons from Thirty-Five years of The Royal Australian Air Force F/A-18 A/B Hornet Aircraft Structural Integrity Program," *International Journal of Fatigue*, vol. 133, no. 7, p. 426, 2020. <https://doi.org/10.1016/j.ijfatigue.2019.105426>

- [3] M. J. Scott, W. J. Verhagen, M. T. Bieber, and P. Marzocca, "A Systematic Literature Review of Predictive Maintenance for Defence Fixed-Wing Aircraft Sustainment and Operations," *Sensors*, vol. 22, no. 18, p. 7070, 2022. <https://doi.org/10.3390/s22187070>
- [4] L.-H. Zhang, W.-J. Li, C. Zhang and S. Wang, "Outsourcing Strategy of an Original Equipment Manufacturer in a Sustainable Supply Chain: Whether and How Should a Contract Manufacturer Encroach?," *Transportation Research Part E: Logistics and Transportation Review*, vol. 174, no. 3, p. 132, 2023, <https://doi.org/10.1016/j.tre.2023.103132>
- [5] M. A. Sezal and F. Giunelli, "Technology Transfer and Defence Sector Dynamics: The Case of Netherlands," *European Security*, vol. 31, no. 4, p. 558, 2022. <https://doi.org/10.1080/09662839.2022.2028277>
- [6] V. Cusati, S. Corcione and V. Memmolo, "Impact of Structural Health Monitoring on Aircraft Operating Costs by Multidisciplinary Analysis," *Sensors*, vol. 21, no. 20, p. 938, 2021. <https://doi.org/10.3390/s21206938>
- [7] M. Orlovsky, A. Priymak and V. Voytenko, "Concept of Continued Airworthiness of Aircraft at Different Stages of Life Cycle," *Open Information and Computer Integrated Technologies*, vol. 12, no. 90, p. 45, 2020.
- [8] S. Zhang and M. Mikulich, "Parametric CAD Modelling of Aircraft Wings for FEA Vibration Analysis," *Journal of Applied Mathematics and Physics*, vol. 9, no. 5, p. 889, 2021. <https://doi.org/10.4236/jamp.2021.95060>
- [9] A. Bacciaglia, A. Ceruti and A. Liverani, "Surface Smoothing for Topological Optimized 3D Models," *Structural and Multidisciplinary Optimization*, vol. 64, no. 6, p. 3453, 2021. <https://doi.org/10.1007/s00158-021-03027-6>
- [10] A. Mazier, A. Bilger, A. E. Forte, I. Peterlik, J. S. Hale, and S. P. Bordas, "Inverse Deformation Analysis: An Experimental and Numerical Assessment Using the FENICS Project," *Engineering with Computers*, vol. 38, no. 5, p. 99, 2022. <https://doi.org/10.1007/s00366-021-01597-z>
- [11] Y. Cai, D. Rajaram and D. N. Mavris, "Simultaneous Aircraft Sizing and Multi-Objective Optimization considering Off-Design Mission Performance during Early Design," *Aerospace Science and Technology*, vol. 126, no. 10, p. 662, 2022. <https://doi.org/10.1016/j.ast.2022.107662>
- [12] A. Bazerghi and J. A. Van Mieghem, "Last Time Buys during Product Rollovers: Manufacturer & Supplier Equilibria," *Production and Operations Management*, vol. 33, no. 3, p. 757, 2024 <https://doi.org/10.1177/10591478241231859>
- [13] A. A. Pohya, J. Wehrspohn, R. Meissner, and K. Wicke, "A Modular Framework for the Life Cycle Based Evaluation of Aircraft Technologies, Maintenance Strategies, and Operational Decision Making Using Discrete Event Simulation," *Aerospace*, vol. 8, no. 7, p. 187, 2021. <https://doi.org/10.3390/aerospace8070187>
- [14] I. Kabashkin, V. Perekrestov, T. Tyncherov, L. Shoshin and V. Susannin, "Framework for Integration of Health Monitoring Systems in Life Cycle Management for Aviation Sustainability and Cost Efficiency," *Sustainability*, vol. 16, no. 14, p. 154, 2024. <https://doi.org/10.3390/su16146154>
- [15] J. Lin, "Durability and Damage Tolerance Analysis Methods for Lightweight Aircraft Structures: Review and Prospects," *International Journal of Lightweight Materials and Manufacturing*, vol. 5, no. 2, p. 224, 2022. <https://doi.org/10.1016/j.ijlmm.2022.02.001>
- [16] P. Korba, S. Al-Rabeei, M. Hovanec, I. Sekelová, and U. Kale, "Structural Design and Material Comparison for Aircraft Wing Box Beam Panel," *Heliyon*, vol. 10, no. 5, 2024. <https://doi.org/10.1016/j.heliyon.2024.e27403>
- [17] Y. Tian et al., "Optimal Design and Analysis of a Deformable Mechanism for a Redundantly Driven Variable Swept Wing," *Aerospace Science and Technology*, vol. 146, no. 10, p. 993, 2024. <https://doi.org/10.1016/j.ast.2024.108993>
- [18] L. Félix, A. A. Gomes and A. Suleman, "Topology Optimization of the Internal Structure of An Aircraft Wing Subjected to Self-Weight Load," *Engineering Optimization*, vol. 52, no. 7, pp. 1119-1135, 2020. <https://doi.org/10.1080/0305215X.2019.1639691>
- [19] W. Skarka, R. Kumpati and M. Skarka, "Failure Analysis of a Composite Structural Spar and Rib-to-Skin Joints," *Procedia Structural Integrity*, vol. 54, no. 4, pp. 490-497, 2024. <https://doi.org/10.1016/j.prostr.2024.01.111>
- [20] N. R. Berger, S. G. Russell and D. N. Mavris, "Preliminary Weight Study Comparing Multi-Rib and Multi-Spar Wing Box Configurations using SPANDSET," in *Scitech 2021 Forum*, Reston, VA 2021, vol. 4, no. 8: AIAA, p. 922. <https://doi.org/10.2514/6.2021-0922>
- [21] P. V. Kumar, I. R. Raj, M. S. Reddy and N. S. Prasad, "Design and Finite Element Analysis of Aircraft Wing Using Ribs and Spars," *Turkish Journal of Computer and Mathematics Education*, vol. 12, no. 8, p. 3224, 2021.
- [22] J. Slota, A. Kubit, T. Trzepieciński, B. Krasowski and J. Varga, "Ultimate Load-Carrying Ability of Rib-Stiffened 2024-T3 And 7075-T6 Aluminium Alloy Panels Under Axial Compression," *Materials*, vol. 14, no. 5, p. 1176, 2021. <https://doi.org/10.3390/ma14051176>
- [23] P. Dwivedi, A. N. Siddiquee and S. Maheshwari, "Issues and Requirements for Aluminum Alloys Used In Aircraft Components: State of the Art Review," *Russian Journal of Non-Ferrous Metals*, vol. 62, no. 4, pp. 212-225 2021. <https://doi.org/10.3103/S1067821221020048>
- [24] S. De, M. Jrad and R. K. Kapania, "Structural Optimization of Internal Structure of Aircraft Wings with Curvilinear Spars and Ribs," *Journal of Aircraft*, vol. 56, no. 2, pp. 707-718 2019. <https://doi.org/10.2514/1.C034818>
- [25] C. Collier and S. Jones, "Unified Analysis of Aerospace Structures through Implementation of Rapid Tools into a Stress Framework," in *Scitech 2020 forum*, Orlando, Florida, 2020, vol. 41, no. 12: AIAA p. 1478. <https://doi.org/10.2514/6.2020-1478>
- [26] J. Kudela and R. Matousek, "Recent Advances and Applications of Surrogate Models for Finite Element Method Computations: A Review," *Soft Computing*, vol. 26, no. 24, 13709,13733, 2022. <https://doi.org/10.1007/s00500-022-07362-8>
- [27] A. Haider, "Efficiency Enhancement Techniques in Finite Element Analysis: Navigating Complexity for Agile Design Exploration," *Aircraft Engineering and Aerospace Technology*, 2024. <https://doi.org/10.1108/AEAT-02-2024-0053>
- [28] A. Haider, "Enhancing Transparency and Reproducibility in Finite Element Analysis through Comprehensive Reporting Parameters: A Review," *El-Cezeri Journal*. <https://doi.org/10.31202/ecjse.1436203>
- [29] T. V. Kumar, A. W. Basha, M. Pavithra and V. Srilekha, "Static & Dynamic Analysis of a Typical Aircraft Wing Structure Using MSC NASTRAN," *Int. J. Res. Aeronaut. Mech. Eng.*, vol. 3, no. 7, pp. 1-12, 2015.
- [30] A. H. Bhutta, "Optimizing Structural Integrity of Fighter Aircraft Wing Stations: a Finite Element Analysis Approach," *Ingenius*, vol. 1, no. 32, pp. 90-100, 2024. <https://doi.org/10.17163/ings.n32.2024.09>
- [31] R. Kumar B, "Investigation on Buckling Response of the Aircraft's Wing Using Finite-Element Method," *Australian Journal of Mechanical Engineering*, vol. 18, no. Sup1, pp. S122-S131, 2020. <https://doi.org/10.1080/14484846.2018.1483467>
- [32] J. S. M. Ali, W. M. H. Embong and A. Aabid, "Effect of Cut-out Shape on the Stresses in Aircraft Wing Ribs Under Aerodynamic Load," *CFD Letters*, vol. 13, no. 11, pp. 87-94, 2021. <https://doi.org/10.37934/cfdl.13.11.8794>
- [33] F. Sarka, "Examination of Bolt Connection with Finite Element Method," in *Vehicle and Automotive Engineering*: Springer, 2022, pp. 212-222.
- [34] J. H. Jang and S. H. Ahn, "FE Modeling Methodology for Load Analysis and Preliminary Sizing of Aircraft Wing Structure," *International Journal of Aviation, Aeronautics, and Aerospace*, vol. 6, no. 2, p. 1, 2019. <https://doi.org/10.15394/ijaaa.2019.1301>
- [35] S. Fu and N. P. Avdelidis, "Prognostic and Health Management of Critical Aircraft Systems and Components: An Overview," *Sensors*, vol. 23, no. 19, p. 8124, 2023. <https://doi.org/10.3390/s23198124>
- [36] W. K. Liu, S. Li and H. S. Park, "Eighty Years of the Finite Element Method: Birth, Evolution, and Future," *Archives of Computational Methods in Engineering*, vol. 29, no. 6, pp. 4431-4453, 2022. <https://doi.org/10.1007/978-981-19-3363-9>
- [37] D. Arndt et al., "Finite Element Library: Design, Features, And Insights," *Computers & Mathematics with Applications*, vol. 81, no. 22, pp. 407-422, 2021. <https://doi.org/10.1016/j.camwa.2020.02.022>
- [38] M. Ainsworth and C. Parker, "Unlocking the Secrets of Locking: Finite Element Analysis in Planar Linear Elasticity," *Computer Methods in Applied Mechanics and Engineering*, vol. 395, no. 11, p. 115034, 2022. <https://doi.org/10.1016/j.cma.2022.115034>
- [39] C. Hagigat, "Elaboration of Degrees of Freedom in NASTRAN/PATRAN by comparing "Rod" and "Beam" Elements," *Journal of Innovative Ideas in Engineering and Technology*, vol. 1, no. 1, p. 8, 2022.

- [40] N. Yang, "Methodology of Aircraft Structural Design Optimisation," *International Journal of Computer Applications in Technology*, vol. 70, no. 3, p. 145, 2022. <https://doi.org/10.1504/IJCAT.2022.130874>
- [41] A. H. Bhutta, "Appropriate Boundary Condition for Finite Element Analysis of Structural Members Isolated from Global Model," *NED*

- University Journal of Research*, vol. 18, no. 3, pp. 61-75, 2021. <https://doi.org/10.35453/NEDJR-STMECH-2021-0001>.
- [42] S. Ereiz, I. Duvnjak and J. F. Jiménez-Alonso, "Review of Finite Element Model Updating Methods for Structural Applications," *Structures*, Atlanta, Georgia, 2022, vol. 41, no. 12, pp. 684-723. Elsevier. <https://doi.org/10.1016/j.istruc.2022.05.041>

# Model for estimating soil chemical properties with RGB drone images

Manuel Álava Bermeo<sup>1</sup>, Antony García Solórzano<sup>2</sup>, Henry Pacheco Gil<sup>3</sup>, Cristhian Delgado Marcillo<sup>4</sup>

**Abstract** — Precision agriculture optimizes crop management by providing accurate data on soil chemical properties, thereby improving agricultural productivity and sustainability. This study aims to develop models to estimate soil chemical properties, such as pH, electrical conductivity (EC), and organic matter (OM), by analyzing drone-captured RGB images. The methodology included photogrammetric flights with a DJI Phantom 4 Pro drone equipped with a 20 Mpx camera and simultaneous sampling, laboratory analysis and on-site measurements, with Royal Eijkelpamp EC meter set voor grond multiparameter sensors and pH meter set voor soil and water. The aerial images were processed with the PIX4Dmapper software, to generate the orthophoto and spectral bands. With the resulting orthophoto of 1.6 cm/pixel, eight spectral indices were calculated, using the spatial analysis tools of ArcGIS software. The in situ results showed an average pH value of 5.83, indicating a slightly acidic soil, and an EC of 1.09 dS/m, suggesting a soil with a low concentration of dissolved salts. Laboratory analyses showed a medium-high content of OM, with an average of 5.19 %. A strong correlation was found between OM and pH\_index with coefficients of determination  $R^2=0.55$ , while moderate correlations were also observed between pH with pH\_index and EC with sal\_index6 with coefficients of determination  $R^2=-0.39$  and  $R^2=0.42$  respectively. The aforementioned results allowed the generation of two models for the estimation of these variables from RGB images.

**Keywords:** precision agriculture; spectral indices; Phantom 4 Pro; PIX4Dmapper, ArcGIS.

**Resumen** — La agricultura de precisión optimiza la gestión de cultivos al proporcionar datos precisos sobre las propiedades químicas del suelo, mejorando así la productividad y sostenibilidad agrícola. Este estudio tiene como objetivo desarrollar modelos para estimar propiedades químicas del suelo, como pH, conductividad eléctrica (CE) y materia orgánica (MO), mediante el análisis de imágenes RGB capturadas por dron. La metodología incluyó vuelos fotogramétricos con un dron DJI Phantom 4 Pro equipado con una cámara de 20 Mpx y la toma simultánea de muestras de análisis de laboratorio y mediciones in situ, con sensores multiparámetros Royal Eijkelpamp EC meter set voor

grond y pH meter set for soil and water. Las imágenes aéreas fueron procesadas con el software PIX4Dmapper, para generar la ortofoto y bandas espectrales. Con la ortofoto resultante de 1.6 cm/píxel, se calcularon ocho índices espectrales, usando las herramientas de análisis espacial del software ArcGIS. Los resultados in situ mostraron un valor promedio de pH de 5.83, indicando un suelo ligeramente ácido, y una CE de 1.09 dS/m, sugiriendo un suelo con baja concentración de sales disueltas. Los análisis de laboratorio evidenciaron un contenido medio-alto de MO, con un promedio de 5.19 %. Se encontró una correlación fuerte entre la MO y el pH\_index con coeficientes de determinación  $R^2=0.55$ , por su parte también se observaron correlaciones moderadas entre pH con el pH\_index y CE con el sal\_index6 con coeficientes de determinación  $R^2=-0.39$  y  $R^2=0.42$  respectivamente. Los resultados mencionados permitieron generar dos modelos para la estimación de estas variables a partir de imágenes RGB.

**Palabras Clave:** agricultura de precisión; índices espectrales; Phantom 4 Pro; PIX4Dmapper, ArcGIS.

## I. INTRODUCTION

AGRICULTURE is an essential activity for the survival of the human being, which significantly influences the economy of Ecuador with 10 % of GDP, promoting development and reducing poverty contributing 19 % to the generation of employment [1].

By using advanced spatial analysis tools, such as Geographic Information Technologies (GIT), agriculture and soil management specialists can make informed decisions to optimize agricultural practices [2].

Soil quality is fundamental for agricultural productivity, it is a complex ecosystem [3], it needs to evaluate chemical parameters such as organic matter (OM), hydrogen potential (pH) and electrical conductivity (EC) to improve its structure, retain water and nutrients [4].

Understanding pH, electrical conductivity (EC), and organic matter (OM) is crucial for assessing soil quality in agriculture. pH affects nutrient availability and plant growth, while EC indicates salt concentration, which can impact water and nutrient uptake. OM improves soil structure, water retention, and microbial biodiversity. Together, these parameters enable more precise soil management, optimizing conditions for healthy and sustainable crop development [5].

The limitation in determining the chemical variables of the soil lies in the constant need to evaluate the productive capacity of the soil through exhaustive laboratory analyses [6]. However, this practice faces several obstacles, as it is costly, time-consuming in processing samples and, in many cases, is not carried out due to a lack of knowledge on the part of producers [7].

1. Manuel Álava Bermeo. Filiation: Universidad Técnica de Manabí. Email: malava7130@utm.edu.ec, ORCID: <https://orcid.org/0009-0008-4027-4950>.

2. Antony García Solórzano. Filiation: Universidad Técnica de Manabí. Email: agarcia6793@utm.edu.ec, ORCID: <https://orcid.org/0009-0003-0124-2423>

3. Henry Pacheco Gil. Filiation: Universidad Técnica de Manabí. Email: henry.pacheco@utm.edu.ec, ORCID: <https://orcid.org/0000-0002-9997-9591>

4. Cristhian Delgado Marcillo. Filiation: Universidad Técnica de Manabí. Email: cristhian.delgado@utm.edu.ec, ORCID: <https://orcid.org/0009-0006-7248-6718>

Manuscript Received: 09/08/2024

Revised: 02/09/2024

Accepted: 09/09/2024

DOI: <https://doi.org/10.29019/enfoqueute.1078>

To address this problem, it is proposed to use spectral calculation from the RGB bands (corresponding to the red, green and blue wavelengths), of aerial images captured by low-cost drones, with the aim of developing a model adapted to local conditions that provides reliable and fast data on key chemical properties of the soil. Such as pH, electrical conductivity and organic matter content [8].

The research by Krestenitis et al. [9] presents an innovative path planning method for UAVs in precision agriculture. The goal is to acquire high-quality data in the shortest possible flight time by adjusting the UAV's speed.

The integration of remote sensing technologies is presented as a promising tool to study the chemical properties of soil, offering accurate and relevant data [10].

Petrovic's research confirms that Agriculture 5.0 has now begun with the widespread use of robotic systems in various field operations, supported by the Internet of Things (IoT), autonomous self-driving devices (robots and drones), and artificial intelligence [11].

Precision agriculture in Ecuador is used in the floriculture, banana, and sugar sectors, mainly for the implementation of automated irrigation systems, pest monitoring and control, moisture management, and ventilation. In this context, drones are used for pest detection and monitoring, as well as for topographic surveys in order to optimize crop management [12].

The implementation of TIG in the study of soil chemical properties involves the acquisition, organization and analysis of detailed geospatial data on pH, EC and OM, through the use of specialized tools that allow the generation of layers of information and the performance of spatial analyses to identify patterns and distributions where modeling techniques are used to predict the distribution of soil properties in unsampled areas. In order to optimize agricultural practices, improve crop management and maximize productivity in an efficient and sustainable way [13].

UAV equipped with high-definition cameras and sensors like LiDAR, are essential tools in agricultural remote sensing. They enable georeferencing data and creating accurate maps of crop health, estimating bio-physical characteristics such as growth and yield. They offer an advanced alternative to traditional field exploration, providing detailed views at the plant and leaf level due to their high resolution and segmentation algorithms [14].

Mao et al. [15], point out that the use of low-end unmanned aerial vehicles (UAVs) has many advantages, such as low cost, high resolution, and considerable spatial coverage giving value to remote sensing data. Remote sensing is based on collecting data from various aerial photographs at different spectral ranges [16].

The next innovation in smart UAVs aims to transform agriculture with cost savings and increased yields. However, they face cybersecurity risks, which could be mitigated through Blockchain and 5G networks [17].

Tan et al. [18], highlights that drones equipped with hyperspectral sensors are crucial for agricultural monitoring, capturing changes in vegetation and soil, and providing spectral information to monitor salinity. The use of regression algorithms, such as Random Forest, has matured as an effective solution for predicting properties like soil salinity, handling nonlinear fitting problems and high-dimensional data.

In the context of soil analysis, the technology of RGB image analysis algorithms is effectively deployed. This approach involves the application of statistical and mathematical methods to the images acquired by a drone equipped with an RGB digital camera. Through this process, the precise identification and quantification of the wavelengths contained in the images is achieved, thus allowing a detailed analysis of soil properties in a non-invasive and reliable way [19].

Recent research by Lintes et al. [20] developed a radar method using two unmanned aerial vehicles in a bistatic system. This system irradiates the Earth's surface obliquely to create the Brewster effect, which enhances the reflection of radio signals from subsurface horizons, allowing for the determination of their physical and chemical parameters.

In a study by Ngabire et al. [21], in the Shiyang River basin, remote sensing was applied to analyze soil salinization in arid and semi-arid environments. A multiple linear regression model was used with 80 samples, divided for training and validation using the Kennard-Stone algorithm. Multicollinearity identification was performed with the variance inflation factor (VIF), adjusting covariates to ensure proper model specification. The results showed outstanding performance, with a coefficient of determination  $R^2=0.898$  and a mean square error (RMSE) of 1.653. These findings are of vital importance to support the integration of remote sensing into the analysis of soil chemical properties.

This soil analysis study focused on addressing the imperative need to efficiently estimate the chemical parameters of the soil through image geoprocessing techniques, taking advantage of remote sensing and RGB digital camera tools. This strategy is based on the precise determination and evaluation of electrical conductivity (EC), pH and organic matter content in the soil, thus offering a significant contribution to the advancement of sustainable management of agricultural resources [22].

## II. METHODOLOGY

### *Location of the study area*

This study was carried out on a plot of 0.38 hectares, located in the Lodana parish of the Santa Ana canton belonging to the province of Manabí. Its geographical location is 80°23'13.60"W, 1°10'25.51"S (Fig. 1). The average temperature is 27.6°C and its average annual rainfall is 83.60 mm [23].



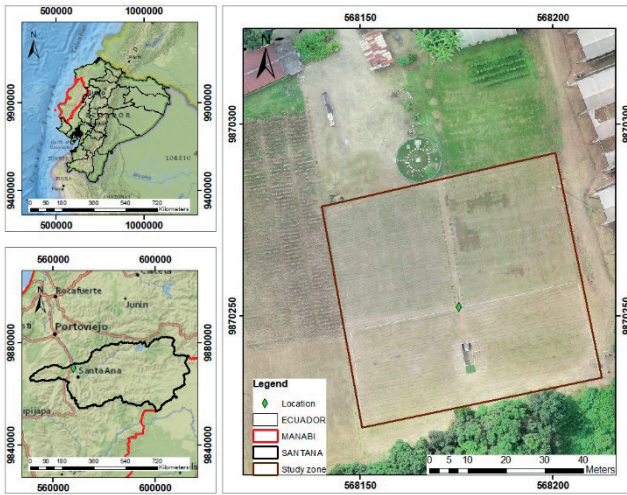


Fig 1. Location of the study area

*On-site measurements and field sampling.*

To define the sampling points systematically, a system of diagonal transects [24] was used in the study area as shown in (Fig. 2). A total of 45 sampling points were surveyed Between July 20 and 22, 2023, coinciding with the end of the drought period in the area, which were georeferenced by means of a topographic implement called RTK (Real Time Kinematics) GPS model Topcon GR-5. With the coordinates generated by the RTK, a shapefile vector file was constructed, using ArcGIS software tools. Fields with the variables pH, EC and MO were added to the attribute table of the shapefile file with the data measured in the field and laboratory.

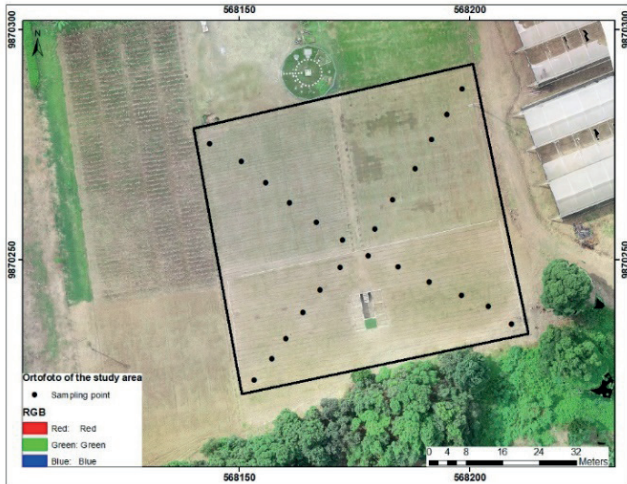


Fig. 2. Orthophoto of the area where the soil samples were obtained.

At each sampling point, the chemical parameters electrical conductivity (EC) and hydrogen potential (pH) were measured in situ using EC-pH meters [25] multiparameter sensors, which are equipment that have an automatic calibration and allow measuring pH on a scale of 0 to 14 with an accuracy of 0.01 pH units while for EC it performs it in a measurement range 0.1  $\mu$ S/cm to 200 mS/cm with an accuracy of 0.01  $\mu$ S/cm (Fig. 3).

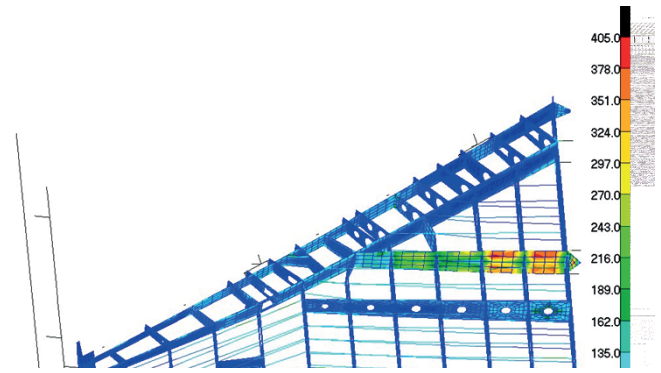


Fig. 3. On-site sampling with electrical conductivity (EC) and hydrogen potential (pH) meters.

Before the on-site measurements were made, the ground was prepared by tilling the soil, with a metal tip, to loosen the first 5 cm of the surface layer, thus facilitating the correct insertion of the sensor head. Once the sensor was inserted, it was waited for it to stabilize before proceeding to record the electrical conductivity (EC) and hydrogen potential (pH) data. Each parameter was measured in three replications and the average value obtained was recorded.

Field sampling involved the extraction of soil samples, each of approximately 500 gr, using a field drill to reach depths of 20 and 40 cm, which was mixed and homogenized to generate a composite sample at each sampling site. The samples were deposited in duly labeled sample holder sleeves, and transported to the water and soil laboratory of the Faculty of Agricultural Engineering of the Technical University of Manabí for the respective analyses.

*Laboratory tests*

The laboratory analysis consisted of the determination of soil organic matter (OM) content by means of the loss-on-ignition (LOI) or gravimetric method proposed by Schulte and Hopkins [26]. To determine OM, samples were kiln dried at 105°C for 24 hours, cooled in a desiccator and then weighed 5g of sample and placed in crucibles before being calcined at 600°C for 2h in a Lindberg/blue M muffle furnace. After combustion, the samples were cooled in a desiccator and re-weighed on an analytical balance. With these values, the percentage of OM was calculated using [1].

$$LOI = \frac{(PSS_{105^{\circ}C} - PSI_{600^{\circ}C})}{(PSS_{105^{\circ}})} * 100 \tag{1}$$

Where PSS represents the dry weight of the soil and PSI the weight after ignition.

*Aerial image processing with drone*

The aerial image capture was done with the DJI Phantom 4 Pro drone, equipped with a 20 MPX RGB camera, capable of detecting the wavelengths of the color red, green, and blue in the visible electromagnetic spectrum [13]. The flight planning was carried out using the DJI GO4 software, this software allowed to define the region of interest, the flight height was 60

m, speed 3.3m/sec, the pixel resolution was 1.5 cm/pixel, the superposition of images, as well as the strategic choice of take-off and landing points.

The RGB images obtained with the drone were subjected to an analysis process using the PIX4Dmapper photogrammetry software. This process was carried out in the Scientific Model and Calculation laboratory of the Faculty of Agricultural Engineering of the UTM, with a high-end computer.

The processing methodology encompassed the import of images and coordinates of the control points, as well as the implementation of necessary adjustments in each phase of the process. These adjustments were executed in order to ensure exhaustive control over the quality of the data obtained through image processing by means of GIS [27], this process allowed the generation of quality photogrammetric products such as orthophoto, RGB bands, digital surface and terrain models, as well as the 3D point cloud.

With the RGB spectral bands, the respective calculation of the indices shown in Table I was carried out. These have been reported in the literature as medium-power indices [28], [29] and [30], to determine chemical parameters of the soil (pH, salinity and organic matter), because they have only three bands of the electromagnetic spectrum [31].

TABLE I  
SPECTRAL INDICES TO ESTIMATE SOIL CHEMICAL PROPERTIES

| Parameter  | Index  |
|------------|--|
| pH_index   | (Red/Green)/Blue   |
| sal_index1 | $\sqrt{Blue * Red}$  |
| sal_index2 | $\sqrt{Green * Red}$   |
| sal_index3 | $\sqrt{Green^2 * Red^2}$                                     |
| sal_index4 | Blue/Red   |
| sal_index5 | (Green * Red)/Blue   |
| sal_index6 | (Blue * Red)/Green   |
| carb_index | $(-0.008 * Red) + (-0.008 * Green) + (0.008 * Blue) + 0.807$ |

#### Statistical analysis

IBM SPSS Statistics (Statistical Package for Social Sciences) statistical software tools were used to perform correlation and regression analyses, in order to model and relate the data obtained in the field and laboratory such as pH, EC, MO and spectral indices. Due to the nature of the data, Pearson's correlation was used, which varies between -1 and 1 evidenced in Table II, quantifies the strength and direction of the linear relationship between two continuous variables; it is preferred for analyses where a precise linear relationship between variables is anticipated [32].

TABLE II  
PEARSON'S CORRELATION COEFFICIENT

| Condition   | Degree of correlation    |
|-------------|--------------------------|
| 0.00 - 0.10 | Non-existent correlation |
| 0.10 - 0.29 | Weak correlation         |
| 0.30 - 0.50 | Moderate correlation     |
| 0.50 - 1.00 | Strong correlation       |

### III. RESULTS AND DISCUSSION

#### Chemical parameters of the soil

Soil chemical parameters were determined, including pH, electrical conductivity (EC), and organic matter (OM) content. According to the values in the table indicated, the classification of electrical conductivity exhibits non-saline characteristics, with average values of 1.09 dS/m, belonging to the category of soils with low concentration of dissolved salts according to the classification of [33], shown in Table III.

TABLE III  
CLASSIFICATION OF THE ELECTRICAL CONDUCTIVITY OF SOIL

| dS/m   | Classification    |
|--------|-------------------|
| < 2    | Not saline        |
| 2 a 4  | Slightly saline   |
| 4 a 8  | Moderately saline |
| 8 a 16 | Strongly saline   |
| > 16   | Extremely saline  |

Based on the soil pH classification presented in Table IV, the soil was determined to be slightly acidic, with an average value of 5.86 according to the classification of [34]. This value indicates moderate acidity, which can influence nutrient availability and soil microbial activity, which are crucial for agricultural productivity and ecosystem health [22].

TABLE IV  
CLASSIFICATION OF SOIL HYDROGEN POTENTIAL

| pH           | Classification      |
|--------------|---------------------|
| 0.00 a 4.50  | Very acid           |
| 4.50 a 5.50  | Moderately acidic   |
| 5.50 a 6.50  | Slightly acidic     |
| 6.50 a 7.50  | Neutral             |
| 7.50 a 8.50  | slightly alkaline   |
| 8.50 a 9.50  | Moderately alkaline |
| 9.50 a 14.00 | Very alkaline       |

Regarding organic matter, an average of 5.19 % of organic matter was found in the soil, considered a medium-high percentage, according to the classification shown in Table V, [35], it is beneficial due to its positive effects on soil structure, water and nutrient retention, as well as on the promotion of microbiological activity [31].

TABLE V  
PERCENTAGE OF SOIL ORGANIC MATTER

| %          | Range              |
|------------|--------------------|
| 0.00 -1.00 | Low                |
| 1.00-2.50  | Medium bass        |
| 2.50-4.00  | Half               |
| 4.00-5.50  | Medium high        |
| 5.50-7.00  | High               |
| 7.00-8.50  | Very high          |
| 8.50-10.00 | Exceptionally high |

*Aerial images and spectral indices.*

Fig. 4 shows the calculation of the spectral indices that yielded the best results. The pH\_index stands out for indicating the degree of alkalinity of the soil, while the sal\_index6 reflects the content of dissolved salts.

*Orthophoto resolution and quality*

The orthophoto acquired on July 20, 2023 at 10:30 AM presents a high quality thanks to its spatial resolution of 1.6 cm/pixel, which allows an exceptional level of detail in the repre-

sentation of the terrain. The image covers an area of 0.44 hectares, captured under optimal atmospheric conditions, with clear skies, which ensures superior clarity and sharpness in the RGB bands used. In addition, the orthophoto is fully compatible and integrated with ArcGIS software because it is generated in a GEOTIFF format, facilitating its use in GIS applications and ensuring its efficiency in geospatial analysis.

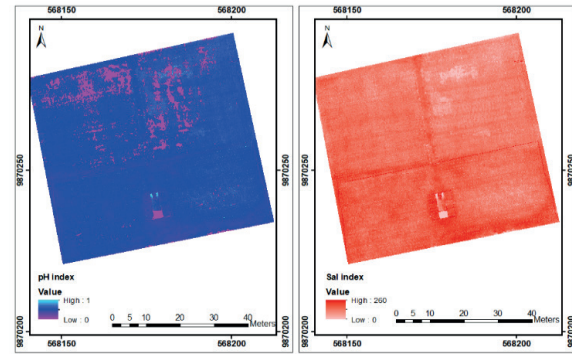


Fig. 4. Processing of aerial images and indexes

*Index statistics*

Table VI shows the soil data obtained in the field and laboratory, as well as the spectral indices calculated with the photogrammetric products.

TABLE VI  
FIELD, LABORATORY AND PHOTOGRAMMETRIC PRODUCT VALUES

| Data | CE   | pH   | MO   | Red | Green | Blue | ph_index | sal_index1 | sal_index2 | sal_index3 | sal_index4 | sal_index5 | sal_index6 | carb_index |
|------|------|------|------|-----|-------|------|----------|------------|------------|------------|------------|------------|------------|------------|
| 1    | 1.50 | 6.20 | 6.00 | 221 | 212   | 192  | 0.00521  | 205.99     | 216.45     | 46852      | -0.0702    | 244.02     | 200.15     | -1.121     |
| 2    | 1.20 | 5.70 | 4.00 | 212 | 204   | 177  | 0.00565  | 193.71     | 207.96     | 43248      | -0.0900    | 244.34     | 183.94     | -1.105     |
| 3    | 1.20 | 5.80 | 4.00 | 211 | 204   | 171  | 0.00585  | 189.95     | 207.47     | 43044      | -0.1047    | 251.72     | 176.87     | -1.145     |
| 4    | 0.90 | 5.80 | 4.00 | 196 | 192   | 150  | 0.00667  | 171.46     | 193.99     | 37632      | -0.1329    | 250.88     | 153.13     | -1.097     |
| 5    | 0.90 | 5.30 | 6.00 | 195 | 190   | 153  | 0.00654  | 172.73     | 192.48     | 37050      | -0.1207    | 242.16     | 157.03     | -1.049     |
| 6    | 1.10 | 5.40 | 6.00 | 204 | 195   | 175  | 0.00571  | 188.94     | 199.45     | 39780      | -0.0765    | 227.31     | 183.08     | -0.985     |
| 7    | 0.90 | 5.30 | 6.00 | 152 | 143   | 125  | 0.00800  | 137.84     | 147.43     | 21736      | -0.0975    | 173.89     | 132.87     | -0.553     |
| 8    | 1.00 | 5.30 | 2.00 | 204 | 195   | 175  | 0.00571  | 188.94     | 199.45     | 39780      | -0.0765    | 227.31     | 183.08     | -0.985     |
| 9    | 1.00 | 5.40 | 4.00 | 217 | 211   | 190  | 0.00526  | 203.05     | 213.98     | 45787      | -0.0663    | 240.98     | 195.40     | -1.097     |
| 10   | 1.50 | 6.30 | 6.00 | 208 | 196   | 175  | 0.00571  | 190.79     | 201.91     | 40768      | -0.0862    | 232.96     | 185.71     | -1.025     |
| 11   | 1.20 | 5.70 | 6.00 | 207 | 200   | 172  | 0.00581  | 188.69     | 203.47     | 41400      | -0.0923    | 240.70     | 178.02     | -1.073     |
| 12   | 1.30 | 5.50 | 5.49 | 189 | 182   | 151  | 0.00662  | 168.94     | 185.47     | 34398      | -0.1118    | 227.80     | 156.81     | -0.953     |
| 13   | 0.60 | 6.60 | 2.45 | 185 | 186   | 161  | 0.00000  | 172.58     | 185.50     | 34410      | -0.0694    | 213.73     | 160.13     | -0.873     |
| 14   | 1.00 | 6.40 | 5.47 | 193 | 184   | 162  | 0.00617  | 176.82     | 188.45     | 35512      | -0.0873    | 219.21     | 169.92     | -0.913     |
| 15   | 1.30 | 6.40 | 5.68 | 179 | 171   | 149  | 0.00671  | 163.31     | 174.95     | 30609      | -0.0915    | 205.43     | 155.97     | -0.801     |
| 16   | 1.10 | 6.20 | 5.25 | 183 | 178   | 152  | 0.00658  | 166.78     | 180.48     | 32574      | -0.0925    | 214.30     | 156.27     | -0.865     |
| 17   | 1.00 | 6.20 | 5.39 | 193 | 187   | 154  | 0.00649  | 172.40     | 189.98     | 36091      | -0.1124    | 234.36     | 158.94     | -1.001     |
| 18   | 0.80 | 5.50 | 5.38 | 211 | 205   | 168  | 0.00595  | 188.28     | 207.98     | 43255      | -0.1135    | 257.47     | 172.92     | -1.177     |

| Data     | CE   | pH   | MO   | Red    | Green  | Blue   | ph_index | sal_index1 | sal_index2 | sal_index3 | sal_index4 | sal_index5 | sal_index6 | carb_index |
|----------|------|------|------|--------|--------|--------|----------|------------|------------|------------|------------|------------|------------|------------|
| 19       | 1.10 | 6.00 | 5.57 | 204    | 201    | 181    | 0.00553  | 192.16     | 202.49     | 41004      | -0.0597    | 226.54     | 183.70     | -0.985     |
| 20       | 1.10 | 5.80 | 6.15 | 178    | 173    | 162    | 0.00617  | 169.81     | 175.48     | 30794      | -0.0471    | 190.09     | 166.68     | -0.705     |
| 21       | 1.30 | 5.90 | 5.69 | 187    | 187    | 168    | 0.00595  | 177.25     | 187.00     | 34969      | -0.0535    | 208.15     | 168.00     | -0.841     |
| 22       | 1.00 | 6.00 | 6.32 | 183    | 180    | 169    | 0.00592  | 175.86     | 181.49     | 32940      | -0.0398    | 194.91     | 171.82     | -0.745     |
| 23       | 1.00 | 6.00 | 6.17 | 160    | 158    | 141    | 0.00709  | 150.20     | 159.00     | 25280      | -0.0631    | 179.29     | 142.79     | -0.609     |
| 24       | 1.20 | 6.00 | 5.46 | 190    | 183    | 168    | 0.00595  | 178.66     | 186.47     | 34770      | -0.0615    | 206.96     | 174.43     | -0.833     |
| Averages | 1.09 | 5.86 | 5.19 | 194.25 | 188.21 | 164.21 | 0.01     | 178.55     | 191.20     | 36820.13   | -0.08      | 223.10     | 169.49     | -0.94      |

5. Correlation analysis and regression models

Pearson’s correlation coefficients are shown in Table VII.

TABLE VII  
CORRELATIONS

|    | Red    | Green  | Blue   | ph_index | sal_index1 | sal_index2 | sal_index3 | sal_index4 | sal_index5 | sal_index6 | carb_index |
|----|--------|--------|--------|----------|------------|------------|------------|------------|------------|------------|------------|
| CE | .303   | .227   | .354   | .305     | .342       | .267       | .271       | .135       | .118       | .421*      | -.161      |
| pH | -.369* | -.350* | -.339* | -.394    | -.051      | -.093      | -.113      | .222       | -.168      | -.027      | .151       |
| MO | -.279  | -.316  | -.199  | .545**   | -.246      | -.298      | -.293      | .122       | -.321      | -.168      | .324       |

In relation to soil organic matter (OM) content, a strong correlation was observed with the pH index (pH\_index), evidenced by a coefficient of determination  $R^2=0.55$  and RMSE 0.72 (Fig. 6). This finding suggests that pH\_index is closely related to the content of OM in the soil. The significance of the data obtained reinforces the usefulness of the pH\_index as a reliable indicator to estimate the percentage of OM in the soil. This robust correlation highlights the importance of this index in the assessment of soil fertility and health, providing a valuable tool for agricultural management.

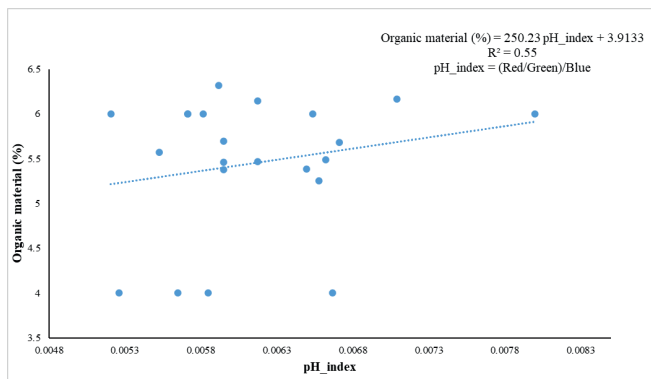


Fig. 6. Scatterplot of the correlation between WM and pH index.

Regarding pH, a moderate correlation was observed, with an  $R^2=-0.39$  and RMSE 0.35 between pH and pH index (Fig. 7). This indicates that an increase in pH is associated with a decrease in the pH index, revealing an inverse relationship that underscores the significant influence of pH on the characteristics assessed by the index.

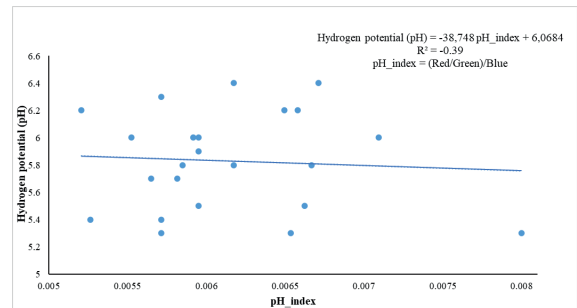


Fig. 7. Scatterplot of the correlation between pH and pH index.

In relation to electrical conductivity (EC), a moderate correlation was observed with the salinity index (sal\_index6), with a coefficient of determination  $R^2=0.42$  and RMSE 0.17 (Fig. 8). This result indicates a significant relationship between soil EC and sal\_index6, suggesting that this index may be a useful indicator for estimating the soluble salt content of soil. The moderate correlation observed highlights the relevance of this index in the evaluation of soil chemical properties.

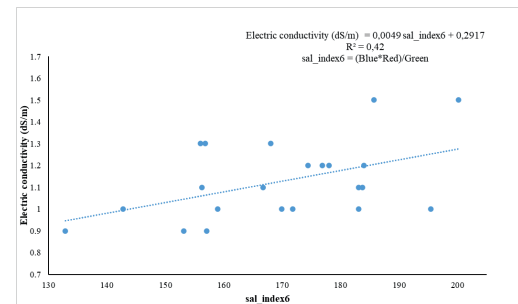


Fig. 8. Scatterplot of the correlation between electrical conductivity and sal\_index6.

The simple linear regression estimation model presents some limitations that may be related to the presence of multicollinearity or outliers. To improve the implementation of these models, it is suggested to incorporate artificial intelligence algorithms, such as artificial neural networks [36].

The implementation of RGB spectral indices for soil analysis and estimation of their chemical properties has significant advantages over the most advanced multispectral techniques. RGB sensors are much cheaper and therefore accessible to a wide audience, from small farmers to researchers with limited budgets. In addition, these sensors are often available in common devices such as smartphones and drones, making them easy to use in various agricultural and research applications [37].

The use of this technique is simpler to implement, as these sensors are easier to handle, allowing users to capture and analyze images without the need for specialized equipment. Its accessibility translates into faster processing and analysis, as RGB data is less complex to manage than multispectral data. Algorithms for processing RGB images are simpler and less demanding in terms of computational resources [38].

The images generated by these technologies are easily integrated into common photo analysis platforms and tools, avoiding the need for specialized software, although they do not provide the same spectral depth as advanced sensors, they are effective in detecting visual changes in soil and crops, in addition, these cameras are less sensitive to environmental variations such as humidity and lighting, facilitating the capture of images in various conditions without constant adjustments [39].

#### IV. CONCLUSION

The average electrical conductivity of the soil was 1.09 dS/m, indicating non-saline conditions. The soil was determined to be slightly acidic, with an average pH value of 5.86.

The organic matter presented an average of 5.19 %, which is considered within a medium-high range.

Photogrammetric flight generated a high-quality orthophoto with a resolution of 1.6 cm per pixel. Eight RGB spectral indices were calculated, of which only pH\_index showed a strong correlation with organic matter, with a coefficient of determination  $R^2=0.54$

On the other hand, the sal\_index6 and presented a moderate correlation with electrical conductivity (EC), with a coefficient of determination  $R^2=0.42$ .

Additionally, a moderate negative correlation was observed between pH and pH\_index, with an  $R^2=-0.39$ .

The rest of the indices studied showed weak relationships with respect to the chemical properties of the soil.

Three models were proposed to estimate soil chemical properties from spectral indices as useful indicators that can result in time and money savings, as well as a decrease in the environmental impacts of agricultural activities.

The results obtained confirm the potential of drone-captured RGB images as a cost-effective and accessible alternative to traditional methods of soil chemical analysis.

It is essential to validate these models in various agricultural environments to ensure their applicability and accuracy

under different agroecological conditions. This validation will extend the robustness and reliability of the proposed approach, allowing its widespread adoption in different productive areas.

#### REFERENCES

- [1] L. Toledo, R. L. Changoluisa Chiguano and O. Viteri Salazar, "Influencia de la agricultura en la economía y su contraste frente a los objetivos de desarrollo sostenible: caso Ecuador," *Revista Científica de Ciencias Sociales y Humanas*, vol. 2, no. 83, pp. 28-49, 2023. <https://doi.org/10.33324/uv.v2i83.697>
- [2] F. González Soto, D. Ullón and J. Loján, "Análisis multitemporal de cambios de uso del suelo en la isla Santa Cruz, archipiélago de las Galápagos, periodo 1991-2023," *Revista Ciencia y Tecnología*, vol. 17, no. 1, pp. 1-9, 2024. <https://doi.org/10.18779/cyt.v17i1.521>
- [3] R. Vicente Salar, M. Castelló Bueno, S. Logan de la Rosa and J. C. Padró García, "Efecto de los usos y las cubiertas del suelo y las políticas ambientales en el comportamiento de las temperaturas superficiales en campus universitarios: El caso de la Universidad Autónoma de Barcelona," *Revista Documents d'Analisi Geogràfica*, vol. 70, no. 2, pp. 261-289, 2024. <https://doi.org/10.5565/rev/dag.875>
- [4] W. Zárate Martínez, M. Felipe Victoriano, F. E. Martínez Silva, K. Moreno León, J. L., Arispe Vázquez and J. F. Díaz Nájera, "Propiedades químicas del suelo y calidad del agua en Miahuatlán de Porfirio Díaz y Ejutla de crepo, Oaxaca, México," *Revista de Ecosistemas y Recursos Agropecuarios*, vol. 11, no. 1, pp. 2-10, 2024. <https://doi.org/10.19136/era.a11n1.3948>
- [5] A. Vélez, M. Vera, S. Valdez, D. Martínez and F. Cutipa, "Methods to determine enzymatic activity in contaminated soils," *South Sustainability*, vol. 5, no. 1, pp. 1-11, 2024. <https://doi.org/10.21142/SS-0501-2024-e092>
- [6] A. Gonzales and L. Castellanos, "Impacto de diferentes prácticas agrícolas sobre las características fisicoquímicas del suelo: un análisis crítico," *Revista Ambiental Agua, Aire y Suelo*, vol. 15, no. 1, 90-105, 2024. <https://doi.org/10.24054/raaas.v15i1.2916>
- [7] R. Enesi, M. Dyck, M. Thilakarathna, S. Strelkov, and L. Gorim, "Calibrated SoilOptix estimates of soil pH and exchangeable cations in three agricultural fields in western Canada – implications for managing spatially variable soil acidity". *Journal Heliyon*, vol. 10 no. 17, pp. 1–18, 2024. <https://doi.org/10.1016/j.heliyon.2024.e37106>
- [8] S. Boubehziz, C. Piccini, M. A. Jiménez González and G. Almendros, "Distribución espacial de los descriptores de calidad del carbono orgánico del suelo que determinan los factores que afectan su secuestro en el Noreste de Argelia", *Revista de Gestión Ambiental*, vol. 358, pp. 1-10, 2024. <https://doi.org/10.1016/j.jenvman.2024.120772>
- [9] M. Krestenitis, E. Raptis, A. Kapoutsis, K. Ioannidis, E. Kosmatopoulos and S. Vrochidis, "Overcome the fear of missing out: active sensing UAV scanning for precision agriculture," *Robotics and Autonomous Systems*, pp. 1-13, 2024. <https://doi.org/10.1016/j.robot.2023.104581>
- [10] J. M. Guzmán Albores, M. de J. Matuz Cruz, J. Y. Arana Llanes, E. López Carrasco, V. Gómez Vázquez and N. González Cárdenas, "Avances y perspectivas de la agricultura de precisión para la sostenibilidad agrícola", *XIKUA Boletín Científico de La Escuela Superior de Tlahuelilpan*, vol. 12, no. 24, pp. 1-6, 2024. <https://doi.org/10.29057/xikua.v12i24.12790>
- [11] B. Petrović, R. Bumbálek, T. Zoubek, R. Kuneš, L. Smutný and P. Bartoš, "Application of precision agriculture technologies in Central Europe-review," *Journal of Agriculture and Food Research*, vol. 15, no. 1, pp. 1-10, 2024. <https://doi.org/10.1016/j.jafr.2024.101048>
- [12] L. E. Sánchez Palacios, F. R. Martínez Alcivar, S. T. Torres Sánchez, A. C. Lascano Montes and G. N. Terán Guajala, "Agricultura de Precisión en El Ecuador", *Ciencia Latina Revista Científica Multidisciplinar*, vol. 8, no. 1, pp. 1532-1542, 2024. [https://doi.org/10.37811/cl\\_rcm.v8i1.9547](https://doi.org/10.37811/cl_rcm.v8i1.9547)
- [13] R. Nitin Lilandhar, P. C. Saurabh, "Detección remota (rs), uav/drones y aprendizaje automático (ml) como potentes técnicas para la agricultura de precisión: eficaces aplicaciones en agricultura". *International Research Journal of Modernization in Engineering Technology and Science*, vol. 5, pp. 4375-4395, 2023. <https://doi.org/10.56726/irj-mets36817>

- [14] P. Vigneault, J. Lafond-Lapalme, A. Deshaies, K. Khun, S. de la Sablonnière, M. Fillion, L. Longchamps and B. Mimee, "An integrated data-driven approach to monitor and estimate plant-scale growth using UAV", *ISPRS Open Journal of Photogrammetry and Remote Sensing*, vol. 11, pp. 1-13, 2024. <https://doi.org/10.1016/j.ophoto.2023.100052>
- [15] Y. Mao *et al.*, "Rapid monitoring of tea plants under cold stress based on UAV multi-sensor data", *Computers and Electronics in Agriculture*, vol. 213, pp. 1-13, 2023. <https://doi.org/10.1016/j.compag.2023.108176>
- [16] D. Kaimaris, "Aerial Remote Sensing Archaeology—A Short Review and Applications", *Article Land*, vol. 13, no. 7, pp. 1-27, 2024. <https://doi.org/10.3390/land13070997>
- [17] M. Raj, H. N. B., S. Gupta, M. Atiqzaman, O. Rawley, and L. Goel, "Leveraging precision agriculture techniques using UAVs and emerging disruptive technologies," *Energy Nexus*, vol. 14, pp. 1-25, 2024. <https://doi.org/10.1016/j.nexus.2024.100300>
- [18] J. Tan, J. Ding, Z. Wang, L. Han, X. Wang, Y. Li, Z. Zhang, S. Meng, W. Cai, and Y. Hong, "Estimating soil salinity in mulched cotton fields using UAV-based hyperspectral remote sensing and a Seagull Optimization Algorithm-Enhanced Random Forest Model," *Computers and Electronics in Agriculture*, vol. 221, pp. 1-10, 2024. <https://doi.org/10.1016/j.compag.2024.109017>
- [19] Y. Han, "Application of Unmanned Aerial Vehicle Remote Sensing for Agricultural Monitoring", *E3S Web of Conferences*, pp. 1-6, 2024. <https://doi.org/10.1051/e3sconf/202455302022>
- [20] G. Linets, A. Bazhenov, S. Malygin, N. Grivennaya, S. Melnikov and V. Gorchakov, "Method for remote measurement of specific conductivity and moisture of subsurface soil horizons," *Smart Agricultural Technology*, vol. 8, pp. 1-9, 2024. <https://doi.org/10.1016/j.atech.2024.100503>
- [21] M. Ngabire *et al.*, "Mapeo de la salinización del suelo en diferentes tipos de cobertura terrestre arenosa en la cuenca del río Shiyang: un enfoque de teledetección y regresión lineal múltiple," *Remote Sensing Applications: Society and Environment*, vol. 28, pp. 1-18, 2024. <https://doi.org/10.1016/j.rsase.2022.100847>
- [22] O. Yuzugullu, N. Fajraoui and F. Liebis, "Soil Texture and Ph Mapping Using Remote Sensing and Support Sampling," *IEEE Journal of Selected Topics in Applied Earth Observations and Remote Sensing*, pp. 1-21, 2024. <https://doi.org/10.1109/JSTARS.2024.3422494>
- [23] INAMHI, "Datos meteorológicos de la estación La Teodomira Manabí, Santa Ana," *Inst. Nac. de Meteorología e Hidrología, Manabí, Ecuador*, Rep. 2023.
- [24] S. Schweizer Lassaga, "Muestreo y análisis de suelos para diagnóstico de fertilidad," 1ª ed. Reading, MA: M. Mesén Villalobos and L. Ramírez Cartín, 2011. <https://www.mag.go.cr/bibliotecavirtual/P33-9965.pdf>
- [25] Eijkelkamp, "EC-pH meters", 2024. [www.eijkelkamp.com](http://www.eijkelkamp.com).
- [26] S. Barrezueta Undas, A. Cervantes Alava, M. Ullauri Espinoza, J. Barrera Leon, and A. Condoy Gorotiza, "Evaluación del método de ignición para determinar materia orgánica en suelos de la provincia el Oro-Ecuador", *FAVE Sección Ciencias Agrarias*, vol. 19, no. 2, pp. 25-36, 2020. <https://doi.org/10.14409/fa.v19i2.9747>
- [27] L. M. Dos Santos-Tonial, M. Schimit Colla, J. Bassetto Carra, M. Fabris and V. Aparecido de Lima, "Classification and total carbon determination of the soils using RGB digital images combined with machine learning", *Communications in Soil Science and Plant Analysis*, vol. 54, no. 2, pp. 1-13, 2023. <https://doi.org/10.1080/00103624.2022.2110891>
- [28] R. Shrestha Prasad, S. Qasim and S. Bachri, "Investigating remote sensing properties for soil salinity mapping: A case study in Korat province of Thailand," *Environmental Challenges*, vol. 5, pp. 1-10, 2021. <https://doi.org/10.1016/j.envc.2021.100290>
- [29] Y. K. Sonn *et al.*, "Development of models to estimate total soil carbon across different croplands at a regional scale using RGB photography", *International Journal of Environmental Research and Public Health*, vol. 19, no. 15, pp. 2-11, 2022. <https://doi.org/10.3390/ijerph19159344>
- [30] V. Kumar, B. Kumar Vimal, R. Kumar, M. Kumar and K. Vigyan Kendra, Determination of soil pH by using digital image processing technique. *Journal of Applied and Natural Science*, vol. 6, no. 1, pp. 14-18, 2014. <https://doi.org/10.31018/jans.v6i1.368>
- [31] S. Yeon Kyu *et al.*, Development of Models to Estimate Total Soil Carbon across Different Croplands at a Regional Scale Using RGB Photography. *International Journal of Environmental Research and Public Health*, vol. 19, no. 15, pp. 2-11, 2022. <https://doi.org/10.3390/ijerph19159344>
- [32] M. F. Ikhwan, W. Mansor, Z. I. Khan, M. K. A. Mahmood, A. Bujiang, and K. Haddadi, "Pearson Correlation and Multiple Correlation Analyses of the Animal Fat S Parameter", *TEM Journal*, vol. 13 no. 1, pp. 155-160, 2024, <https://doi.org/10.18421/TEM131-15>
- [33] C. Omuto, R. Vargas, K. Viatkin and Y. Yigini, "Mapeo de suelos afectados por salinidad", *Modelo espacial de suelos afectados por salinidad*, 2021, <http://www.wipo.int/amc/en/mediation/rules>
- [34] D. Ibarra Castillo, J. A. Ruiz Corral, D. R. González Eguiarte, J. G. Flores Garnica and G. Díaz Padilla, "Distribución espacial del pH de los suelos agrícolas de Zapopan, Jalisco, México", *Agricultura Técnica En México*, vol. 35, no. 3, pp. 267-276, 2009.
- [35] N. C. Arzola Pina and J. Machado de Armas, "Soil aptitude for the production of sugarcane. Part I. Calibration in experimental and production conditions," *Centro Agrícola*, vol. 42, no. 2, pp. 33-38, 2015. [http://ca-gricola.uclv.edu.cu/descargas/pdf/V42-Numero\\_2/cag05215.pdf](http://ca-gricola.uclv.edu.cu/descargas/pdf/V42-Numero_2/cag05215.pdf)
- [36] G. Mesías Ruiz, J. Peña, A. Castro, I. Borra Serrano and J. Dorado, "Detección y clasificación de malas hierbas mediante drones y redes neuronales profundas: creación de mapas para tratamiento localizado Weed detection and classification using UAVs and deep neural networks: mapping for localized treatment," *Revista de Ciencias Agrarias*, vol. 47, no. 1, pp. 175-179, 2024, <https://doi.org/10.19084/rca.34973>
- [37] L. Biró, V. Kozma-Bognár and J. Berke, "Comparison of RGB Indices used for Vegetation Studies based on Structured Similarity Index (SSIM)," *Journal of Plant Science and Phytopathology*, vol. 8, no. 1, pp. 007-012, 2024, <https://doi.org/10.29328/journal.jpssp.1001124>
- [38] A. Dwi Priyo, R. Isnain Rachmanto, Mujiyo and Komariah, "The accuracy of soil moisture prediction using an RGB camera on maize and peanut plantation", *E3S Web of Conferences*, pp. 1-6, 2023. <https://doi.org/10.1051/e3sconf/202346701031>
- [39] F. J. Diaz, A. Ahmad, L. Parra, S. Sendra and J. Lloret, "Low-Cost Optical Sensors for Soil Composition Monitoring", *Sensors*, vol. 24, no. 4, pp. 1-20, 2024. <https://doi.org/10.3390/s24041140>

# Effect of cutting age on the productive indicators and nutritional quality of *Brachiaria hybrid* vs. Mulato I

Jonathan B. López-Bósquez<sup>1</sup>, Juan P. Salazar-Arias<sup>1</sup>, Danis M. Verdecia-Acosta<sup>2\*</sup>, Luis G. Hernández-Montiel<sup>3</sup>, Edilberto Chacón-Marcheco<sup>1</sup>, Jorge L. Ramírez-de la Ribera<sup>2</sup>

**Abstract** — with the objective of determining the productive components, chemical characterization, digestibility and energy contribution of the *Brachiaria hybrid* vs Mulato I at different ages of cuts in both periods of the year. For which a randomized block design with four repetitions was used. It was sampled in plots of 25 m<sup>2</sup>, to which a uniformity cut was applied 10 cm from the ground, without irrigation or fertilization. The yield of total dry matter, leaves and stems was determined; the length and width of the leaves; the leaf-stem ratio, chemical composition (CP, NDF, ADF, ADL, CC, Si, P, Ca, ash and OM), energy contributions and digestibility. A double classification analysis of variance was applied to each variable studied and the means were compared according to Duncan. Crude protein decreased with age for both periods, showing significant differences between all ages. The best values were shown at 30 days of cut (9.47 and 10.40 % in the rainy and dry periods respectively), the fiber increased with age with its best values at 75 days with (71.39 and 70.11 % in the rainy periods and little rain), aspects that conditioned the quality with a decrease in digestibility and energy intake. The yield of the plant was affected by the periods of the year, being higher in the rainy period. It is concluded that the increase in regrowth age directly influences the depression of nutritional quality and yield in both periods of the year.

**Keywords:** chemical composition, energy, digestibility, protein, performance

**Resumen** — Con el objetivo de determinar los componentes productivos, caracterización química, digestibilidad y aporte energético del *Brachiaria híbrido* vs Mulato I a diferentes edades de corte en ambas épocas del año. Para lo cual se utilizó un diseño de bloques al azar con cuatro repeticiones. Se muestreó en parcelas de 25 m<sup>2</sup>, a las cuales se les aplicó un corte de uniformidad a 10 cm

del suelo, sin riego ni fertilización. Se determinó el rendimiento de materia seca total, hojas y tallos; el largo y ancho de las hojas; la relación hoja-tallo, composición química (PB, FDN, FDA, LAD, CC, Si, P, Ca, cenizas y MO), aportes energéticos y digestibilidad. Se aplicó un análisis de varianza de clasificación doble a cada variable estudiada y se compararon las medias según Duncan. La proteína cruda disminuyó con la edad para ambos períodos, mostrando diferencias significativas entre todas las edades. Los mejores valores se presentaron a los 30 días de corte (9,47 y 10,40 % en los períodos lluvioso y poco lluvioso respectivamente), la fibra se incrementó con la edad con sus mejores valores a los 75 días con (71,39 y 70,11 % en los períodos lluvioso y poco lluvioso), aspectos que condicionaron la calidad con una disminución en la digestibilidad y el aporte energético. El rendimiento de la planta se vio afectado por los períodos del año, siendo mayor en el período lluvioso. Se concluye que el aumento de la edad de rebrote influye directamente en la disminución de la calidad nutricional en ambos períodos del año.

**Palabras clave:** composición química, energía, digestibilidad, proteína, rendimiento

## I. INTRODUCTION

AMONG the resources and alternative sources available to producers for livestock feeding in Cuba and other developing countries, grasses and forages are fundamental. These resources account for approximately 70 % of the energy needs and 65 % of the protein requirements for cattle production. However, the productivity of these resources varies significantly across different ecosystems, influenced by factors such as soil and climatic conditions, animal load, irrigation availability, and the specific varieties of grasses used [1].

In tropical countries where grain and cereal production falls short of desired levels, developing livestock supplementation strategies using locally available resources is essential. This approach is a cornerstone of effective livestock programs and is crucial for achieving greater independence and competitiveness in the sector [2].

In Cuba, the production of milk, meat, and their derivatives must primarily rely on livestock management practices that optimize production while utilizing pastures and forages. This strategy is ground in the economics of these products, which do not compete with food needs for direct human consumption, and it leverages the potential of unsuitable, unproductive, or marginal lands for livestock grazing. Given the current economic challenges, the ongoing deterioration of the environment, and

1. The current investigation was carried out as a result of the financing project: Nutritional Evaluation of grasses for the Purpose of Feeding Ruminants. Financing: CITMA Funds.

\*Corresponding author: [dverdeciaacosta@gmail.com](mailto:dverdeciaacosta@gmail.com)

1. Universidad Técnica de Cotopaxi, Ecuador. Email: [jonathan.lopez9292@utc.edu.ec](mailto:jonathan.lopez9292@utc.edu.ec), ORCID: <https://orcid.org/0000-0002-6146-9748>. Email: [juan.salazar0@utc.edu.ec](mailto:juan.salazar0@utc.edu.ec), ORCID: <https://orcid.org/0000-0002-1609-0085>. Email: [edilberto.chacon@utc.edu.ec](mailto:edilberto.chacon@utc.edu.ec), ORCID: <https://orcid.org/0000-0001-9590-6451>.

2. Universidad de Granma, Cuba. Email: [dverdeciaacosta@gmail.com](mailto:dverdeciaacosta@gmail.com), ORCID: <https://orcid.org/0000-0002-4505-4438>. Email: [jramirezrivera1971@gmail.com](mailto:jramirezrivera1971@gmail.com), ORCID: <https://orcid.org/0000-0002-0956-0245>.

3. Centro de Investigaciones Biológicas del Noroeste, Baja California Sur, México. Email: [lhernandez@cibnor.mx](mailto:lhernandez@cibnor.mx), ORCID: <https://orcid.org/0000-0002-8236-1074>.

Manuscript Received: 20/03/2024

Revised: 25/05/2024

Accepted: 28/08/2024

DOI: <https://doi.org/10.29019/enfoqueute.1043>

the limited feasibility of continuing high-input livestock operations, relying on pastures and forages emerges as the most viable option for livestock feeding, maximizing their potential [3].

One of the primary limiting factors for animal production in the tropical regions of Latin America is the limited availability and poor quality of forage. Consequently, grasslands are predominantly composed of naturalized species. This inadequate nutritional level significantly contributes to the low productivity of tropical livestock, particularly in areas characterized by low natural soil fertility and seasonal droughts. To address this challenge, it is essential to introduce adapted species with high potential for improved forage quality and availability [4].

In this context, Silva-Cardoso, et al. [5], reported that the introduction of grasses and forages is one of the oldest methods of genetic improvement in crops. Today, this approach enables countries lacking adequate infrastructure for genetic enhancement to incorporate more productive varieties into their commercial varietal structures. However, it is essential to identify species with the highest potential for success in the specific environments where the crops are intended to be introduced, necessitating prior research.

Therefore, the objective of this work was to determine the effect of cutting age on the productive components, chemical characterization, digestibility and energy contribution of the *Brachiaria hybrid* vs Mulato I under current climatic conditions.

## II. METHODS

### A. Research area, climate, and soil

The experiment was conducted in areas belonging to the Teaching-Productive Department of the University of Granma, located in the southeastern region of Cuba's Granma Province, approximately 17.5 km from the city of Bayamo. The study spanned a two-year period from 2020 to 2021 and considered two distinct seasons: the rainy season (May to October) and the dry season (November to April).

The soil in the study area was classified as a calcic haptucept [6], with a pH of 6.4. The levels of phosphorus pentoxide ( $P_2O_5$ ), potassium oxide ( $K_2O$ ), and total nitrogen (N) were 2.6, 37.5, and 34 mg.100g<sup>-1</sup> of soil, respectively, with an organic matter content of 3.4 %.

During the rainy season, precipitation reached 712.8 mm. The average, minimum, and maximum temperatures recorded were 27.33 °C, 22.67 °C, and 35.44 °C, respectively, with relative humidity values of 80.04 %, 50.86 %, and 94.33 % for the average, minimum, and maximum, respectively. In the drier period, rainfall totaled 265 mm, with average, minimum, and maximum temperatures of 25.12 °C, 19.38 °C, and 32.65 °C, respectively. The relative humidity ranged from an average minimum of 44.03 % to an average maximum of 95.31 %.

### B. Treatment and experimental design

The experiment employed a randomized block design, with treatments consisting of four different cutting ages (30, 45, 60, and 75 days) and four replications.

### C. Experiment management

The experimental plots measured 25 m<sup>2</sup> (5x5 m) and were planted in February 2020, with a spacing of 50 cm between rows and 20 cm between plants. The plants underwent an establishment period until July 2020, when a uniformity cut was performed. Thereafter, sampling was conducted at 30, 45, 60, and 75 days after cutting, with a 50 cm edge effect eliminated. All harvestable material was cut 10 cm above ground level. The following parameters were evaluated: total dry matter yield, leaf and stem yields, leaf length and width, and leaf-to-stem ratio [7]. For each treatment and replicate, two kilograms of samples were collected for subsequent laboratory analysis. No fertilization, irrigation, or chemical weed control measures were applied. At the start of the experiment, the plant population in the plots was 97 %.

### D. Determination of chemical composition, digestibility and energy

After collection, the samples were dried in a forced-air circulation oven at 65 °C, ground to a particle size of 1 mm, and stored in amber bottles until laboratory analysis. The following parameters were determined: dry matter (DM), crude protein (CP), ash, organic matter (OM), phosphorus (P), and calcium (Ca) according to AOAC [8]; neutral detergent fiber (NDF), acid detergent fiber (ADF), acid detergent lignin (ADL), cellulose (Cel), hemicellulose (Hcel), and cell contents (CC) according to Goering and Van Soest, [9]; Dry matter digestibility was quantified using Aumont, et al. [10] and metabolizable and net lactation energy were established according to Cáceres and González, [11]. All analyses were performed in duplicate and by replication.

### E: Statistical analysis

An analysis of variance was performed according to the experimental design and the mean values were compared using Duncan's Multiple Range and Multiple F Tests, [12] after verifying the normality of the data with the Kolmogorov-Smirnov test [13] and the homogeneity of the variance with the Bartlett test [14].

## III. RESULTS

The dry matter yield of the *Brachiaria hybrid* variety Mulato I increases with cutting age, demonstrating significant differences at  $p < 0.05$ . The highest yields were observed at 75 days, measuring 6.84 t DM ha<sup>-1</sup> cut during the rainy season and 3.69 t.DM.ha<sup>-1</sup>.cut<sup>-1</sup> during the less rainy season. Conversely, the lowest yields were recorded at 30 days, with values of 1.69 t.DM.ha<sup>-1</sup>.cut<sup>-1</sup> in the rainy season and 1.51 t.DM ha<sup>-1</sup>.cut<sup>-1</sup> in the less rainy season (Fig. 1)



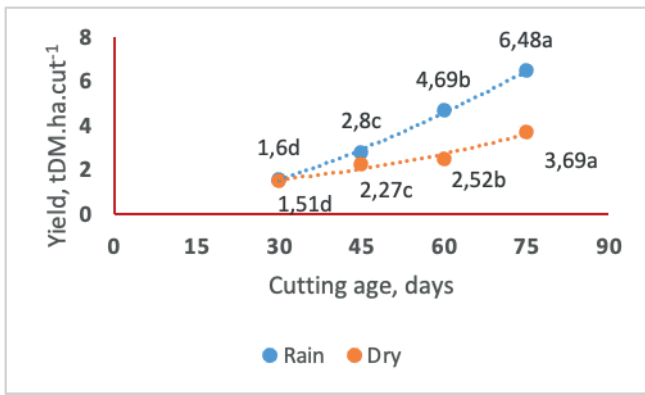


Fig. 1. Performance of the *Brachiaria hybrid* vc Mulato I in the two seasons of the year

As shown in figures 2 and 3, the dry matter yield of both leaves and stems increases with cutting age, exhibiting significant differences at  $p < 0.05$  during both periods of the year. The highest yields were recorders at 75 days, with values of 3.1 t.DM.ha<sup>-1</sup>.cut<sup>-1</sup> for leaves and 1.92 t.DM.ha<sup>-1</sup>.cut<sup>-1</sup> for stems, during the rainy season 3.7 t.DM.ha<sup>-1</sup>.cut<sup>-1</sup> for leaves and 1.17 t.DM.ha<sup>-1</sup>.cut<sup>-1</sup> for stems during the dry season.

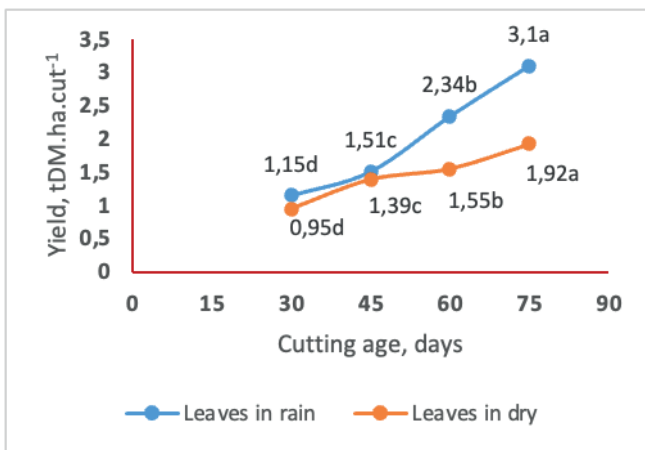


Fig. 3. Yield of stems of the *Brachiaria hybrid* vc Mulato I during the two seasons of the year

TABLE I  
LENGTH AND WIDTH OF THE LEAVES AND LEAF-TO-STEM RATIO OF THE *BRACHIARIA HYBRID* VC MULATO IN THE TWO SEASONS OF THE YEAR

| Age, days | Length and width of the leaves, cm |                   |                    |                   | Leaf-to-stem ratio, % |                    |                    |                    |
|-----------|------------------------------------|-------------------|--------------------|-------------------|-----------------------|--------------------|--------------------|--------------------|
|           | Rain                               |                   | Dry                |                   | Rain                  |                    | Dry                |                    |
|           | Length                             | width             | Length             | width             | Leaves                | Stems              | Leaves             | Stems              |
| 30        | 20.60 <sup>a</sup>                 | 1.55 <sup>a</sup> | 13.00 <sup>a</sup> | 0.90 <sup>a</sup> | 68.13 <sup>a</sup>    | 31.87 <sup>a</sup> | 70.52 <sup>a</sup> | 29.48 <sup>a</sup> |
| 45        | 25.90 <sup>a</sup>                 | 1.78 <sup>a</sup> | 15.83 <sup>b</sup> | 1.23 <sup>b</sup> | 53.71 <sup>b</sup>    | 46.29 <sup>b</sup> | 61.20 <sup>b</sup> | 38.80 <sup>b</sup> |
| 60        | 32.90 <sup>b</sup>                 | 1.93 <sup>a</sup> | 20.00 <sup>c</sup> | 1.55 <sup>c</sup> | 49.07 <sup>c</sup>    | 48.31 <sup>c</sup> | 60.03 <sup>c</sup> | 37.00 <sup>c</sup> |
| 75        | 47.80 <sup>c</sup>                 | 2.68 <sup>b</sup> | 29.00 <sup>d</sup> | 1.90 <sup>d</sup> | 43.20 <sup>d</sup>    | 50.05 <sup>d</sup> | 50.30 <sup>d</sup> | 40.00 <sup>d</sup> |
| SE±       | 3.009                              | 0.122             | 1.570              | 0.096             | 2.379                 | 1.859              | 1.889              | 1.064              |
| P         | 0.02                               | 0.03              | 0.01               | 0.001             | 0.001                 | 0.001              | 0.001              | 0.001              |

abcd Values with different letters differ at  $P < 0.05$  [12]

Fig. 2. Yield of leaves of the *Brachiaria hybrid* vc Mulato I during the two seasons of the year

As shown in Table 1, both the length and width of the leaves increase with the age of regrowth, with significant differences observed between some cutting ages. The highest values were recorders at 75 days, measuring 47.80 cm in length and 2.68 cm in width during the rainy season, and 29.00 cm in length and 1.90 cm in width during the dry season.

The leaf-stem proportion decreased with the age of the grass, showing significant differences for  $p < 0.05$  (Table 1), among all ages in the study. The proportion of leaves decrease with age, with the highest values observed at 30 days and the lowest at 75 days. During this period, the decrease was 36.59 % in the rainy season and 28.67 % in the dry season. In contrast, the proportion of stems increased, showing rises of 36.32% in the rainy season and 26.3 % in the dry season.

As shown in Table 3, during the rainy season, the chemical composition of the grass exhibits the following changes, cell wall components increase with cutting age, with values at 75 days exceeding those at other ages (71.39 %), ADF (33.29 %), ADL (3.23 %), and silica (5.32 %). Crude protein (CP) and cell contents (CC) decrease with age, with the highest values recorded at 30 days (9.47 % and 36.28 %, respectively). Minerals, ash, and organic matter show fluctuations in their behavior across cutting ages.

During the dry season (Table 3), a similar trend was observe, albeit with different numerical values. The highest values were recorders at 30 days, with crude protein (CP) at 10.40 %, cell contents (CC) at 35.38 %, and organic matter (OM) at 88.84 %. These components decrease with age. In contrast, the structural components NDF, ADF, ADL, silica (Si), calcium (Ca), and ash increase with maturity, reaching their highest percentages at 75 days, with values of 70.11 %, 30.15 %, 3.43 %, 8.09 %, 0.45 %, and 13.04 %, respectively.

TABLE II  
CHEMICAL COMPOSITION OF *BRACHIARIA HYBRID* VC. MULATO I RAINY SEASON

| Age, days | Chemical composition, % |                    |                    |                   |                    |                   |                   |                     |                    |                    |
|-----------|-------------------------|--------------------|--------------------|-------------------|--------------------|-------------------|-------------------|---------------------|--------------------|--------------------|
|           | CP                      | NDF                | ADF                | ADL               | CC                 | Si                | Ca                | P                   | Ash                | OM                 |
| 30        | 9.47 <sup>a</sup>       | 63.72 <sup>d</sup> | 26.99 <sup>c</sup> | 0.99 <sup>d</sup> | 36.28 <sup>a</sup> | 3.66 <sup>d</sup> | 0.53 <sup>b</sup> | 0.015 <sup>a</sup>  | 12.65 <sup>c</sup> | 87.35 <sup>a</sup> |
| 45        | 8.34 <sup>b</sup>       | 67.29 <sup>c</sup> | 31.13 <sup>b</sup> | 1.47 <sup>c</sup> | 32.71 <sup>b</sup> | 3.99 <sup>c</sup> | 0.62 <sup>a</sup> | 0.014 <sup>a</sup>  | 16.29 <sup>a</sup> | 83.71 <sup>b</sup> |
| 60        | 7.32 <sup>c</sup>       | 69.10 <sup>b</sup> | 32.00 <sup>a</sup> | 2.08 <sup>b</sup> | 30.90 <sup>c</sup> | 4.65 <sup>b</sup> | 0.42 <sup>c</sup> | 0.012 <sup>ab</sup> | 11.62 <sup>d</sup> | 87.38 <sup>a</sup> |
| 75        | 6.39 <sup>d</sup>       | 71.39 <sup>a</sup> | 33.29 <sup>a</sup> | 3.23 <sup>a</sup> | 28.61 <sup>d</sup> | 5.32 <sup>a</sup> | 0.53 <sup>b</sup> | 0.017 <sup>b</sup>  | 13.76 <sup>b</sup> | 86.24 <sup>a</sup> |
| SE±       | 0.345                   | 0.794              | 1.635              | 0.776             | 0.884              | 0.332             | 0.005             | 0.001               | 0.543              | 1.523              |
| P         | 0.0001                  | 0.0001             | 0.001              | 0.0001            | 0.0001             | 0.0001            | 0.01              | 0.001               | 0.0001             | 0.01               |

<sup>abcd</sup> Values with different letters differ at P<0,05 [12]

TABLE III  
CHEMICAL COMPOSITION OF *BRACHIARIA HYBRID* VC. MULATO I DRY SEASON

| Age, days | Chemical composition, % |                    |                    |                   |                    |                   |                   |                     |                    |                    |
|-----------|-------------------------|--------------------|--------------------|-------------------|--------------------|-------------------|-------------------|---------------------|--------------------|--------------------|
|           | CP                      | NDF                | ADF                | ADL               | CC                 | Si                | Ca                | P                   | Ash                | OM                 |
| 30        | 10.40 <sup>a</sup>      | 61.62 <sup>d</sup> | 26.07 <sup>b</sup> | 0.99 <sup>d</sup> | 38.38 <sup>a</sup> | 4.33 <sup>d</sup> | 0.28 <sup>c</sup> | 0.014 <sup>c</sup>  | 11.16 <sup>d</sup> | 88.84 <sup>a</sup> |
| 45        | 9.83 <sup>b</sup>       | 65.15 <sup>c</sup> | 27.26 <sup>b</sup> | 1.11 <sup>c</sup> | 34.85 <sup>b</sup> | 4.66 <sup>c</sup> | 0.38 <sup>b</sup> | 0.017 <sup>a</sup>  | 12.97 <sup>c</sup> | 87.03 <sup>b</sup> |
| 60        | 7.17 <sup>c</sup>       | 67.58 <sup>b</sup> | 29.32 <sup>a</sup> | 2.08 <sup>b</sup> | 32.42 <sup>c</sup> | 5.99 <sup>b</sup> | 0.41 <sup>b</sup> | 0.016 <sup>ab</sup> | 13.32 <sup>b</sup> | 86.68 <sup>c</sup> |
| 75        | 6.33 <sup>d</sup>       | 70.11 <sup>a</sup> | 30.15 <sup>a</sup> | 3.43 <sup>a</sup> | 29.89 <sup>d</sup> | 8.09 <sup>a</sup> | 0.45 <sup>a</sup> | 0.015 <sup>bc</sup> | 13.54 <sup>a</sup> | 86.46 <sup>c</sup> |
| SE±       | 0.432                   | 0.612              | 1.543              | 0.711             | 0.664              | 0.321             | 0.003             | 0.005               | 0.212              | 1.432              |
| P         | 0.0001                  | 0.0001             | 0.01               | 0.0001            | 0.0001             | 0.0001            | 0.01              | 0.01                | 0.0001             | 0.001              |

<sup>abcd</sup> Values with different letters differ at P<0,05 [12]

Tables 4 and 5 show that during both the rainy and dry seasons, the energy contribution and digestibility indicators of the forage decreased with increasing cutting age. During the rainy season, dry matter digestibility (DMD), organic matter digestibility (OMD), metabolizable energy (ME), net lactation energy (NLE), and net energy for fattening (NEF) decrease by 10.68 %, 11.03 %, 1.66 MJ.kg<sup>-1</sup> DM, 1.12 MJ.kg<sup>-1</sup> DM, and 0.82 MJ.kg<sup>-1</sup> DM. Although the trend was similar during the dry season, the magnitude of the decreases was lower, with DMD, OMD, ME, NLE, and NEF declining by 3.98 %, 2.75 %, 1.09 MJ.kg<sup>-1</sup> DM, 0.68 MJ.kg<sup>-1</sup> DM, and 0.36 MJ.kg<sup>-1</sup> DM, respectively.

TABLE IV  
QUALITY OF *BRACHIARIA HYBRID* VC. MULATO I RAINY SEASON

| Age, days | %                  |                    |                    | MJ.kg <sup>-1</sup> DM |                   |  |
|-----------|--------------------|--------------------|--------------------|------------------------|-------------------|--|
|           | DMD                | OMD                | ME                 | NLE                    | NEF               |  |
| 30        | 58.25 <sup>a</sup> | 60.06 <sup>a</sup> | 8.78 <sup>a</sup>  | 4.96 <sup>a</sup>      | 4.47 <sup>a</sup> |  |
| 45        | 55.93 <sup>b</sup> | 57.29 <sup>a</sup> | 8.04 <sup>ab</sup> | 4.56 <sup>ab</sup>     | 4.25 <sup>a</sup> |  |
| 60        | 54.12 <sup>c</sup> | 55.97 <sup>b</sup> | 7.86 <sup>b</sup>  | 4.19 <sup>b</sup>      | 4.06 <sup>b</sup> |  |
| 75        | 47.57 <sup>d</sup> | 49.03 <sup>c</sup> | 7.12 <sup>c</sup>  | 3.84 <sup>c</sup>      | 3.65 <sup>c</sup> |  |
| SE±       | 1.022              | 0.841              | 0.023              | 0.033                  | 0.032             |  |
| P         | 0.0001             | 0.001              | 0.001              | 0.001                  | 0.001             |  |

<sup>abcd</sup> Values with different letters differ at P<0,05 [12]

TABLE V  
QUALITY OF *BRACHIARIA HYBRID* VC. MULATO I DRY SEASON

| Age, days | %                  |                    | MJ.kg <sup>-1</sup> DM |                    |                   |
|-----------|--------------------|--------------------|------------------------|--------------------|-------------------|
|           | DMD                | OMD                | ME                     | NLE                | NEF               |
| 30        | 57.42 <sup>a</sup> | 58.05 <sup>a</sup> | 8.45 <sup>a</sup>      | 4.93 <sup>a</sup>  | 4.42 <sup>a</sup> |
| 45        | 56.86 <sup>b</sup> | 56.76 <sup>b</sup> | 7.86 <sup>b</sup>      | 4.48 <sup>ab</sup> | 4.13 <sup>a</sup> |
| 60        | 51.12 <sup>c</sup> | 53.68 <sup>b</sup> | 7.04 <sup>c</sup>      | 4.05 <sup>b</sup>  | 3.99 <sup>b</sup> |
| 75        | 53.44 <sup>d</sup> | 55.30 <sup>d</sup> | 7.36 <sup>d</sup>      | 4.25 <sup>c</sup>  | 4.06 <sup>c</sup> |
| SE±       | 1.734              | 1.964              | 0.044                  | 0.036              | 0.041             |
| P         | 0.0001             | 0.0001             | 0.0001                 | 0.001              | 0.001             |

<sup>abcd</sup> Values with different letters differ at P<0,05 [12]

If we consider the potential productive improvements that can be achieved using this species in livestock systems in tropical regions, employing it in monoculture or silvopastoral systems could yield significant benefits. The expected investment for implementing these practices ranges from \$844 to \$1110, depending on production volumes and nutrient contributions. If the species is utilized at an average age of 60 days, production rates could increase by 15-30 %, resulting in outputs of 3329 to 3,764 liters per cow per day. Consequently, income could fluctuate between \$6742.51 and \$7623.73. These benefits are particularly relevant for small and medium-sized producers, who

account for more than 60 % of the region's livestock. The improvements could also translate into enhanced public services, such as health, education, housing, roads, and communication. To ensure the sustainability of these results, it is essential to design innovative seed production and marketing schemes that provide the livestock sector with an adequate supply in terms of volume, quality, and price

#### IV. DISCUSSION

Globally, livestock farming is one of the primary sources of greenhouse gas emissions, contributing to temperature increases of 1-6 °C in tropical regions. This rise in temperature is expected to enhance evaporation per unit area, leading to alterations in the natural water balance of plants, including grassland species [15]. These effects can be particularly detrimental in areas dominated by dry land farming, where rising temperatures may be accompanied by either decrease or excessive precipitation, directly influencing the productive response of forage species [16].

In a study evaluating two cutting heights (0.4 and 0.5 m) and four levels of nitrogen fertilization (0, 50, 100, and 150 kg.ha<sup>-1</sup>) in *Brachiaria hybrid* variety Mulato II, Marques, et al. [17] reported positive responses in biomass production and dry matter yield, with values of 6.61 t.ha<sup>-1</sup> and 1.14 t.ha<sup>-1</sup>, respectively, under average temperatures of 23.2 °C and total precipitation of 1,759.9 mm. Similarly, Faria, et al. [16] under comparable conditions with *B. decumbens* and *B. ruziziensis*, reported yields of 1.12 t.ha<sup>-1</sup> and 1.6 t.ha<sup>-1</sup>, respectively. These responses highlight that nitrogen fertilization has an immediate and significant impact on the structural characteristics of forage, thereby enhancing productivity.

While, Ramírez, et al. [18] evaluate *Brachiaria decumbens* variety Basilisk in the Cauto Valley, eastern Cuba, during the rainy season (average temperature of 24.3 °C and 130 mm of rain) and the dry season (27.2 °C and 759 mm of rain). They report dry matter yields of 6.06 t.ha<sup>-1</sup> and 1.83 t.ha<sup>-1</sup>, respectively, noting a 43 % decrease in the number of leaves between the two periods. This variation was associated with the influence of climatic factors on productive and morphological indicators (Fig. 1 and 2). It is important to note that the differences in leaf and stem content throughout the year serve as indicators for establishing yield composition. A higher proportion of leaves suggests an increase likelihood of enhancing the photosynthetic process, greater potential for growth substance production, and improved reserve accumulation for regrowth.

Cruz-López, et al. [19] and Tamele, et al. [20] studies the interaction between plant height and climatic season, reporting a negative linear relationship between the two factors. During the summer (350 mm rainfall, 23 °C) and winter (30 mm, 18 °C), leaf appearance increased with plant height. However, leaf and stem growth was negatively affected in winter, as evidenced by R<sup>2</sup> values of -0.88 and -0.84, respectively. In contrast, summer saw increases in plant height for both leaves and stems, with R<sup>2</sup> values of 0.94 and 0.92. *Brachiaria* grass pastures are characterized by higher stem and leaf elongation rates and lower leaf emergence rates, particularly in the upper strata. Grasses exhibit significant variability in their tolerance

to water deficit stress. In some cases, they undergo adaptations or escape mechanisms to mitigate the negative effects of stress. *Brachiaria* species are known for producing numerous decumbent stems that generate tillers under optimal moisture conditions, leading to increased leaf and stem production during summer [21].

Changes in morphological composition are influenced by edaphic and climatic conditions, which can either enhance or inhibit the growth of leaves and stems, as well as alter their proportions. These aspects are evident in the results presented in Table 1. Ortega-Aguirre, et al. [22] and Cruz-Hernández, et al. [23] found that leaf emergence increases when temperatures range from 20 to 32.5 °C but decreases when temperatures exceed 35 °C. During the dry season, changes in growth may have been inhibited by low temperatures, while water stress further limited growth. This suggests that plant age plays a crucial role in determining the distribution of dry matter among morphological components.

The proportion of leaves in harvest forage decreases as the interval between harvests increases, primarily due to enhanced stem growth when environmental conditions are favorable for plant development, such as during the rainy season. Therefore, the management of defoliation in a pasture significantly influences growth rate, production, botanical composition, quality, and persistence [24]. This indicates that it is essential to consider not only forage yield but also the leaf-to-stem ratio, which can help explain the behavior of the morphological indicators studied here.

The observed variations in crude protein (CP) and cell contents (CC) were 1.08 % and 2.16 %, respectively, while the components of the cell wall NDF, ADF, ADL, cellulose, and hemicellulose were 1.82 %, 2.03 %, 0.87 %, 1.15 %, and 0.33 %, respectively (Tables 2 and 4). The lower concentrations in areas with higher rainfall can be attributed to the dilution effect of nutrients present in grasses in regions with abundant precipitation. This phenomenon has been reported by Martín, et al. [3]; Ramírez, et al. [18]; Santos-Cruvinel, et al. [25] and De Abreu-Faria, et al. [26] in cultivars such as *B. decumbens* (Basilisk), *B. brizantha* (Marandu, Piata, Xaraes), and the hybrid CIAT BRO2/1752 (Cayman), demonstrating variability between rainy and dry periods.

Faria, et al. [16] and Marques, et al. [17] reported a directly proportional relationship for crude protein (CP) and an inverse linear relationship for neutral detergent fiber (NDF) and acid detergent fiber (ADF) with nitrogen fertilization. They observed increases of 2 % in protein values (ranging from 12 % to 14 %) and reductions of 20 percentage points for NDF and 6 percentage points for ADF in Mulato II, *B. decumbens*, and *B. brizantha*. In another study, De Almeida-Moreira, et al. [27] evaluated 26 *Brachiaria* varieties under mesothermal climate conditions and red-yellowish soil, finding that *B. ruziziensis* clones performed best, with CP, NDF, ADF, and acid detergent lignin (ADL) values ranging from 13.5 % to 16.49 %, 50 % to 60 %, 21 % to 30 %, and 3.9 % to 4.06 %, respectively. The *B. ruziziensis* clones exhibit higher percentages of CP and lower percentages of cell wall components compared to the *decumbens* variety used as a control. This indicates that the improved clones

have higher nitrogenous component values and lower structural carbohydrates and phenolic compounds, suggesting a greater leaf-to-stem ratio. The observed differences can guide new crosses in breeding programs aimed at complementing agronomic indicators for the development of superior genotypes.

Regarding ash, mineral, and organic matter content, the highest mineral and ash results were recorded during periods of low rainfall. Ramirez, et al. [28] and De Lucena-Costa, et al. [29] investigated the relationship between climatic factors and mineral content in *B. hybrid* variety Mulato I and *B. brizantha* variety Piatá, reporting high correlations ( $R^2 > 0.77$ ) between rainfall and average temperatures during both rainy and dry periods for calcium and phosphorus content. Additionally, multiple linear regression equations were established with coefficients greater than  $R^2 0.81$ , showing better fits for age, total rainfall, and solar radiation. It was evident that the variability of these mineral elements is primarily due to their higher abundance in the young and growing parts of the plant, particularly in the shoots, young leaves, and root tips. The observed variation in minerals with increasing age is related to the dilution effect caused by vegetative development and water accumulation during the rainy season.

On the other hand, Jiménez, et al. [30] reported data for *B. humidicola* in warm and humid climate conditions, with average temperatures of 26 °C, rainfall of 2,123 mm, and humic Acrisol soil. They found values of 16.38 %, 0.015 %, 0.44 %, and 88.04 % for ash, calcium, phosphorus, and organic matter, respectively. Avelar-Magalhães, et al. [31] studied *B. brizantha* variety Marandú in a humid tropical climate characterized by latosolic soil, an average temperature of 28 °C, and rainfall of 1,300 mm, reporting values of 16.46 %, 0.02 %, 0.52 %, and 88.21 % for ash, calcium, phosphorus, and organic matter, respectively. Similarly, Mutimura, et al. [32] evaluated *B. brizantha* variety Piatá in a semi-arid climate with average temperatures of 29 °C and rainfall of 600 mm, finding ash, calcium, phosphorus, and organic matter contents of 16.56 %, 0.025 %, 0.60 %, and 88.41 %, respectively. These results align with those reported by Ramírez, et al. [28].

Considering the variability observed in quality results (Tables 4 and 5), these findings are consistent with those of Tamele, et al. [20] who investigated the interaction between cutting height and climatic zone. They noted greater development of leaves and stems in areas with higher solar radiation intensity, precipitation, and average temperatures, concluding that the variability of these elements influences the structural characteristics of forages. It is important to emphasize that the proportions of leaves and stems serve as indicators of forage quality; a higher proportion of leaves indicates greater nutrient content, palatability, and digestibility, as animals tend to consume more leaves than stems.

The digestibility values fall within the range reports in the literature; however, it is noteworthy that the effects of variety play a significant role in the variability of these indicators. De Almeida-Moreira, et al. [27] evaluated several *Brachiaria* varieties (*B. ruziziensis*, *B. brizantha* variety Marandú, and *B. decumbens* variety Basilisk as a control) with a cut-

ting frequency of every 27 days and a cutting height of 10 cm. They found significant differences in dry matter digestibility (DMD), with the best results (66.69 %) for *B. ruziziensis*. Factors identified as responsible for the variability in digestibility of tropical grasses include climate, plant maturity, soil type, fertilization level and type, growing season, and variability in fiber-nitrogen fractions. Changes in these factors can affect the plant's morphological structure (the proportion of leaves and stems), along with the intrinsic characteristics of each species (genetic improvement) and their adaptability to edaphoclimatic conditions, which may explain the lack of differences found between climatic zones.

The differences observed in the digestibility of matter and organic matter may be linked to the growth and development achieved. This process induces changes in the cell wall structure, particularly in the primary wall, which reduces the intercellular space where nutrients, such as proteins, are located. This reduction is influenced by the relative proportions of each chemical component and their individual digestibility. Additionally, the increase in structural components, such as silica and monomeric lignin, also plays a significant role in this process [31].

Jiménez et al. [30] in their study conducted in The Sabana of Huimanguillo, Tabasco, Mexico, found that *Brachiaria humidicola* exhibit the highest in situ dry matter digestibility (ISDMD) values during the winter (dry) season, with percentages exceeding 50 %. The authors suggest that the seasonal differences can be attributed to variations in climatic factors, such as ambient temperature and precipitation, which significantly affect the growth and structure of the grass. On the other hand, Mutimura, et al. [32] reported that *B. brizantha* cv. Piatá contributed 8.19 MJ of energy and 8.1 kg of milk per day. They concluded that forages with high digestibility and an appropriate fiber-to-nitrogen ratio enhance milk consumption and production. The energy contributions from forages are influenced by the plant's maturity, which leads to chemical and biochemical changes in its components, including a decrease in soluble carbohydrates, digestible proteins, and overall dry matter digestibility. Furthermore, it is important to note that the energy value of forages is closely linked to the digestibility of organic matter, which is inherently related to the plant's composition [33].

## V. CONCLUSIONS AND RECOMMENDATIONS

The yield of total dry matter, leaves, and stems increased with the age of regrowth, reaching the highest values at 75 days. During this period, the yield increased by 75.29 % and 59.08 % in the rainy and dry seasons, respectively. This finding suggests that *Brachiaria hybrid* Mulato I can serve as a viable option for animal feed during the dry season.

Despite exhibiting similar growth patterns in both climatic seasons, *Brachiaria hybrid* Mulato I showed lower performance during the dry season in terms of leaf growth, cell wall components, digestibility, and energy contribution. However, these results confirm the adaptability and potential of this forage species in ecosystems with limited rainfall.

## REFERENCES

- [1] D. Cheruiyot, C. A. Midega, J. O. Pittchar, J. A. Pickett, Z. and R. Khan, "Farmers' perception and evaluation of Brachiaria Grass (*Brachiaria* spp.) Genotypes for Smallholder Cereal-livestock Production in East Africa," *Agriculture*, vol. 10, no. 7, pp. 268-281, 2020. [Online]. Available: <https://doi.org/10.3390/agriculture10070268>
- [2] L. Castañeda-Pimienta, Y. Olivera-Castro and H. B. Wencom-Cárdenas, "Evaluación agronómica y selección de accesiones de *Brachiaria* spp. en suelos de mediana fertilidad," *Pastos y Forrajes*, vol. 40, no. 4, pp. 290-295, 2017. [Online]. Available: [http://scielo.sld.cu/pdf/pyf/v40n4/en\\_pyf05417.pdf](http://scielo.sld.cu/pdf/pyf/v40n4/en_pyf05417.pdf)
- [3] R. Martín, J. M. Dell'Amico and P. J. Cañizares, "Response to cayman grass (*Brachiaria* hybrid cv. CIAT BRO2/1752) to water deficit," *Cultivos Tropicales*, vol. 39, no. 1, pp. 113-118, 2018. [Online]. Available: <https://ediciones.inca.edu.cu/index.php/ediciones/article/view/1435/pdf>
- [4] M. Galdos, E. Brown and C.A. Rosolem, "Brachiaria species influence nitrate transport in soil by modifying soil structure with their root system," *Scientific Reports*, vol. 10, no. 1, pp. 5072, 2020. [Online]. Available: <https://doi.org/10.1038/s41598-020-61986-0>
- [5] A. D. Silva-Cardoso, R. P. Barbero, E. P. Romanzini, R. W. Teobaldo, F. Ongaratto, M. H. Fernandes and R. A. Reis, "Intensification: A key strategy to achieve great animal and environmental beef cattle production sustainability in Brachiaria grasslands," *Sustainability*, vol. 12, no. 16, pp. 6656, 2020. [Online]. Available: <https://doi.org/10.3390/su12166656>
- [6] Soil Survey Staff, *Keys to soil taxonomy*, 12th ed., vol. 97, no. 123. Lincoln, NE, USA: United States Department of Agriculture, Natural Resources Conservation Service, 2014.
- [7] R. S. Herrera, M. García and A. M. Cruz, "Study of some climate indicators at the Institute of Animal Science from 1967 to 2013 and their relation with grasses," *Cuban Journal of Agricultural Science*, vol. 52, no. 4, pp. 411-421, 2018. [Online]. Available: <https://www.cjasience.com/index.php/CJAS/article/view/831>
- [8] AOAC, "Official Methods of Analysis of AOAC International" 18<sup>th</sup> ed., AOAC International, 2005. [Online]. Available: <https://t.ly/3NZDV>
- [9] H. K. Goering, P. J. Van Soest, "Forage fiber analyses," (*apparatus, reagents, procedures, and some applications*) (No. 379). US Agricultural Research Service, 1970.
- [10] G. Aumont, I. Caudron, G. Saminadin and A. Xandé, "Sources of variation in nutritive values of tropical forages from the Caribbean," *Animal Feed Science and Technology*, vol. 51, no. 1-2, pp. 1-13, 1995. [Online]. Available: [https://doi.org/10.1016/0377-8401\(94\)00688-6](https://doi.org/10.1016/0377-8401(94)00688-6)
- [11] O. Cáceres and E. González, "Metodología para la determinación del valor nutritivo de los forrajes tropicales," *Rev. Pastos y Forrajes*, vol. 23, pp. 87-89, 2000. [Online]. Available: <https://hal.science/hal-01190063/>
- [12] D. B. Duncan, "Multiple Range and Multiple F Test," *Biometrics*, vol. 11, no. 1, pp. 1-42, 1955. [Online]. Available: <https://doi.org/10.2307/3001478>
- [13] F. J. Massey, "The Kolmogorov-Smirnov Test for Goodness of Fit," *Journal of the American Statistical Association*, vol. 4, no. 543, pp. 68-78, 1951. [Online]. Available: <https://dx.doi.org/10.2307/2280095>
- [14] M. Bartlett, "Properties of Sufficiency and Statistical Tests," *Proceedings of the Royal Society of London. Serie A*, vol. 160, no. 2, pp. 268-282, 1937. [Online]. Available: <https://doi.org/10.1098/rspa.1937.0109>
- [15] J. M. Bravo-Alves and M. Santos-Diniz, "Um estudo preliminar de possíveis efeitos de mudanças climáticas no nordeste do Brasil," *RBGF-Revista Brasileira de Geografia Física*, vol. 2, no. 2, pp. 11-18, 2009. [Online]. Available: <https://doi.org/10.26848/rbgf.v2.2.p11-18>
- [16] B. M. Faria, M. J. Frota-Morenz, D. S. Campos-Paciullo, F.C. Ferraz-Lopes, C.A. de Miranda-Gomide, "Growth and bromatological characteristics of *Brachiaria decumbens* and *Brachiaria ruziziensis* under shading and nitrogen," *Revista Ciência Agronômica*, vol. 49, no. 3, pp. 529-536, 2018. [Online]. Available: <https://doi.org/10.5935/1806-6690.20180060>
- [17] D. L. Marques, A. F. Franca, L. G. Oliveira, E. Arnhold, R. N. Ferreira, D. S. Correa, D. C. Bastos and L. C. Brunes, "Production and chemical composition of hybrid *Brachiaria* cv. Mulato II under a system of cuts and nitrogen fertilization," *Bioscience Journal*, vol. 33, no. 3, pp. 685-696, 2017. [Online]. Available: <https://doi.org/10.14393/BJ-v33n3-32956>
- [18] J. L. Ramírez, R. S. Herrera, I. Leonard, D. Verdecia, Y. Álvarez, "Rendimiento y calidad de la *Brachiaria decumbens* en suelo fluviosol del Valle del Cauto, Cuba," *REDVET Revista Electrónica de Veterinaria*, vol. 13, no. 4, pp. 1-11, 2012. [Online]. Available: <https://www.redalyc.org/pdf/636/63623403003.pdf>
- [19] P. I. Cruz-López, A. Hernández-Garay, J. F. Enríquez-Quiroz, S. I. Mendoza-Pedroza, A. R. Quero-Carrillo and B. M. Joaquín-Torres, "Agronomic performance of *Brachiaria humidicola* (Rendle) Schweickert genotypes in the Mexican humid tropics," *Revista Fitotecnia Mexicana*, vol. 34, no. 2, pp. 123-131, 2011. Available: <https://www.scielo.org.mx/pdf/rfm/v34n2/v34n2a11.pdf>
- [20] O. H. Tamele, O. A. A. Lopes-de Sá, T. F. Bernardes, M. A. S. Lara, D. R. Casagrande, "Optimal defoliation management of *Brachiaria* grass-forage peanut for balanced pasture establishment," *Grass and Forage Science*, vol. 73, no. 2, pp. 522-531, 2017. [Online]. Available: <https://doi.org/10.1111/gfs.12332>
- [21] J. J. Reyes, Y. Ibarra, A. V. Enríquez, V. Torres, "Performance of *Brachiaria decumbens* cv. Basilisk, subjected to two grazing intensities in the rainy season," *Cuban Journal of Agricultural Science*, vol. 53, no. 1, pp. 21-28, 2019. [Online]. Available: <https://cjasience.com/index.php/CJAS/article/view/856>
- [22] C. A. Ortega-Aguirre, C. Lemus-Flores, J. O. Bugarín-Prado, G. Alejo-Santiago, A. Ramos-Quirarte, O. Grageola-Núñez and J. A. Bonilla-Cárdenas, "Características agronómicas, composición bromatológica, digestibilidad y consumo animal en cuatro especies de pastos de los generos *brachiaria* y *Panicum*," *Tropical and Subtropical Agroecosystems*, vol. 18, no. 3, pp. 291-301, 2015. [Online]. Available: <http://dspace.uan.mx:8080/jspui/handle/123456789/374>
- [23] A. Cruz-Hernández, A. Hernández-Garay, H. Vaquera-Huerta, A. Chay-Cantul, J. Enríquez-Quiroz and S. Ramirez-Vera, "Componentes morfológicos y acumulación del pasto mulato a diferente frecuencia e intensidad de pastoreo," *Revista mexicana de ciencias pecuarias*, vol. 8, no. 1, pp. 101-109, 2017. [Online]. Available: <https://doi.org/10.22319/rmcp.v8i1.4310>
- [24] N. N. Nantes, V. P. B. Euclides, D. B. Montagner, B. Lempp, R. A. Barbosa and P. O. Gois, "Animal performance and sward characteristics of *piatã* palisade grass pastures subjected to different grazing intensities," *Pesquisa Agropecuária Brasileira*, vol. 48, no. 1, pp. 114-121, 2013. [Online]. Available: <https://doi.org/10.1590/S0100-204X2013000100015>
- [25] W. Santos-Cruvinel, K.A. de Pinho-Costa, A. Guerra-da Silva, E. da Costa-Severiano and M. Gonçalves-Ribeiro, "Intercropping of sunflower with *Brachiaria brizantha* cultivars during two sowing seasons in the interim harvest," *Semina: Ciências Agrárias*, vol. 38, no. 5, pp. 3173-3191, 2017. [Online]. Available: <https://doi.org/10.5433/1679-0359.2017v38n5p3173>
- [26] L. De Abreu-Faria, F. H. Silva-Karp, P. Pimentel-Righeto, A. L. Abdalla-Filho, R. C. Lucas, M. Canto-Machado, A. Santana-Natel, T. C. Graciano and A. L. Abdalla, "Nutritional quality and organic matter degradability of *Brachiaria* spp. agronomically biofortified with selenium," *Journal of Animal Physiology and Animal Nutrition*, vol. 102, no. 6, pp. 1464-1471, 2018. [Online]. Available: <https://doi.org/10.1111/jpn.12971>
- [27] E. de Almeida-Moreira, S. Motta-de Souza, A. Lima-Ferreira, T. Ribeiro-Tomich, J. A. Gomes-Azevêdo, F. De Souza-Sobrinho, F. R. Gandolfi-Benites, F. Samarini-Machado, M. Magalhães-Campos and L. G. Ribeiro-Pereira, "Nutritional diversity of *Brachiaria ruziziensis* clones," *Ciência Rural*, vol. 48, no. 02, pp. 1-8, 2018. [Online]. Available: <https://dx.doi.org/10.1590/0103-8478cr20160855>
- [28] J. L. Ramírez, I. Leonard, D. Verdecia, Y. Pérez, Y. Arceo and Y. Álvarez, "Relación de dos minerales con la edad y los elementos del clima en un pasto tropical," *REDVET Revista Electrónica de Veterinaria*, vol. 15, no. 05, pp. 1-8, 2014. [Online]. Available: <https://www.redalyc.org/pdf/636/63633881008.pdf>
- [29] N. de Lucena-Costa, A. N. Azevedo-Rodrigues, J. Avelar-Magalhães, A. Burlamaqui-Bendahan, B. H. Nunes-Rodrigues and F. J. De Seixas-Santos, "Forage yield, chemical composition and morphogenesis of *Brachiaria brizantha* cv. Piatã under regrowth periods," *Research, Society and Development*, vol. 9, no. 1, pp. 133911801, 2020. [Online]. Available: <http://dx.doi.org/10.33448/rsd-v9i1.1499>
- [30] O. M. M. Jiménez, L. Granados, J. Oliva, J. Quiroz and M. Barrón, "Calidad nutritiva de *Brachiaria humidicola* con fertilización orgánica en suelos ácidos," *Archivos de Zootecnia*, vol. 59, no. 228, pp. 561-570, 2010. [Online]. Available: <https://scielo.isciii.es/pdf/azoo/v59n228/art9.pdf>
- [31] J. Avelar-Magalhães, M. S. de Souza-Carneiro, A. Carvalho-Andrade, E. Sales-Pereira, B. H. Nunes-Rodrigues, N. de Lucena-Costa, F. H.

- dos Santos-Fogaça, K. N. de Carvalho-Castro and C. Ramalho-Townsend, "Composição bromatológica do capim-Marandu sob efeito de irrigação e adubação nitrogenada," *Semina: Ciências Agrárias*, vol. 36, no. 2, pp. 933-941, 2015. [Online]. <https://doi.org/10.5433/1679-0359.2015v36n2p933>
- [32] M. Mutimura, C. Ebong, I. M. Rao and I. V. Nsahlai. "Effects of supplementation of *Brachiaria brizantha* cv. Piatá and Napier grass with *Desmodium distortum* on feed intake, digesta kinetics and milk production in crossbred dairy cows," *Animal Nutrition*, vol. 4, no. 2, pp. 222-227, 2018. [Online]. <https://doi.org/10.1016/j.aninu.2018.01.006>
- [33] H. Aniano-Aguirre, M. D. L. Á. Maldonado-Peralta, L. Gasga-Pérez, U. V. Pelaez-Estrada, J. A. Hernández-Marín and A. R. Rojas-García, "Características estructurales de pastos: Mulato II, Convert 330 y Convert 431 (*Urochloa* híbrido)," *Revista Mexicana de Ciencias Agrícolas*, vol. 13, no. 5, pp. 863-872, 2022. [Online]. <https://doi.org/10.29312/remexca.v13i5.3230>

# Assessment of animal drinking water quality in livestock farms in Galapagos Islands

Andrea Belén Casanova Intriago<sup>1</sup>, María Emilia Zambrano Loor<sup>1</sup>, María Fernanda Pincay Cantos<sup>1</sup> and José Manuel Calderón Pincay<sup>1</sup>

**Abstract** — The purpose of this research was to determine the quality of water for bovine consumption on livestock farms in the El Progreso parish - Galapagos by applying a quality index following the Brown methodology proposed by the National Sanitation Foundation of the United States. Information was collected from the livestock farms through a socio-environmental diagnosis of the area, where five localities were considered: San Joaquín, Las Goteras, Cerro Verde, Puerto Chino and El Progreso from which fifteen livestock farms were selected for the respective sampling of the sources of water. Therefore, nine parameters were considered for the analysis of the respective water sources: pH, TDS, Fecal Coliforms, electrical conductivity, hardness, nitrites, phosphates, temperature and turbidity. Of the total livestock farms monitored, three of them presented a rating of Good quality in a range of 70 to 90, while the remaining farms recorded values with a Medium classification, which are those that recorded AQI values between 51 to 70 according to the criteria established by the NSF. This research highlights the importance of frequently carrying out analyzes of the water sources from which cattle drink to determine the quality of the resource, and also provide technical advice to ranchers in the area on the management and cleaning of the reservoirs.

**Keywords:** reservoirs, canals, quality index, livestock farms, NSF, physicochemical parameters.

**Resumen** — El propósito de esta investigación fue determinar la calidad del agua para consumo bovino en fincas ganaderas de la parroquia El Progreso-Galápagos mediante la aplicación de un índice de calidad siguiendo la metodología de Brown propuesta por la Fundación Nacional de Saneamiento de Estados Unidos. Se recolectó información de las fincas ganaderas mediante un diagnóstico socioambiental de la zona, donde se consideraron cinco localidades: San Joaquín, Las Goteras, Cerro Verde, Puerto Chino y El Progreso, de las cuales se seleccionaron quince fincas ganaderas para el respectivo muestreo de las fuentes de agua. Por lo tanto, se consideraron nueve parámetros para el análisis de las respectivas fuentes de agua: pH, TDS, Coliformes Fecales, conductividad eléctrica, dureza, nitritos, fosfatos, temperatura y turbidez. Del total de fincas ganaderas monitoreadas, tres de ellas presentaron una calificación de Buena calidad en un rango de 70 a 90, mientras

que las fincas restantes registraron valores con una clasificación Media, que son aquellas que registraron valores de ICA entre 51 a 70 según los criterios establecidos por la NSF. Esta investigación resalta la importancia de realizar análisis frecuentes de las fuentes de agua de las que bebe el ganado para determinar la calidad del recurso, así también de brindar asesoría técnica a los ganaderos de la zona sobre el manejo y limpieza de los reservorios.

**Palabras Clave:** reservorios, encañadas, índice de Calidad, granjas ganaderas, NSF, parámetros fisicoquímicos.

## I. INTRODUCTION

SINCE water resources have a significant impact on the ecosystem, environmental health, and sustainable development [1], it is crucial to study water quality, particularly that of resources meant for animal consumption, in order to ensure both their continued good condition and the safety of all those who use them [2].

A great deal of water management efforts in Ecuador have concentrated on increasing the quantity of available water, with little regard for the resource's quality [3]. In addition, the conservation of primary water sources is beset by difficulties related to accessibility and limited economic resources, particularly in the island region because of its hydrogeological features [4].

Vulnerable populations are mostly responsible for the problem of water resource contamination in less developed nations as a result of inadequate basic sanitation [5]. The few studies on the water quality of San Cristóbal Island's El Progreso parish, however, leave a lot of problems unanswered, particularly about the suitability of the water for animal use.

The geological richness of the Galapagos Islands, comprising volcanic, sedimentary, and metamorphic rocks, and their volcanic origin are what define them [6]. This becomes important for study since the area's geological makeup, which is primarily composed of sedimentary, metamorphic, or volcanic rocks, affects the physical-chemical properties of the surface water, including its odor [7].

The ravines that form on the island's slopes are the primary source of water for the productive farms in the El Progreso- San Cristóbal parish. These ravines are used directly for agricultural production and cattle hydration [8]. In order to prevent circumstances that could negatively impact the behavior and health of the animals, it is imperative that a water quality index (ICA-NSF) be used in this study to ascertain the incidence in water for animal consumption [9]. The study's goal is to assess the water quality for animal usage on profitable farms in the El Progreso parish (Galápagos). Additionally, it is established as

Corresponding author: [jose.calderon@espam.edu.ec](mailto:jose.calderon@espam.edu.ec)

1. Escuela Superior Politécnica Agropecuaria de Manabí Manuel Félix López, 10 de Agosto N.82 y Granda Centeno, 59304, Calceta, Ecuador. Email: [andrea.casanova@espam.edu.ec](mailto:andrea.casanova@espam.edu.ec), ORCID: <https://orcid.org/0009-0004-9761-0098>. Email: [maria.zambrano@espam.edu.ec](mailto:maria.zambrano@espam.edu.ec), ORCID: <https://orcid.org/0009-0006-8220-3507>. Email: [maria.pincay@espam.edu.ec](mailto:maria.pincay@espam.edu.ec), ORCID: <https://orcid.org/0000-0001-8431-4418>. Email: [jose.calderon@espam.edu.ec](mailto:jose.calderon@espam.edu.ec), ORCID: <https://orcid.org/0000-0002-3315-997X>.

Manuscript Received: 03/07/2024

Revised: 16/08/2024

Accepted: 20/08/2024

DOI: <https://doi.org/10.29019/enfoqueute.1068>

a hypothesis that, based on the National Health Foundation of the United States' (NHF) classification of the index, the quality of water for animal consumption on productive farms is medium quality (between 51 and 70 points).

## II. MATERIALS AND METHODS

### A. Study area

This research was carried out in September 2023, during the rainy season, in fifteen livestock farms in the El Progreso parish of the San Cristóbal canton, Galapagos province, Republic of Ecuador. The parish is located at the eastern end of the archipelago, between  $0^{\circ} 40' 40''$  and  $0^{\circ} 57' 00''$  south latitude and  $89^{\circ} 14' 10''$  and  $89^{\circ} 37' 30''$  west longitude, as shown in figure 1. The altitude of the farms ranges between 320 and 600 meters above sea level.

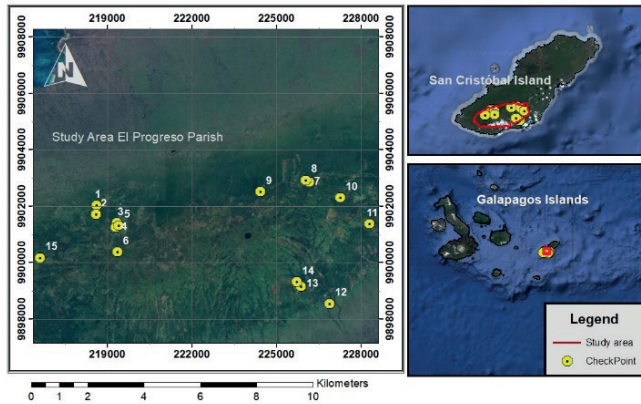


Fig. 1. Geographic location of the study area - "El Progreso Parish". Images taken from [10] and [11].

The study was descriptive in nature, non-experimental, and involved analyzing and interpreting the current nature and composition of pertinent aspects of each detected water sample in order to calculate the water quality index [12]. There are roughly 535 people living in the El Progreso parish. Based on the findings, of the total of 76 cattle ranchers registered in the database of the Ministry of Agriculture and animal of San Cristóbal's Technical Office an intentional sample of 20% was selected, resulting in 15 animal farms to carry out this study [8]. Due to the number of producers, farms were chosen that have participated in the Livestock Field School programs carried out by the technical office and that have water reservoirs to give livestock drinking, which facilitated the study of monitoring water for animal consumption [11].

### B. Socio-environmental diagnosis of the livestock farms of the El Progreso parish (Galápagos)

In order to identify the research area of the El Progreso parish (Galápagos), the base information was processed using ArcGIS version 10.5. A GARMIN eTrex 10 GPS model was used to calculate the farms' geographic coordinates and height [14]. Then, a survey was made up by fourteen questions adapted from [15], [16], and [17]; this instrument was used to find out

the current state of water management and storage on livestock farms. It was divided into three sections: sociodemographic, productive, and cattle water consumption [8]. Using Microsoft Excel software, the survey data were tallied, and pie charts were used to illustrate the average response [18].

### C. Determination of the water quality index in the livestock farms of the El Progreso Galapagos parish

Using the US EPA Standards-600/4-79-0120 "Methods for the Collection and Analysis of Water and Waste," the samples were taken straight from the surface of the livestock drinking fountains. Each point was measured for pH, total dissolved solids (TDS), and temperature in a sterile bottle (500 mL) [16].

A HANNA brand pH meter, given by the Environmental Chemistry laboratory of the Escuela Superior Politécnica Agropecuaria de Manabí Manuel Félix López, was used to measure pH, TDS, and temperature. Total coliform analysis was done at the ESPAM MFL facilities; nitrite and phosphate analysis were done at the Technical University of Manabí, which is situated in Portoviejo. The turbidity analysis was done in the Terrestrial Ecology Laboratory, which is part of the Universidad San Francisco de Quito, San Cristóbal Campus, Galapagos Science Center. Table I displays the techniques.

Brown's methodology, which is a modified version of the UWQI (Universal Water Quality Index), was used to obtain a simplified index to establish the quality of water used for animal consumption [19] through the weighted arithmetic average of nine variables, this research being a pioneer in the evaluation of the quality of animal drinking water in the livestock sector of the island of San Cristóbal-Galapagos, evidenced a need to develop applied research in livestock areas that are aligned with the precepts of environmental sustainability.

TABLE I  
PARAMETERS TO BE ANALYSED (NSF)  
IN THE STUDY. ADAPTED FROM [20], [21]

| Parameter                    | Method                        | Weight NSF |
|------------------------------|-------------------------------|------------|
| Total coliforms              | AOAC 991.14                   | ---        |
| pH                           | Multiparameter meter          | 0.12       |
| Water hardness               | Test Strips                   | ---        |
| Electrical conductivity      |                               | ---        |
| Temperature                  | Pocket meter                  | 0.1        |
| Total Dissolved Solids (TDS) |                               | 0.08       |
| Turbidity                    | Turbidimetric                 | 0.08       |
| Nitrates                     | Ultraviolet spectrophotometry | 0.17       |
| Phosphates                   | Checker Hanna HI706           | 0.17       |

The determination of the water quality index was carried out using Microsoft Excel software, automatically calculating the parameters that directly influence water quality. With the quality factor, the weighting factor and the equation defined for the calculation, the ICA-NSF index was determined for each



farm [23]. [24] mention that the weighting factor is obtained from the value of the laboratory analysis of the parameter in the quality curves, which reflect the professional criteria of responses on a scale (Q) of 0-100, which decreases with the increase in water pollution. To calculate the Brown Index, the additive method was used, which consists of the weighted linear sum of the by-products of each quality parameter and the weights assigned to each one.

The water quality index was determined through the equation 1 [22]:

$$WQI = \sum_{i=1}^{i=n} (Q_i * W_i) \tag{1}$$

Where:

$W_i$ : represents the importance or weighting factor of the variable (i) with respect to the remaining variables that make up the index.

$Q_i$ : corresponds to the scale factor of the variable, depends on the magnitude of the variable and is independent of the rest.  
i: represents the variable or parameter considered.

For the determination of the water quality index, a summary matrix was developed with the parameters analyzed according to their methods and corresponding weights described in table 1 according to [20], as well as with the result of the analysis by parameter obtained from the laboratory and the Q value obtained from the relevant graphs, as indicated in table 2, this table is a projection of how the AQI was calculated during the data analysis.

TABLE II  
MATRIX MODEL DESIGNED FOR THE CALCULATION OF THE ICA-NSF WATER QUALITY INDEX. ADAPTED FROM [23]

| Parameter              | Result | Unit       | Q. Value | Weighting factor | Subtotal |
|------------------------|--------|------------|----------|------------------|----------|
| Dissolved oxygen [DO]  |        | mg/L       |          | 0.17             |          |
| Faecal coliforms       |        | UFC/100 mL |          | 0.15             |          |
| pH                     |        | -          |          | 0.12             |          |
| DBO <sub>5</sub>       |        | mg/L       |          | 0.10             |          |
| Nitrates               |        | mg/L       |          | 0.10             |          |
| Phosphates             |        | mg/L       |          | 0.10             |          |
| Temperature            |        | °C         |          | 0.10             |          |
| Turbidity              |        | NTU        |          | 0.08             |          |
| Total dissolved solids |        | mg/L       |          | 0.08             |          |

The NSF quality indicators were established using the methods suggested by [21], [25] then used the derived ICA values to classify the results as excellent, good, half-bad, bad, and very bad, as shown in table III.

TABLE III  
WATER QUALITY CLASSIFICATION ADAPTED FROM [26]

| Range  | Class     | Color  |
|--------|-----------|--------|
| 0-25   | Very bad  | Red    |
| 26-50  | Bad       | Orange |
| 51-70  | Medium    | Yellow |
| 71-90  | Good      | Green  |
| 91-100 | Excellent | Blue   |

### III. RESULTS AND DISCUSSION

Of the total number of farmers surveyed, 87 % consider their water source to be crystal clear, while 13 % indicate the presence of turbidity as reflected in figure 2a. While for the odor variable, 100 % of respondents consider that the water sources of their farms for cattle consumption do not have an odor, as evidenced in figure 2b.

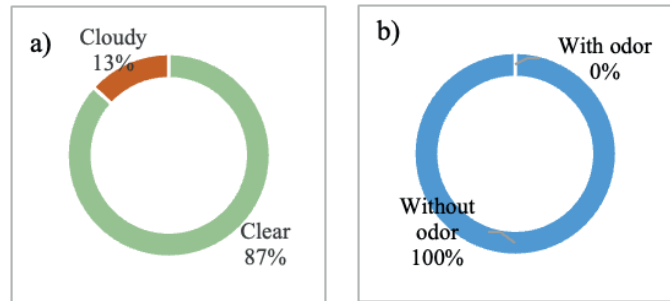


Fig. 2. Perception of surveyed farmers regarding a) color and b) odor of water sources for bovine consumption.

For [27], physicochemical factors such as iron, manganese and tannins, organic matter, which is produced when the remains of plants and animals decompose, cause water to color, generating an impact on organoleptic characteristics such as color, smell and taste. According to [28], the number of total coliforms influences the water's odor. Similarly, the presence of other dissolved contaminants, including heavy metals, impacts the water's quality and suitability for human uses, including agriculture and raising cattle.

The findings of the biological and physicochemical analyses of the 15 farms in the parish of "El Progreso" are shown in Table IV.

TABLE IV  
RESULTS OF THE PHYSICOCHEMICAL AND BIOLOGICAL PARAMETERS EVALUATED

| POINT | PLACE        | pH    | T(°C) | PO <sub>4</sub> (mg/l) | NO <sub>3</sub> (mg/l) | TDS (mg/l) | TURBIDITY (NTU) | HARDNESS (ppm) | EC  | TOTAL COLIFORMS (UFC / 100 mL) |
|-------|--------------|-------|-------|------------------------|------------------------|------------|-----------------|----------------|-----|--------------------------------|
| 1     | San Joaquín  | 7.32  | 20    | 2.45                   | 5.33                   | 44         | 3.70            | 445            | 93  | <1.0                           |
| 2     | San Joaquín  | 6.67  | 20    | 2.25                   | 2.10                   | 14         | 1.46            | 267            | 29  | <1.0                           |
| 3     | San Joaquín  | 10.07 | 20    | 1.22                   | 2.23                   | 36         | 2.03            | 267            | 76  | <1.0                           |
| 4     | San Joaquín  | 8.4   | 20    | 1.53                   | 0.33                   | 10         | 1.61            | 356            | 21  | 9.0 × 10 <sup>1</sup>          |
| 5     | San Joaquín  | 8.12  | 20    | 1.84                   | 3.84                   | 13         | 4.27            | 356            | 27  | <1.0                           |
| 6     | San Joaquín  | 7.4   | 20    | 3.67                   | 0.33                   | 14         | 2.36            | 267            | 42  | <1.0                           |
| 7     | Las Goteras  | 7.79  | 20    | 1.53                   | 0.68                   | 10         | 1.83            | 267            | 21  | <1.0                           |
| 8     | Las Goteras  | 7.5   | 20    | 0.61                   | 1.84                   | 12         | 1.26            | 89             | 25  | 1.0 × 10 <sup>1</sup>          |
| 9     | Las Goteras  | 6.5   | 20    | 3.37                   | 1.55                   | 17         | 0.82            | 89             | 36  | <1.0                           |
| 10    | Cerro Verde  | 6.55  | 20    | 1.22                   | 0.5                    | 12         | 1.50            | 445            | 25  | <1.0                           |
| 11    | Cerro Verde  | 7.10  | 20    | 1.53                   | 0.35                   | 51         | 0.36            | 445            | 108 | <1.0                           |
| 12    | Puerto Chino | 7.36  | 20    | 1.22                   | 1.23                   | 44         | 0.99            | 445            | 93  | <1.0                           |
| 13    | Puerto Chino | 7.45  | 20    | 3.98                   | 1.16                   | 36         | 0.54            | 178            | 76  | 1.0 × 10 <sup>1</sup>          |
| 14    | Puerto Chino | 7.08  | 20    | 1.22                   | 1.72                   | 35         | 4.45            | 445            | 74  | 2.0 × 10 <sup>1</sup>          |
| 15    | El Progreso  | 8.16  | 20    | 5.2                    | 5.58                   | 55         | 8.26            | 356            | 117 | <1.0                           |

It was found that, in comparison to the other farms that maintain a neutral pH, farms 3, 4, 5, and 15 in the town of San Joaquín had high pH values. The water sources in the various locations maintained a temperature of 20°C. El Progreso recorded the greatest total dissolved solids content, with a maximum of 55 mg/L, while Cerro Verde recorded 51 mg/L. Farm 15 had a turbidity rating of 8.26 NTU, a value below the maximum acceptable level in drinking water for animals [29]. With hard water in mind, the hardness measured values at Puerto Chino, San Joaquín, and Cerro Verde were 445 PPM. At last, farm 4 was found to have a higher concentration of total coliforms, measuring 9.0 × 10<sup>1</sup> nmp / 100 mL.

The following conditions must be met by water used for livestock: a pH between 6 and 9, a maximum of 3000 mg/L of total dissolved solids (TDS), a maximum of 1000 NMP of fecal coliforms, and a maximum of 50 mg/L of nitrates (NO<sub>3</sub>), as stated in Ministerial Agreement 097-A [30].

Farm 3's pH exceeds the maximum allowable limit (10.07), which can be explained by high photosynthetic activity caused by the community of bacteria and algae found in surface water sources. This would supersaturate the aquatic system with oxygen, depleting carbon dioxide and raising the pH of the water. This is one explanation offered [31] for the alkaline pH values observed. Nonetheless, [7] clarify that the values of the various parameters in the water are changed by the geological makeup of the region where surface or subsurface runoff passes, which is primarily composed of volcanic, sedimentary, or metamorphic rocks.

For instance, the discharge of minerals like iron from volcanic rocks can lower the pH of the water by acidifying it [32], [33]. However, carbonates found in sedimentary rocks can function as pH buffers, maintaining a neutral or slightly alkaline pH [34], [35] Similarly, minerals released by metamorphic

rocks might affect the water's alkalinity [36]. Table V presents the classification according to the NSF ICA index.

TABLE V  
RESULTS OF THE NSF WATER QUALITY INDEX.

| Farm | Place       | WQI NSF | Classification NSF |
|------|-------------|---------|--------------------|
| 1    | San Joaquín | 63.96   | Medium             |
| 2    | San Joaquín | 62.70   | Medium             |
| 3    | San Joaquín | 55.45   | Medium             |
| 4    | San Joaquín | 68.00   | Medium             |
| 5    | San Joaquín | 61.50   | Medium             |
| 6    | San Joaquín | 67.70   | Medium             |
| 7    | Las Goteras | 69.00   | Medium             |
| 8    | Las Goteras | 73.00   | Good               |
| 9    | Las Goteras | 63.00   | Medium             |
| 10   | Cerro Verde | 66.04   | Medium             |
| 11   | Cerro Verde | 71.00   | Good               |
| 12   | El Chino    | 71.00   | Good               |
| 13   | El Chino    | 67.10   | Medium             |
| 14   | El Chino    | 66.40   | Medium             |
| 15   | El Progreso | 60.70   | Medium             |

Based on the NSF's established criteria, farms 8, 11, and 12 were classified as having good quality, with AQI values between 51 and 70. The remaining farms were rated as having a medium quality. These results are based on the results of the water quality index. The water sources with the highest values for pH, hardness, total dissolved solids, turbidity, and total co-

liforms were classified as medium. Figure 3 depicts how water supplies behave on farms raising livestock.

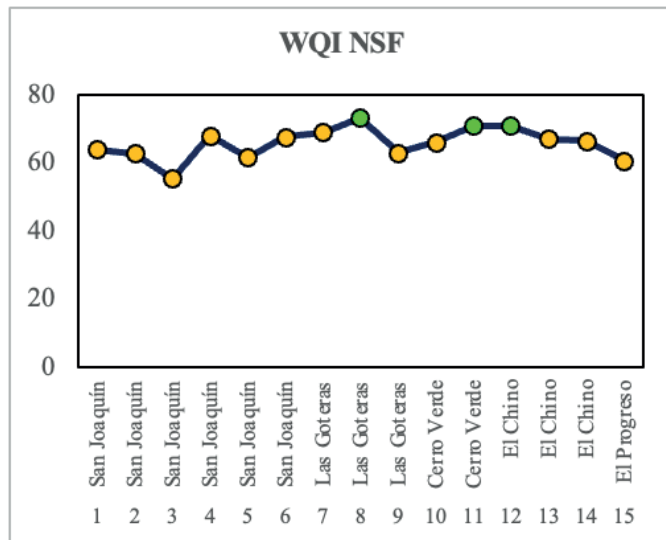


Fig. 3. Behavior of the Water Quality Index of the farms.

Regarding what solutions can be proposed to improve water quality, considering the nature of the special regime that the Galapagos Islands have, there are three possible solutions to be implemented in cattle farms: a treatment with hydrogen peroxide to reduce the microbiological load to 3 % to eliminate the microbiological load of the drinking water [37], a chlorination treatment (1:5 NaClO 15 % m/v is diluted in water (36 g/L)) as it improves growth performance without detrimental side effects on health or nutrient digestibility [38] and a third treatment with oxygen-enriched drinking water that has potential effects on cattle fattening performance [39].

The results of this research become a key piece to reduce knowledge and technology gaps in the livestock sector, allowing the strengthening of local capacities of livestock farmers; this is related to what is described by [40] who mention that livestock activity has one of the largest environmental footprints and therefore should promote practices that reduce these impacts.

The situation of livestock in Galapagos is going through a series of difficulties and limitations for its maintenance and development within the framework of sustainability [41]; since it is a protected natural area with unique characteristics, it is necessary to minimize the impact of anthropic activities without conditioning the satisfaction of the basic needs of the island's inhabitants [42]; that is why getting traditional livestock farming to transition to more sustainable livestock farming with access to information on animal and environmental health will lead to better decision-making in the livestock sector.

With regard to environmental health, the monitoring of water quality through a physicochemical analysis is of utmost importance for its productivity since, in ruminants, especially cattle, water consumption is directly related to dry matter consumption, so an animal that drinks little water due to its availability, palatability or low quality can manifest stress and consequently meat or milk production will be decreased [43].

#### IV. CONCLUSION AND RECOMMENDATION

The average ICA NSF water quality index was 65.78, placing it in the medium quality category. Of the total number of participating farms, 20 % (3 farms) have good quality water and 80 % (12 farms) have medium quality water. The quality of water on cattle farms is affected by sanitation problems, mainly due to the way water is stored and exposure to the elements.

The results obtained serve as a basis for future studies that analyze the quality of water for bovine consumption in different seasons between dry and rainy seasons, which could be carried out in the coming years, including in the analysis of water the study of minerals or heavy metals depending on how each livestock farm obtains water.

#### ACKNOWLEDGMENTS

Authors acknowledge the support provided by Galapagos Science Center from University of San Francisco de Quito, Mr. Edy Becerra-President of the El Progreso Parish GAD, Dr. Diego Castillo and the technicians of the San Crisóbal-Santa Cruz-Isabela Zonal Office of the Ministry of Agriculture and Livestock of Ecuador and Escuela Superior Politécnica Agropecuaria de Manabí Manuel Félix López.

#### REFERENCES

- [1] C. D. Paucar Peñaranda, V. H. González Carrasco, H. D. Álvarez Pucha, B. A. Madrid Celi, C. A. De Gracia Pérez and A. R. Flores Acosta, "Aplicación del índice de calidad del agua (ICA) caso de estudio: río Jubones, Ecuador," *Ciencia Latina*, vol. 7, n.º 4, Art. n.º 4, jul. 2023. <https://doi.org/10.37811/clrcm.v7i4.6953>
- [2] R. del P. Freire Rosero, M. Pino Vallejo, P. Andrade and A. Mejía López, "Evaluación de la calidad del agua del Río Chambo en época de estiaje utilizando el índice de calidad del agua ICA-NSF," *Perfiles*, vol. 1, n.º 23, Art. n.º 23, 2020. [Online]. Available: <http://dspace.espoche.edu.ec/handle/123456789/14581>
- [3] E. Terneus Jácome and P. Yanez-Moreta, "Principios fundamentales en torno a la calidad del agua, el uso de bioindicadores acuáticos y la restauración ecológica fluvial en Ecuador," *Igr*, vol. 27, n.º 1, Art. n.º 1, ene. 2018. <https://doi.org/10.17163/igr.n27.2018.03>
- [4] W. Vernaza et al., "Agua para Galápagos: un programa de monitoreo de la calidad del agua en las islas Galápagos," *Esferas*, vol. 2, n.º 1, Art. n.º 1, abr. 2021. <https://doi.org/10.18272/esferas.v2i.2026>
- [5] L. N. Pedraza Castillo et al., "Calidad e inocuidad del agua de bebida de sistemas de producción animal: experiencia en municipios del departamento del Meta, Colombia," *CTA*, vol. 23, n.º 3, Art. n.º 3, sep. 2022. [https://doi.org/10.21930/rcta.vol23\\_num3\\_art:2259](https://doi.org/10.21930/rcta.vol23_num3_art:2259)
- [6] Instituto Geofísico Escuela Politécnica Nacional [IG-EPN], "Islas Galápagos," IGEPN. [Online]. Available: <https://www.igepn.edu.ec/islas-galapagos>
- [7] R. P. Rojas Vargas y L. N. Rojas Vizcarra, "Caracterización y Determinación de la Calidad de Agua Superficia," *RI*, vol. 12, n.º 1, Art. n.º 1, mar. 2023. <https://doi.org/10.26788/ri.v12i1.4014>
- [8] V. Barrera, L. Escudero, M. Valverde and J. Allauca, "Productividad y sostenibilidad de los sistemas de producción agropecuaria de las islas Galápagos-Ecuador," En *Libro Técnico*. Quito, Ecuador: Instituto Nacional de Investigaciones Agropecuarias [INIAP], 2019. [Online]. Available: <https://bit.ly/3Z5ewvA>
- [9] Ma. T. Kido-Cruz, C. J. Martínez-Castro, T. Zúñiga-Marroquín, y J. Cotera-Rivera, "Estimación del bienestar animal del bovino lechero en trópico, mediante criterios de acondicionamiento ambiental," *Rev MVZ Córdoba*, vol. 27, n.º 3, Art. n.º 3, may 2024. <https://doi.org/10.21897/rmvz.2676>
- [10] National Geographic [NatGeo], "Islas Galápagos," *Revista NatGeo*. [Online]. Available: <https://www.nationalgeographic.es/tema/lugares/tierra/americadel-sur/ecuador/islas-galapagos>

- [11] Environmental Systems Research Institute [ESRI], "Basemaps," ArcGIS Developers. [Online]. Available: <https://bit.ly/3MrgILY>
- [12] D. N. Ante Bautista and G. E. Pilatasig Achig, "Determinación de la calidad del agua por bioindicadores (macroinvertebrados) e índices EPT, BMWP/COL, ABI y SHANNON-WEAVER del río Pachanlica, provincia de Tungurahua, 2020," Proyecto de Investigación, Universidad Técnica de Cotopaxi [UTC], Latacunga, Ecuador, 2020. [Online]. Available: <http://repositorio.ute.edu.ec/handle/27000/7076>
- [13] L. F. Mucha Hospital, R. Chamorro Mejía, M. E. Oseda Lazo and R. D. Alania-Contreras, "Evaluación de procedimientos que se toman para la población y muestra en trabajos de investigación," *Desafíos*, vol. 12, n.º 1, Art. n.º 1, feb. 2021, <https://doi.org/10.37711/desafios.2021.12.1.253>.
- [14] C. A. Chamba Salavarría, "Implementación de un prototipo de sistema de georreferenciación mediante la tecnología GPS/GSM para personas vulnerables," Trabajo de Titulación, Escuela Superior Politécnica de Chimborazo, Riobamba, Ecuador, 2017. [Online]. Available: <http://dspace.espace.edu.ec/handle/123456789/6367>
- [15] D. G. Benítez Jiménez, J. C. Vargas Burgos, V. Torres Cárdenas and S. Soria Re, "La Incidencia de las Prácticas Ganaderas en la Productividad de los Rebaños de Cría en la Provincia de Pastaza de la Amazonia Ecuatoriana," *Avances en Investigación Agropecuaria*, vol. 20, n.º 3, Art. n.º 3, 2016, [Online]. Available: <https://www.redalyc.org/journal/837/83754344004/html/>
- [16] J. F. Cajape Bravo, "Índice de calidad de agua de las fuentes hídrica que abastecen al ganado bovino, parroquia Quiroga," Trabajo de Titulación, Escuela Superior Politécnica Agropecuaria de Manabí Manuel Félix López [ESPAM MFL], Calceta, Ecuador, 2021. [Online]. Available: <http://repositorio.espam.edu.ec/handle/42000/1393>
- [17] Ministerio de Economía Familiar, Comunitaria, Cooperativa y Asociativa [MEFCCA], Cooperación Suiza en América Central [COSUDE] and Centro Agronómico Tropical de Investigación y Enseñanza [CATIE], *Uso del agua del reservorio en labores agropecuarias*, Cooperación Suiza en América Central [COSUDE], Centro Agronómico Tropical de Investigación y Enseñanza [CATIE]. En Serie Técnica Cosecha de agua, no. 5. Nicaragua, 2018. [Online]. Available: <https://repositorio.catie.ac.cr/handle/11554/8970>
- [18] J. S. Saltz and J. M. Stanton, *An introduction to data science*. Thousand Oaks, California: SAGE Publications, Inc., 2018. ISBN: 978-1-5063-7751-3
- [19] C. A. Caho-Rodríguez and E. A. López-Barrera, "Determinación del Índice de Calidad de Agua para el sector occidental del humedal Torca-Guaymaral empleando las metodologías UWQI y CWQI," *Rev. P+L*, vol. 12, n.º 2, Art. n.º 2, dic. 2017. <https://doi.org/10.22507/pml.v12n2a3>
- [20] P. V. Méndez Zambrano, J. P. Arcos Logroño and X. R. Cazorla Vinuesa, "Determinación del índice de calidad del agua (NSF) del río Copueno ubicado en Cantón Morona," *Dominio de las Ciencias*, vol. 6, n.º 2, Art. n.º 2, 2020. <https://doi.org/10.23857/dc.v6i2.1245>
- [21] C. B. Borrero García, "Metodología para determinación del índice de calidad del agua a partir de parámetros fáciles de medir en campo," Uniandes, 2018. [Online]. Available: <http://hdl.handle.net/1992/34065>
- [22] L. S. Quiroz Fernández, E. Izquierdo Kulich and C. Menéndez Gutiérrez, "Aplicación del índice de calidad de agua en el río Portoviejo, Ecuador," *Ingeniería Hidráulica y Ambiental*, vol. 38, n.º 3, Art. n.º 3, oct. 2017, [Online]. Available: <https://riha.cujae.edu.cu/index.php/riha/article/view/408>
- [23] P. C. Saravía Solares, "Determinación de los Índices de Calidad del Agua ICA-NSF para Consumo Humano de los Ríos Teocinte y Acatán, que Abastecen la Planta de Tratamiento de Agua Santa Luisa Zona 16, Guatemala," *ASA*, vol. 12, n.º 1, Art. n.º 1, nov. 2017. <https://doi.org/10.36829/08ASA.v12i1.1424>
- [24] R. M. Granizo Taboada and V. N. Toa López, *Determinación del índice de calidad de agua (ICA- NSF) de las fuentes de agua resultantes de un plan de manejo de parámos, Parroquia Sucre, Cantón Patate*, [Bachelor thesis], Universidad Estatal Amazónica, 2020. [Online]. Available: <https://repositorio.uea.edu.ec/handle/123456789/827>
- [25] J. A. Gil-Marín, C. Vizcaino and N. J. Montaña-Mata, "Evaluación de la calidad del agua superficial utilizando el índice de calidad del agua (ICA). Caso de estudio: Cuenca del Río Guarapiche, Monagas, Venezuela," *An. cient. U.N.A.*, vol. 79, n.º 1, Art. n.º 1, jun. 2018. <https://doi.org/10.21704/ac.v79i1.1146>
- [26] Md. G. Uddin, S. Nash and A. I. Olbert, "A review of water quality index models and their use for assessing surface water quality," *Ecological Indicators*, vol. 122, p. 107218, mar. 2021. 1 <https://doi.org/10.1016/j.ecolind.2020.107218>
- [27] V. Sánchez Requejo, *Determinación de Parámetros Físicos y Químicos, y su Influencia en las Características Organolépticas en la Quebrada El Herrero, Soritor*, 2015. [Tesis de Licenciatura], Universidad Nacional de San Martín, 2018. [Online]. Available: <https://repositorio.unsm.edu.pe/handle/11458/2999>
- [28] S. Castillo-Herrera, S. Barrezueta-Unda and J. Arbito-Quituisaca, "Evaluación de la Calidad de Aguas Subterráneas de la Parroquia La Peaña, Provincia El Oro, Ecuador," *CU*, vol. 12, n.º 31, Art. n.º 31, sep. 2019. <https://doi.org/10.29076/issn.2528-7737vol12iss31.2019pp64-73p>.
- [29] J. M.ª Llena, "La calidad del agua y sus usos diferentes en ganadería: Seleccionamos Avícolas," pp. 31-35. 2011 Available: <https://bit.ly/4dH9bz4>
- [30] Ministerio del Ambiente del Ecuador [MAE], *Acuerdo Ministerial 097-A, Anexos de Normativa, Reforma Libro VI del Texto Unificado de Legislación Secundaria del Ministerio del Ambiente*, vol. 083-B, n.º Registro Oficial 387 Año III. 2015. [Online]. Available: <https://bit.ly/3WXXH7W>
- [31] S. N. Escobar Arrieta, A. Albuja and F. D. Andueza Leal, "Calidad fisicoquímica del agua de la laguna Colta. Chimborazo. Ecuador," *FIGEMPA: Investigación y Desarrollo*, vol. 11, n.º 1, pp. 76-81, 2021. [Online]. Available: <https://dialnet.unirioja.es/servlet/articulo?codigo=8529807>
- [32] C. M. Ossa Cardona, *Comportamiento de los Contaminantes Retenidos por Schwertmannita durante la Interacción con Agua de Mar*, [Tesis de Máster], Universidad Internacional de Andalucía, 2022. [Online]. Available: <https://bit.ly/3MoJelt>
- [33] J. T. Ovalle *et al.*, "Formation of massive iron deposits linked to explosive volcanic eruptions," *Sci Rep*, vol. 8, n.º 1, oct. 2018, <https://doi.org/10.1038/s41598-018-33206-3>
- [34] J. G. Prato, L. C. González-Ramírez, M. C. Pérez, y M. E. Rodríguez, "Adsorción de la dureza del agua sobre lechos de rocas volcánicas de Ecuador," *Inf. tecnol.*, vol. 32, n.º 2, abr. 2021. <https://doi.org/10.4067/S0718-07642021000200051>
- [35] Servicio Geológico Mexicano, "Rocas metamórficas," Gobierno de México. [Online]. Available: <https://www.sgm.gob.mx/Web/Museo-Virtual/Rocas/Rocas-metamorficas.html>
- [36] Servicio Geológico Mexicano, "Rocas sedimentarias," Gobierno de México. [Online]. Available: <https://www.sgm.gob.mx/Web/Museo-Virtual/Rocas/Rocas-sedimentarias.html>
- [37] D. Y. Ramos Chura, "Efecto del peróxido de hidrogeno en la calidad microbiológica del agua (mesófilos aerobios totales, coliformes totales, escherichia coli y enterobacterias) de bebederos en vacas, vaquillas, vaquillonas y terneros en el Fundo AQP Milk en la Irrigación de Majes-2019," ago. 2021. [Online]. Available: <https://repositorio.ucsm.edu.pe/handle/20.500.12920/10985>
- [38] L. Llonch *et al.*, "Drinking water chlorination in dairy beef fattening bulls: water quality, potential hazards, apparent total tract digestibility, and growth performance," *Animal*, vol. 17, n.º 1, p. 100685, ene. 2023. <https://doi.org/10.1016/j.animal.2022.100685>
- [39] V. Konaç, A. Akbaş and M. Saatçı, "Los efectos del agua potable tratada con oxígeno energizado en el rendimiento de engorde en ganado vacuno," *Harran Univ Vet Fak Derg*, vol. 8, núm. 2, pp. 236-242, 2019. <https://doi.org/10.31196/huvfd.667782>
- [40] R. González-Quintero *et al.*, "Limitaciones para la implementación de acciones de mitigación de emisiones de gases de efecto de invernadero (GEI) en sistemas ganaderos en Latinoamérica," *Livestock Research for Rural Development*, vol. 27, p. Article 249, dic. 2015.
- [41] Consejo de Gobierno del Régimen Especial de Galápagos. Plan de Desarrollo Sustentable y Ordenamiento Territorial del Régimen Especial de Galápagos. -Plan Galápagos. 2016. Puerto Baquerizo Moreno, Galápagos, Ecuador. ISBN-978-9942-22-059-2
- [42] M. E. Godoy Zúñiga and E. P. Vidal Roha, "Manejo turístico de islas sudamericanas: Un estudio de las Islas Galápagos y el Archipiélago de San Andrés, Providencia y Santa Catalina," *TURYDES: Revista sobre Turismo y Desarrollo local sostenible*, vol. 10, n.º 22, p. 61, 2017. [Online]. Available: <https://dialnet.unirioja.es/servlet/articulo?codigo=7932298>
- [43] J. I. Sierra, "Determinación e interpretación de calidad de agua con destino a uso ganadero del Dto. Loventué, provincia de La Pampa," *Semiárida*, vol. 29, n.º 2, Art. n.º 2, 2019. [Online]. Available: <https://cerac.unlpam.edu.ar/index.php/semiárida/article/view/4425>

# The bioaccumulative potential of heavy metals in five forest species living in mining environments in the Ecuadorian Amazon region

Yudel García-Quintana<sup>1</sup>, Dixon Domingo Andi-Grefa<sup>2</sup>, Luis Ramón Bravo-Sánchez<sup>3</sup>, Samantha García-Decoro<sup>4</sup>, Sonia Vega-Rosete<sup>5</sup>, Sting Brayán Luna-Fox<sup>6</sup> and Yasiel Arteaga-Crespo<sup>7</sup>

**Abstract** — Heavy metal contamination of soils and ecosystems is an environmental problem that requires urgent attention due to the ecological problems that it generates. Forest species can be used to mitigate contamination because of their potential to bioaccumulate contaminating metals. The objective of this work was to evaluate the bioaccumulator potential of heavy metals in five forest species that live in mining environments in the Ecuadorian Amazon region. The bioconcentration factor for five forest species, such as: *Cedrela odorata*, *Parkia multijuga*, *Inga edulis*, *Cecropia ficifolia* and *Pourouma cecropiifolia*, commonly found in the Ecuadorian Amazon was analysed, based on the relationship between the concentration of the heavy metal in leaves and the soil. Atomic absorption spectrometry was used to analyse heavy metals in leaves and soil samples of each plant specie. The results showed that *P. cecropiifolia* had the highest bioconcentration factor for lead, *C. odorata* for cadmium and nickel, and *I. edulis* had the highest potential for iron and aluminium absorption. No correlation was found between the concentration of each element in the soil and the leaves, which shows that the bioaccumulation capacity of the species studied does not depend on the concentration of the element in the soil. This provides relevant information for the inclusion of these species for phytoremediation purposes.

**Keywords:** tree species; pollution; mining; leaves; soil; bioconcentration factor.

**Resumen** — La contaminación de suelos y ecosistemas por metales pesados es un problema ambiental que requiere atención urgente debido a los problemas ecológicos que genera. Las especies

forestales se pueden utilizar para mitigar la contaminación debido a su potencial para bioacumular metales pesados. El objetivo de este trabajo fue evaluar el potencial bioacumulador de metales pesados en cinco especies forestales que viven en entornos mineros en la región amazónica ecuatoriana. Se analizó el factor de bioconcentración a partir de la relación entre la concentración de metales pesados en las hojas y el suelo para cinco especies forestales, tales como: *Cedrela odorata*, *Parkia multijuga*, *Inga edulis*, *Cecropia ficifolia* y *Pourouma cecropiifolia*, comúnmente distribuidas en la Amazonía ecuatoriana. Se utilizó espectrometría de absorción atómica para analizar los metales pesados en muestras de hojas y suelo de cada especie vegetal. Los resultados mostraron que *P. cecropiifolia* presentó el mayor factor de bioconcentración de plomo, *C. odorata* de cadmio y níquel, e *I. edulis* mayor potencial para absorción de hierro y aluminio. No se encontró correlación entre la concentración de los elementos en el suelo y las hojas, lo que demostró que la capacidad de bioacumulación de las especies estudiadas no depende de la concentración del elemento en el suelo. Esto facilita información relevante para la inclusión de estas especies con fines de fitorremediación.

**Palabras Clave:** especies arbóreas; contaminación; minería; hojas; suelos; factor de bioconcentración.

## I. INTRODUCTION

HEAVY metals are considered potentially toxic elements and one of the world's largest ecological problems, affecting human health both directly and indirectly [1]. They are natural constituents of the Earth's crust and are found in various components, such as the atmosphere, water bodies, sediments and the biosphere [2]. Among these pollutants, chromium (Cr), nickel (Ni), zinc (Zn), cadmium (Cd), lead (Pb), stand out as having attracted considerable attention due to their environmental persistence, toxicity and bioaccumulation [3]. These elements can bind to particles and be transported for several thousand kilometers by airflow, then deposited again through dry or wet deposition, ultimately resulting in high environmental concentrations [3]. Heavy metals are often associated with fine atmospheric particles and their transport distances depend mainly on meteorological factors, the physical and chemical characteristics of the particles, and atmospheric residence time.

Heavy metals have been investigated in various natural ecosystems [4] in both slightly and highly polluted areas, such as mining areas [5], agricultural regions [6] or urban environments, where heavy metal content originates mainly from various anthropogenic activities [7]. These anthropogenic activities can elevate metal

1. Universidad Estatal Amazónica, km 2 ½ Paso Lateral, vía al Tena. Puyo. Pastaza, Ecuador. Email: [ygarcia@uea.edu.ec](mailto:ygarcia@uea.edu.ec), ORCID: <https://orcid.org/0000-0002-9107-9310>. Corresponding autor.

2. Universidad Estatal Amazónica, km 2 ½ Paso Lateral, vía al Tena. Puyo. Pastaza, Ecuador. Email: [dixon.9572@gmail.com](mailto:dixon.9572@gmail.com), ORCID: <https://orcid.org/0000-0002-3064-2608>.

3. Universidad Estatal Amazónica, km 2 ½ Paso Lateral, vía al Tena. Puyo. Pastaza, Ecuador. Email: [lbravo@uea.edu.ec](mailto:lbravo@uea.edu.ec), ORCID: <https://orcid.org/0000-0001-5756-6628>.

4. Empresa Agroforestal Pinar del Río, Carr. San Luis Km 3 ½. Pinar del Río, Cuba. Email: [garciadecorosamantha@gmail.com](mailto:garciadecorosamantha@gmail.com), ORCID: <https://orcid.org/0009-0009-9883-8883>.

5. Universidad de Alicante, Carr. de San Vicente del Raspeig, s/n, 03690 San Vicente del Raspeig. Alicante, España. Email: [svegarosete@gmail.com](mailto:svegarosete@gmail.com), ORCID: <https://orcid.org/0000-0003-2020-0205>.

6. Universidad Estatal Amazónica, km 2 ½ Paso Lateral, vía al Tena. Puyo. Pastaza, Ecuador. Email: [sb.lunaf@uea.edu.ec](mailto:sb.lunaf@uea.edu.ec), ORCID: <https://orcid.org/0000-0001-6058-7024>.

7. Universidad Estatal Amazónica, km 2 ½ Paso Lateral, vía al Tena. Puyo. Pastaza, Ecuador. Email: [yarteaga@uea.edu.ec](mailto:yarteaga@uea.edu.ec), ORCID: <https://orcid.org/0000-0002-9817-9883>.

Manuscript Received: 27/03/2024

Revised: 01/07/2024

Accepted: 28/08/2024

DOI: <https://doi.org/10.29019/enfoqueute.1031>

concentrations above their normal levels and cause potentially toxic effects in the living world [8]. Although some heavy metals are also essential nutrients (e.g. copper and zinc) [9], they can be extremely toxic at higher concentrations or in a specific chemical form [10]. They tend to accumulate in biological organisms and soil over time, rendering them extremely hazardous [11].

Plants are extremely important because of their role in filtering air and releasing oxygen, regulating air temperature and accumulating potentially toxic substances [12]. Since some organs (roots and leaves) accumulate heavy metals [7, 13], they can serve as biomonitors of environmental pollution. The main sources of heavy metals in plants are their growth media and atmospheric deposition. Trees can absorb both essential and non-essential metals, and the uptake of heavy metals by both roots and leaves increases when the concentration of heavy metals increases in the external environment [7]. The accumulation of metal elements in plants confirms that these elements are present in the soil or air, but in many plants the concentrations of heavy metals can be several times higher than the concentrations of heavy metals in the soil [12]. The toxicity of these elements in plants varies depending on the plant species, type of metal, concentration, chemical form, soil composition, pH, type of sources (natural or anthropogenic) [9, 11]. Therefore, the leaves of specific tree species have been used as biomonitors of heavy metal pollution in several studies [14]. However, metal concentrations in tree organs are not a sufficient indicator of tree contamination, as uptake depends on the plant species and its bioconcentration factors, i.e. the ability of a plant to accumulate heavy metals from soil and air [15].

In the Ecuadorian Amazon, given the proximity of volcanoes, soils may have high levels of heavy metals [16]. In addition, mining operations are a major cause of environmental contamination, where mining waste management is inadequate. Consequently, heavy metals are easily released into the environment, posing a potential risk to human health. Artisanal and small-scale gold mining is among the most important causes of secretion of these elements into ecosystems, leading to severe pollution [17]. This has been widely reported in developing countries, where inefficient or non-existent environmental regulations exacerbate the problem [18]. This fact is particularly worrying in Ecuador as illegal and uncontrolled mining has produced serious environmental pollution, mainly in terms of discharges of potentially toxic elements [19]. These are not the only causes of heavy metal pollution; the population growth is also to blame in that it has led to the diversification of economic activity [20], the intensive use of toxic agrochemicals [21] and so on. Therefore, the objective of this work was to evaluate the bioaccumulator potential of heavy metals in five forest species that live in mining environments in the Ecuadorian Amazon region.

## II. MATERIALS AND METHODS

### A. Study Area

This study was carried out in a mining area near the banks of the Jatunyacu River in the Yutsupino community, Puerto Napo

parish, Napo province, Ecuador (Figure 1), where illegal gold mining activities are carried out.

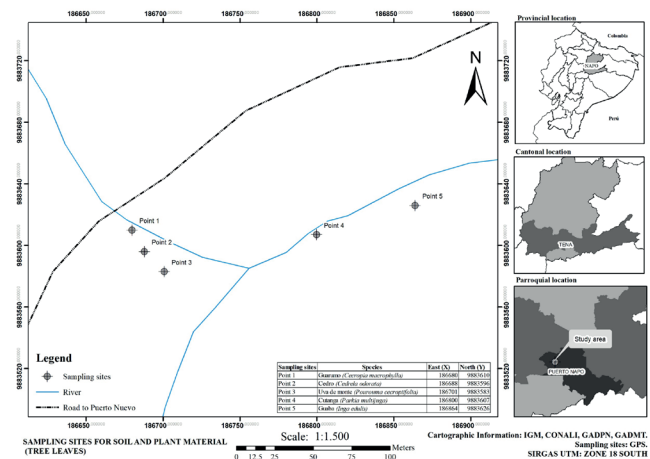


Fig. 1. Geographic location of the leaf and soil sampling sites of five forest species living in mining environments, Yutsupino community, Napo.

### B. Sampling of Plant Material and Soil

For the analysis of heavy metals present in the plant material (leaves), five sampling points and ten trees per point were selected from five tree species that live in an area close to the mining site: *Cedrela odorata* L. (cedro), *Parkia multijuga* Benth. (cutanga), *Inga edulis* Mart. (guaba), *Cecropia ficifolia* Ward (guarumo) and *Pourouma cecropiifolia* Mart. (uba de monte) (<http://www.theplantlist.org/>). The selection of the five sampling points was carried out according to the location of the five species under study present at the mining extraction site. The species were selected based on their abundance, ecological and economic importance for the Amazon region.

The collection of leaf samples was carried out from individuals in an adult state, with exposure to the sun and in good physical condition. The plant material was collected from different sides of the trees, cutting the branches to prevent the leaves from facing the metal scissors. Leaves without mechanical damage or apparent disease were selected.

Soil samples were taken with an auger, at three different points at a depth of 0-30 cm within 30 cm around the selected trees. Soil sampling around the selected trees was in accordance with the methodology used by Greksa et al. [22]. A soil depth between 0 and 30 cm was used, as suggested by other authors [23]. Leaf litter and roots were removed. The samples obtained from different sides of the same tree and corresponding to the same soil unit were mixed in a bucket until the soil was homogenized and a composite sample obtained was representative of the collection, in an amount equivalent to 1000 grams [22]. The samples were placed in a plastic Ziploc bag, appropriately labeled and transferred to the Environmental Sciences Laboratory of the Universidad Estatal Amazónica, located in the main matrix Puyo, Ecuador, for subsequent processing and analysis of heavy metals: lead (Pb), cadmium (Cd), nickel (Ni), iron (Fe) and aluminum (Al).

### C. Analysis of Soil and Leaf Samples

The plant material samples were washed with drinking water and then with distilled water. They were allowed to dry naturally on filter paper for four days and pulverized without the use of sharp metals, until obtaining a sample of 20 g. The soil samples were crushed and sieved through a 2 mm mesh sieve, then dried and a 100 g sample was obtained.

The collected soil and plant material samples were air-dried at room temperature for seven days before being taken to the forced circulation oven (Model ED-S 115, from Germany, with a temperature range from +7 °C to 250 °C) at a temperature of 40°C for 48 hours. The dried samples were placed in an agate mortar for grinding to a completely fine powder. The pulverized material was sieved to obtain particle sizes less than 2 mm [22]. A blank with 68 % nitric acid was used to verify possible contamination during the sample preparation process. A pre-labelled vial to process the digested soil and plant material samples was used. A mass of 0.5 g of each sample was weighed, and then, 7 mL of 68 % nitric acid (HNO<sub>3</sub>), was added, followed by 1 mL of 30 % hydrogen peroxide (H<sub>2</sub>O<sub>2</sub>). The vial was closed and placed in a microwave-assisted digestion apparatus (ETHOS ONE) for 50 minutes. This device used were 50 ml TFM (Modified Fluorine Teflon) containers to carry out the acid decomposition of the samples, ensuring exhaustive control of all reaction factors and compliance with strict safety and quality standards. The containers were placed in the microwave oven, which operated at 800 Watts and reached a temperature of up to 170 °C, for a predefined time until the temperature reached 40 °C. Once the wet digestion process was completed, the sample was allowed to stand at room temperature [24]. Once digested, the samples were transferred to a previously labelled volumetric flask, to which distilled water was added for a final volume of 25 mL. The samples were filtered prior to analysis and lastly, heavy metal determinations were performed on an Aurora Instruments LTD atomic absorption spectrometer with a data processor software Trace 1200 (Perkin Elmer, Model A Analyst 800, dimensions 1524.00 x 1016.00 x 812.80 mm, automatic sampler AS800, weight 136.08 kg), under the following conditions: flame type for the elements Pb, Cd, Ni and Fe, air-acetylene and nitrous oxide-acetylene for Al, with an airflow of 1.5 Lmin<sup>-1</sup> (air pressure 50 psi), acetylene flow of 3.5 Lmin<sup>-1</sup> (acetylene pressure 50 psi) and for hollow cathode lamp conditions, 20 mA current, slit width 0.2 nm and wavelengths of 217 nm, 228.8 nm, 232 nm, 248.3 nm and 309.2 nm for Pb, Cd, Ni, Fe and Al, respectively.

### D. Data Analysis

An analysis of variance (ANOVA) and Tukey's test were performed, to determine the significance of the differences in heavy metals (Pb, Cd, Zn, Fe and Al) concentrations in the species analyzed (*C. odorata*, *P. multijuga*, *I. edulis*, *C. ficifolia* and *P. cecropiifolia*) as well as the concentrations of metals mentioned above in the soil around the place where they grow. A cluster analysis was performed to define the similarity between the heavy metal uptake capacity of the species, and Pearson's correlation coefficient was used to determine the correlations in the concentrations of the heavy metals analyzed in the plants and the soil. A Principal Component Analysis (PCA)

to establish the separation of the analyzed plants according to the concentrations of heavy metals in soil and trees was done. Origin 2021 software was used for the statistical analyses.

The bioconcentration factor (BCF) was employed to measure each plant's ability to absorb heavy metals from the soil [15]. BCF was calculated using Equation (1):

$$BCF = C_{leaves} / C_{soil} \quad (1)$$

where  $C_{leaves}$  and  $C_{soil}$  represent the concentration of the element in the plant and in the soil, respectively.

## III. RESULTS

### A. Concentrations of Heavy Metals in Leaves and Soil

Figure 2a shows the results of the concentration of the heavy metals Pb, Cd, Ni, Fe and Al present in the leaves of *C. odorata*, *P. multijuga*, *I. edulis*, *C. ficifolia* and *P. cecropiifolia*, whilst Figure 2b shows the concentrations in the soils where those species grow. Foliar Pb concentrations ranged from 0.25 mg kg<sup>-1</sup> in *C. odorata* to 7.05 mg kg<sup>-1</sup> for *P. cecropiifolia*. Foliar Cd concentrations ranged from 0.08 mg kg<sup>-1</sup> for *P. cecropiifolia* to 0.98 mg kg<sup>-1</sup> in *C. odorata*. As for Ni, the lowest value was found in *P. multijuga* with a concentration of 1.80 mg kg<sup>-1</sup> and the highest in *C. ficifolia* with 6.93 mg kg<sup>-1</sup>. Fe values were 69.03 mg kg<sup>-1</sup> in *C. ficifolia* and 99.02 mg kg<sup>-1</sup> for *I. edulis*. Al was 109.4 mg kg<sup>-1</sup> in *C. ficifolia* and 149.6 mg kg<sup>-1</sup> for *C. odorata*.

Pb concentrations in soil ranged from 1.18 mg kg<sup>-1</sup> for *C. ficifolia* to 1.89 mg kg<sup>-1</sup> for *P. multijuga*. Cd values ranged from 1.49 mg kg<sup>-1</sup> for *C. odorata* and *P. cecropiifolia* to 1.89 mg kg<sup>-1</sup> in *P. multijuga*. Ni concentrations ranged from 1.98 mg kg<sup>-1</sup> around the place where *C. odorata* was located, to 3.60 mg kg<sup>-1</sup> where *I. edulis* was grown. Fe in the soil had a minimum concentration of 198 mg kg<sup>-1</sup> and a maximum concentration of 390.8 mg kg<sup>-1</sup>, corresponding to *C. ficifolia* and *C. odorata* respectively. Al values ranged from 322.4 mg kg<sup>-1</sup> in the soil around *I. edulis* to 542.2 mg kg<sup>-1</sup> for *P. cecropiifolia*.

The Analysis of variance (ANOVA) and Tukey's test showed statistical differences in the concentration of the metallic elements Pb, Cd, Ni, Fe and Al in the leaves of the species studied, as well as in the soil where the species were grown (Figures 2A and 2B). For instance, *C. odorata* leaves had a significantly lower Pb concentration than *P. cecropiifolia* leaves. However, *C. odorata* had the highest Cd concentration, while *P. cecropiifolia* had the lowest Cd content. As for Ni, *P. multijuga* had the lowest concentration with significant differences to *C. ficifolia*, which was the species with the highest value. Yet *C. ficifolia* showed the lowest Fe and Al concentrations, whilst *I. edulis* and *C. odorata* had the highest Fe and Al values respectively (Figure 2A).

In general, the soil where the species grow showed significant differences in the concentration of heavy metals (Figure 2B). The lowest Pb concentration was in the areas of *I. edulis* and *C. ficifolia*, whereas the highest concentration was in the soil around *P. multijuga* and *C. odorata*. Cd concentration was similar in the locations of *C. odorata* and *P. cecropiifolia*. Indeed, the lowest and highest values of Cd were similar for the

rest of the soil where the other species were found. Moreover, the presence of Ni in the soil had significant differences with lower values in soil surrounding *P. cecropiifolia* than in soil around *I. edulis*. As for the presence of Fe, where *C. odorata* is present, it had a higher content with significant differences to *C. ficifolia*. Al was higher in the soil around *P. cecropiifolia* and lower in *I. edulis* areas.

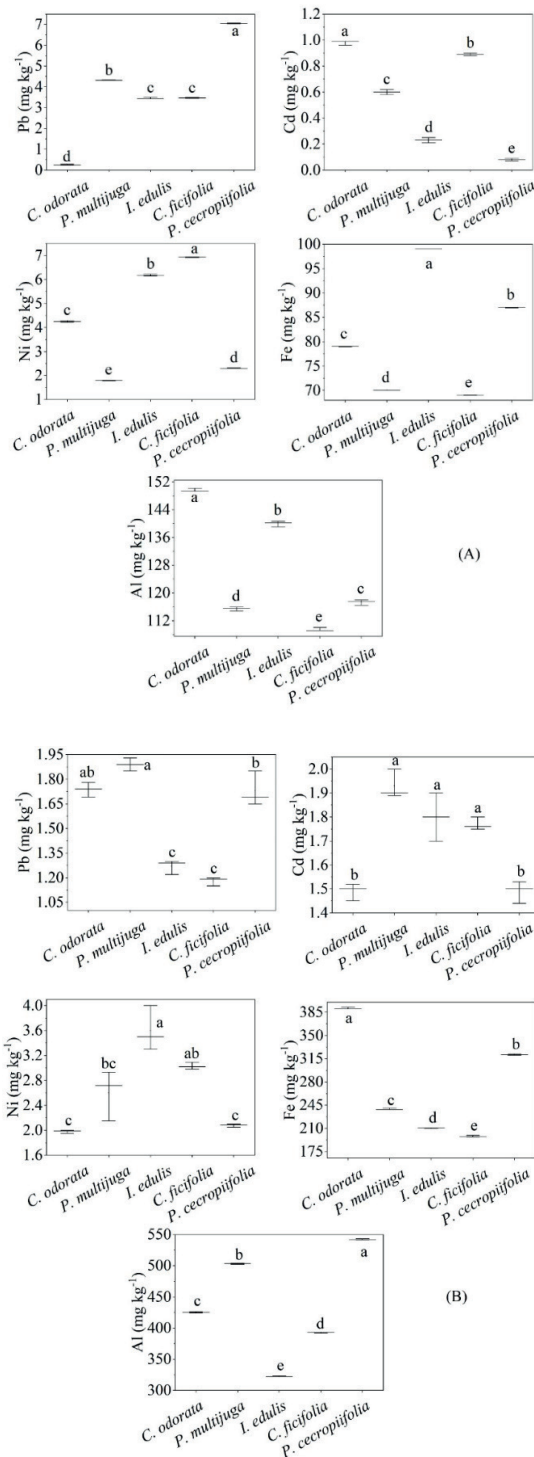


**Fig. 2.** Variation in the concentration of heavy metals (Pb, Cd, Ni, Fe and Al) of five forest species living in mining environments (A) Concentration in the leaves and (B) Concentration in the soil (Unequal letters indicate significant differences between species according to the Tukey test).

According to Pearson’s correlation coefficient (Figure 3), when analyzing the concentration of metals in the leaves of the species studied, only a positive correlation (higher than 50%) was found between Al and Fe ( $r = 0.54$ ). Meanwhile, other elements showed negative correlations: Cd and Pb ( $r = -0.79$ ), Fe and Cd ( $r = -0.71$ ) and Al and Pb ( $r = -0.69$ ). Positive correlations higher than 50% between soil element concentrations were between Ni and Cd ( $r = 0.70$ ), Fe and Pb ( $r = 0.62$ ) and Al and Pb ( $r = 0.80$ ), whereas Ni presented negative correlations with negative Pb, Al and Fe elements ( $r = -0.76$ ,  $r = -0.77$ ,  $r = -0.87$ ), respectively.

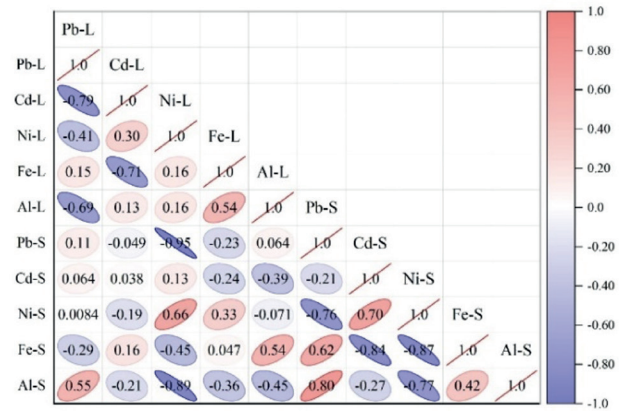


**Fig. 3.** Results of the correlation matrix between the concentration of heavy metals in the leaves and soil of five forest species living in mining environments. (The numerical value corresponds to the Pearson correlation coefficient).

The cluster analysis grouped all studied species into three groups based on the concentrations of heavy metals (Pb, Cd, Ni, Fe and Al) in leaves (Figure 4). Al concentrations in leaves of *C. odorata* and *I. edulis* formed one group; Fe concentrations in *P. cecropiifolia*, *I. edulis*, *C. ficifolia*, *P. multijuga* and *C. odorata*, and Al concentrations in *P. cecropiifolia*, *C. ficifolia* and *P. multijuga* formed the second group; while the third group included Cd, Ni and Pb concentrations.

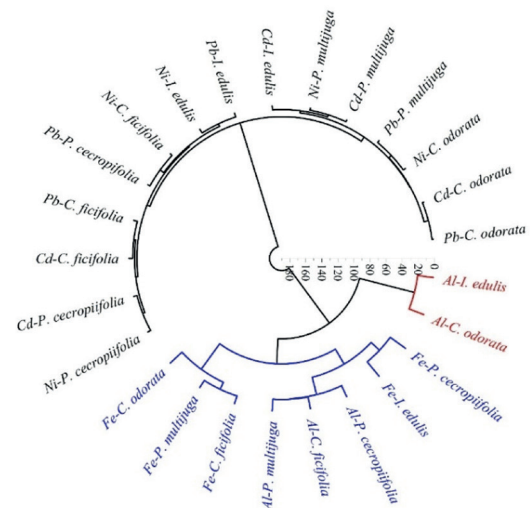


**Fig. 4.** Cluster analysis for the classification of similarity groups based on the concentration of heavy metals (Pb, Cd, Ni, Fe and Al) in leaves of five forest species living in mining environments.



The bioconcentration factor was used to estimate the plants' ability to absorb certain heavy metals from the soil. The BFC values can be seen in Figure 5. The species analyzed differ significantly in their capacity to absorb the heavy metals studied, with *P. cecropiifolia* having the greatest capacity to retain Pb, *C. odorata* accumulating the greatest amount of Cd, and *C. ficifolia* and *C. odorata* absorbing the most Ni. As for Fe and Al, *I. edulis* had the highest bioaccumulation potential for both elements.

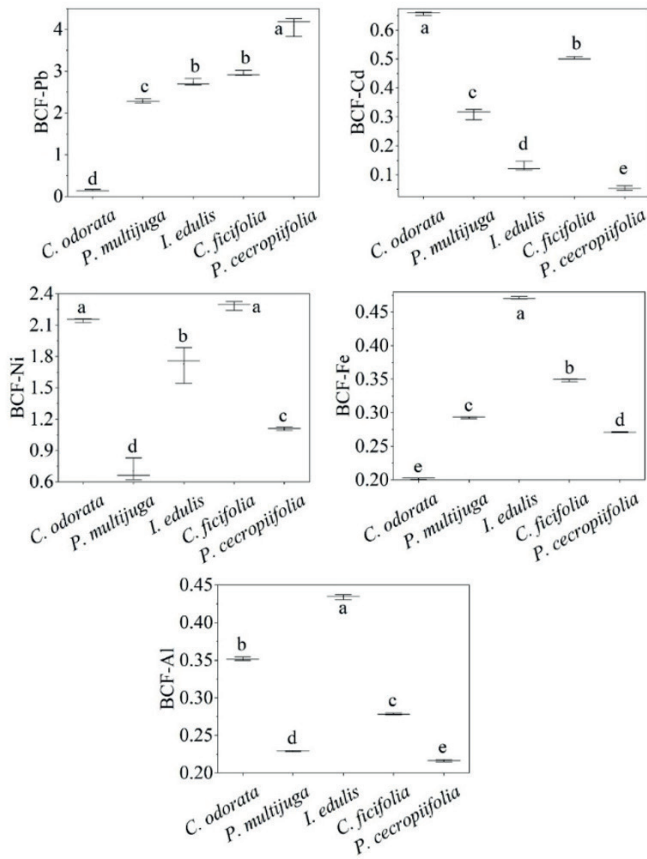


Fig. 5. Variation of heavy metal BCF among five forest species living in mining environments. (Unequal letters indicate significant differences between species according to the Tukey test).

From the eigenvalues of the correlation matrix of the heavy metals studied and using the PCA method, the initial data set was reduced to two principal components that explained 70.6 % of the variability. Based on the PCA analysis, Ni and Cd concentrations in the soil were lower than those of Fe, Pb and Al (PC 1). When looking at the plants in the coordinate system, determined by the principal components, it can be noted that the PC 1 axis separates the species *C. odorata*, *P. cecropiifolia* and *P. multijuga*, which are on the positive side of the axis and had lower values of Cd and Ni in the soil, from *I. edulis* and *C. ficifolia*, which are on the negative side of the axis and are characterized by higher concentrations of Cd and Ni in the soil. The second axis, PC 2, separates the species *C. odorata*, on the positive side of the axis and with a lower Pb concentration, from the rest of the species (Figure 6).

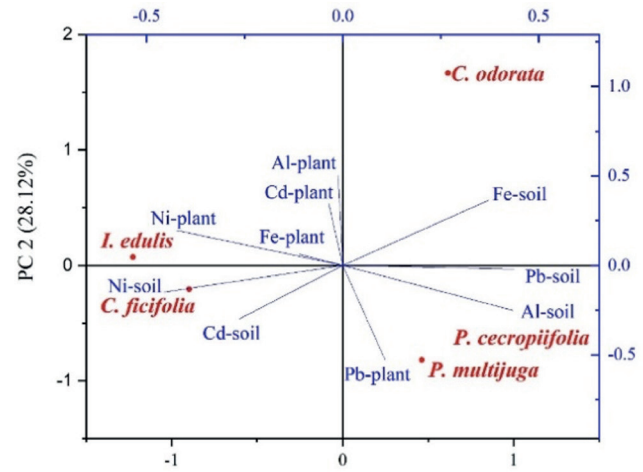


Fig. 6. Results of the PCA analysis of the concentrations of heavy metals (Pb, Cd, Ni, Fe and Al) in leaves and soil of five forest species (*C. odorata*, *P. multijuga*, *I. edulis*, *P. cecropiifolia* and *C. ficifolia*). X axis: PC1 (principal component 1); Y axis: PC2 (main component 2).

#### IV. DISCUSSION

The leaf material of five forest species, *C. odorata*, *P. multijuga*, *I. edulis*, *C. ficifolia* and *P. cecropiifolia*, which commonly inhabit mining areas in the Ecuadorian Amazon region, together with soil samples taken at a depth of 0-30 cm were tested. The objective was to identify which species had the potential to bioaccumulate Pb, Cd, Ni, Fe and Al to mitigate possible contamination by any of these elements in Amazonian ecosystems.

The variation found between the species *C. odorata*, *P. multijuga*, *I. edulis*, *C. ficifolia* and *P. cecropiifolia*, in relation to the concentration of heavy metals at the foliar level and in the soil, indicated a different response of the species as a reflection of the potential to accumulate Pb, Cd, Ni, Fe and Al.

The variability found in the concentration of heavy metals between species agrees with studies carried out for three woody species of ecological importance (*Piptocoma discolor*, *Bambusa vulgaris* and *Ochroma pyramidale*) that inhabit soils contaminated by mining in the province of Napo, Ecuadorian Amazon, which presented differences in the concentration of heavy metals [25]. Generally, the concentration of heavy metals in different parts of the plant depends on the amount of heavy metals in the air and soil, and it is different within and between plant species [26, 27]. The different responses of vascular plants to heavy metals can be attributed to genetic and physiological factors [28].

The concentration of heavy metals in the soil reflected that there is a high concentration of heavy metals in each of the sampling points at a depth of 0-30 cm. These results coincide with those reported by Šichorová et al. and Wu et al. [23, 29], where the maximum concentration was found in the soil layer within this depth range.

However, concentrations of heavy metals may be higher at depths greater than 30 cm, but their chemical forms differ with depth and therefore may not be readily available to plants [23].

The Cd concentration of the species in this study was higher than that reported by Alahabadi et al. [15] for different woody

plants, where the values were between 0.34 and 0.62 mg kg<sup>-1</sup>. According to Ecuadorian regulations [30], it was found that the concentration of Cd exceeded the permissible values (0.5 mg kg<sup>-1</sup>), Pb and Ni were below the established limits, while Fe and Al are not regulated. The exceeded limits of Cd were similar to those reported by Chamba-Eras et al. [31] in a study of native hyperaccumulator plants with differential phytoremediation potential in an artisanal gold mine in the Ecuadorian Amazon. In contrast to what was reported by García et al. [25] in soils contaminated by mining in Napo, who obtained Cd concentration values within the tolerance range (0.04-0.35 mg kg<sup>-1</sup>) for three study species (*P. discolor*, *B. vulgaris* and *O. pyramidale*), while the concentration of Pb resulted in toxicity for the species *P. discolor* in a range of 30-300 mg kg<sup>-1</sup>. It is important to highlight the bioaccumulative potential of the species, regardless of whether the soil can be considered contaminated or not. If plants can absorb some of the elements considered contaminants, then this could be a viable option for bioremediation of contaminated soils.

When the content of heavy metals in the soil reaches levels that exceed the maximum permitted limits, they cause immediate effects such as inhibition of normal growth and development of plants, and a functional disturbance in other components of the environment, as well as the decrease in populations soil microbes [32]. The amount of heavy metals available in the soil can be a function of pH, texture, organic matter, cation exchange capacity and other soil properties [33]. Therefore, it is recommended for future studies to include analysis of the physical and chemical properties of the soil that will make it easier to understand the absorption capacity of heavy metals.

High levels of Cd contamination can cause detrimental effects on plants such as: decreased seed germination rate, lipid content and overall plant growth, induction of phytochelatin production and interference in establishment of the symbiosis between microorganisms and plants [34]. The results of this research reported a higher concentration of heavy metals (Pb, Cd, Ni, Fe and Al) in the soil than in the plant. This corresponds to studies carried out by Barthwal et al. [35] in several sites, which indicated that the level of absorption of heavy metals was higher in the soil than in the plants.

The low correlation found in this research between the concentration of heavy metals in the soil and the leaves could be related to the bioconcentration capacity of each species. The bioaccumulation capacity of plants does not depend entirely on the concentration of heavy metals in the soil but is related to the physiology of the plant and its protection capacity [36]. When plants are stressed by heavy metals, they can actively regulate the concentration of the elements [37].

The behavior that has been found in the species *I. edulis* and *C. ficifolia*, which are characterized by higher concentrations of Cd and Ni in the soil, could be given by the specific physiological mechanisms of bioaccumulation in these species. These results are interesting because they are fast-growing species, which grow naturally in anthropized sites, which suggests their use as phytoremediation species in sites where mining extraction practices are carried out and contamination by heavy metals of Cd has been proven or not.

The bioaccumulation factor (BCF) showed that *C. odorata* had a high capacity for the phytostabilization of Cd and Ni, while *I. edulis* presented a high capacity for Fe and Al and *P. cecropiifolia* a high capacity for Pb. This indicated the tolerance of these species to soils contaminated by these heavy metals, suggesting their use as potential species for phytoremediation. Previous studies have documented the heavy metal biosorption potential of *C. odorata*. For example, Akintola and Bodede [38] studied seedlings grown in landfill soils and deduced that heavy metal concentrations in contaminated soils indicated metal enrichment in plant tissues. Enrichment coefficients and distribution factors showed the potential of *C. odorata* as a bioaccumulator species. Thus, they concluded that seedlings of this species can be used to clean up or rehabilitate soils that are contaminated with the heavy metals studied (Cu, Pb, Zn and Co). This demonstrates the effectiveness and ability of *C. odorata* to accumulate and distribute heavy metals in its parts. In a study carried out at a mining site in Alacrán, Colombia, the Hg bioaccumulator potential of *I. edulis* has also been reported, where it has been used for phytoremediation in a mining site contaminated with this heavy metal [39].

In Ecuador, no reports have been found on the species under study regarding the capacity to accumulate heavy metals. However, in a study carried out in the tropical forests of southern Ecuador, the capacity of two native woody plants (*Erato polymnioides* and *Miconia sp*) to accumulate Cd, Pb, Zn and Hg was estimated, with the aim of developing effective strategies for the phytoremediation of mining sites. These species demonstrated high potential for bioaccumulation of heavy metals [31]. These results are interesting, since the species were characterized by their low productivity and high adaptability to the edaphoclimatic conditions of the region and have been used for the recovery of soils contaminated by mining. In the study, the species *I. edulis* presents similar characteristics to the species of this forest (low productivity and adaptability), so its high potential for accumulation of Fe and Al gives the possibility of including this species for phytoremediation in sites contaminated by mining.

For the species *P. multijuga*, *C. ficifolia* and *P. cecropiifolia*, no studies have been reported on the absorption capacity of heavy metals, so this research reports for the first time the bioaccumulative potential of these species.

These studies demonstrated the importance of research and the polluting effect that mining exploitation practices have without criteria or regulations that allow their use in a responsible manner. Illegal mining in Ecuador and the Ecuadorian Amazon is an environmental concern for the general population [40]. Therefore, phytoremediation emerges as a technique that uses specialized plants to absorb and accumulate heavy metals in their tissues.

Knowledge about the main weaknesses of large-scale mining worldwide constitutes fundamental information for the analysis of the current situation in Ecuador, which has prospects for large-scale production starting in December 2019, so knowing about These good practices and policies constitute application guidelines towards responsible mining [41].

## V. CONCLUSION

The bioconcentration factor made it possible to identify the studied species' (*C. odorata*, *P. multijuga*, *I. edulis*, *P. cecropiifolia* and *C. ficifolia*) capacity to bioaccumulate the heavy metals Pb, Cd, Ni, Fe and Al, making it possible to propose reforestation in areas contaminated with these elements to mitigate the negative impacts they may cause on the ecosystem. For Pb-contaminated soils, *P. cecropiifolia* is recommended as it showed the highest CBF-Pb value. Furthermore, the species *C. odorata* can be used in Cd and Ni contaminated sites, while *I. edulis* showed the highest potential for Fe and Al uptake.

As no correlation was found between the concentration of the element in the soil and the leaves, it can be asserted that absorption depends on the bioconcentration capacity of the species. It is therefore suggested that more forest species inhabiting the Ecuadorian Amazon region could be studied as well as other heavy metals to broaden the identification of potential species, depending on the pollutant.

## REFERENCES

- [1] K. N., S. M., Palansooriya, S. M. Shaheen, S. S. Chen, D. C. W., Tsang, Y. Hashimoto, D. Hou, et al., Soil amendments for immobilization of potentially toxic elements in contaminated soils: A critical review. *Environ Int.*, p. 105046, 2020. <https://doi.org/10.1016/j.envint.2019.105046>
- [2] R. G. Garrett, Natural sources of metals to the environment. *Hum Ecol Risk Assess*, 6, 945-963, 2000. <https://doi.org/10.1080/10807030091124383>
- [3] P. Lazo, T. Stafilov, F. Qarri, S. Allajbeu, L. Bektishi, M. Frontasyeva, et al., Spatial distribution and temporal trend of airborne trace metal deposition in Albania studied by moss biomonitoring. *Ecol Indic.*, 101, 1007-1017, 2019. <https://doi.org/10.1016/j.ecolind.2018.11.053>
- [4] G. Tyler, Changes in the concentrations of major, minor and rare-earth elements during leaf senescence and decomposition in a Fagus sylvatica forest. *For Ecol Manage*, 206, 167-177, 2005. <https://doi.org/10.1016/j.foreco.2004.10.065>
- [5] S. M. Serbula, T.S. Kalinovic, A. A. Ilic, J. V. Kalinovic y M. M. Steharnik, "Assessment of airborne heavy metal pollution using Pinus spp. and Tilia spp.," *Aerosol Air Qual Res.*, 13, 563-573, 2013. <https://doi.org/10.4209/aaqr.2012.06.0153>
- [6] A. K., M., Ratul Hassan, Uddin MK, Sultana MS, Akbor MA, Ahsan MA. Potential health risk of heavy metals accumulation in vegetables irrigated with polluted river water. *Int Food Res J.*, 25, pp. 329-338. 2018
- [7] F. Ugolini, R. Tognetti, A. Raschi, L. Bacci, L., "Quercus ilex as bio-accumulator for heavy metals in urban areas: Effectiveness of leaf washing with distilled water and considerations on the trees distance from traffic," *Urban For Urban Green*, 12, pp. 576-584. 2013. <https://doi.org/10.1016/j.ufug.2013.05.007>.
- [8] D. Neumann, "Heavy Metal Stress in Plants: From Molecules to Ecosystems", *Phytochemistry*, 53, p. 822. 2000. [https://doi.org/10.1016/s0031-9422\(00\)00010-8](https://doi.org/10.1016/s0031-9422(00)00010-8).
- [9] R. A. Wuana and F. E. Okieimen, "Heavy Metals in Contaminated Soils: A Review of Sources, Chemistry, Risks and Best Available Strategies for Remediation," *ISRN Ecol.*, pp. 1-20. 2011. <https://doi.org/10.5402/2011/402647>
- [10] K. Rehman, F. Fatima, I. Waheed and M. S. H. Akash, "Prevalence of exposure of heavy metals and their impact on health consequences," *J Cell Biochem.*, 119, pp. 157-184. 2018. <https://doi.org/10.1002/jcb.26234>
- [11] P. C. Nagajyoti, K. D. Lee and T. V. M. Sreekanth, "Heavy metals, occurrence and toxicity for plants: A review," *Environ Chem Lett.*, 8, pp. 199-216. 2010. <https://doi.org/10.1007/s10311-010-0297-8>
- [12] T. Sawidis, P. Krystallidis, D. Veros and M. Chettri, "A study of air pollution with heavy metals in Athens city and Attica basin using evergreen trees as biological indicators," *Biol Trace Elem Res*, 148, pp. 396-408. 2012. <https://doi.org/10.1007/s12011-012-9378-9>
- [13] J. Liang, H. L. Fang, T. L. Zhang, X. X. Wang and Y. D. Liu, "Heavy metal in leaves of twelve plant species from seven different areas in Shanghai, China," *Urban For Urban Green*, 27, pp. 390-398. 2017. <https://doi.org/10.1016/j.ufug.2017.03.006>
- [14] G. Tóth T. Hermann, M. R. Da Silva and L. Montanarella, "Heavy metals in agricultural soils of the European Union with implications for food safety", *Environ Int.*, 88, pp. 299-309. <https://doi.org/10.1016/j.envint.2015.12.017>
- [15] A. Alahabadi, M. H. Ehrampoush, M. Miri, H. Ebrahimi Aval, S. Yousefzadeh and H. R. Ghaffari et al., "A comparative study on capability of different tree species in accumulating heavy metals from soil and ambient air," *Chemosphere*, 172, pp.459-4667. 2017. <https://doi.org/10.1016/j.chemosphere.2017.01.045>
- [16] N. Mainville J. Webb, M. Lucotte, R. Davidson, O. Betancourt and E. Cueva et al., "Decrease of soil fertility and release of mercury following deforestation in the Andean Amazon, Napo River Valley, Ecuador," *Sci Total Environ.*, 368, pp.88-98. 2006. <https://doi.org/https://doi.org/10.1016/j.scitotenv.200509.064>.
- [17] R. Xiao, S. Wang, R. Li, J. J. Wang and Z. Zhang, "Soil heavy metal contamination and health risks associated with artisanal gold mining in Tongguan, Shaanxi, China," *Ecotoxicol Environ Saf.*, 141, 17-24. 2017. <https://doi.org/10.1016/j.ecoenv.2017.03.002>
- [18] N. H. Tarras-Wahlber, A. Flachier, G. Fredriksson, S. Lane, B. Lundberg and O. Sangfors, "Environmental impact of small-scale and artisanal gold mining in southern Ecuador: Implications for the setting of environmental standards and for the management of small-scale mining operations," *Ambio*, 29, 484-491. 2000. <https://doi.org/10.1579/0044-7447-29.8.484>
- [19] E. Peña-Carpio and J. M. Menéndez-Aguado, "Environmental study of gold mining tailings in the Ponce Enriquez mining area (Ecuador)," *DYNA* 83, pp. 237-245. 2016. <https://doi.org/10.15446/dyna.v83n195.51745>
- [20] S. L. Pimm, C. N. Jenkins, R. Abell, T. M. Brooks, J. L. Gittleman, L. N. Joppa et al., "The biodiversity of species and their rates of extinction, distribution, and protection," *Science*, 344(6187). 2014. <https://doi.org/10.1126/science.1246752>
- [21] P. K. Panday, M.T. Coe, M. N. Macedo, P. Lefebvre and A. D. d. A. Castanho, "Deforestation offsets water balance changes due to climate variability in the Xingu River in eastern Amazonia," *J Hydrol* 523, pp. 822-829. 2015. <https://doi.org/10.1016/j.jhydrol.2015.02.018>
- [22] A. Greksa B. Ljevnaić-Mašić, J. Grabić, P. Benka, V. Radonić, B. Blagojević et al., "Potential of urban trees for mitigating heavy metal pollution in the city of Novi Sad, Serbia," *Environ Monit Assess*, 191, pp. 1-13. 2019. <https://doi.org/10.1007/s10661-019-7791-7>
- [23] Y. Wu, X. Peng and X. Hu, "Vertical distribution of heavy metal in soil of abandoned vehicles dismantling area," *Asian J Chem.*, 25, pp. 8423-8426. 2013. <https://doi.org/10.14233/ajchem.2013.14770>
- [24] Z. Wang, X. Liu and H. Qin, "Bioconcentration and translocation of heavy metals in the soil-plants system in Machangqing copper mine, Yunnan Province, China," *J Geochemical Explor.*, 200, 159-166. 2019. <https://doi.org/10.1016/j.gexplo.2019.02.005>
- [25] Y. García, Y. Arteaga, V. del R. Chico, S. García, S. Luna and C. Bañol, "Potencial bioacumulador de metales pesados para la fitorremediación como alternativa para la recuperación del paisaje forestal en un área de extracción minera, Napo, Ecuador," *Rev Cuba Ciencias For.*, 12, p. e8632024. Availabel: <https://bit.ly/3yX0Qbq>
- [26] D. Satpathy and M. Reddy, "Phytoextraction of Cd, Pb, Zn, Cu and Mn by Indian mustard (*Brassica juncea* L.) grown on loamy soil amended with heavy metal contaminated municipal solid waste compost", *Appl Ecol Environ Res.*, 11, 661-667. 2013. [https://doi.org/10.15666/aecer/1104\\_661679](https://doi.org/10.15666/aecer/1104_661679)
- [27] A. Ipeaiyeda and M. Dawodu, "Assessment of toxic metal pollution in soil, leaves and tree barks: bioindicators of atmospheric particulate deposition within a University community in Nigeria," *Adv Environ Sci.*, p. 6. 2014.
- [28] P. Parmar B. Dave, A. Sudhir, K. Panchal, R. B., "Subramanian Physiological, Biochemical and Molecular Response of Plants Against Heavy Metals Stress," *Int J Curr Res.*, 80-89. 2013.
- [29] K. Šichorová, P. Tlustoš J. Száková, K. Kořínek and J. Balík, "Horizontal and vertical variability of heavy metals in the soil of a polluted area," *Plant, Soil Environ.*, 50, pp. 525-534. 2004. <https://doi.org/10.17221/4069-pse>

- [30] MAE-TULSMA. Texto Unificado de Legislación Secundaria Medio Ambiental. Ministerio de Ambiente de Ecuador. Quito. 2015.
- [31] I. Chamba-Eras, D. M. Griffith, C. Kalinhoff, J. Ramírez and M. J. Gázquez, "Hyperaccumulator Plants with Differential Phytoremediation Potential in an Artisanal Gold Mine of the Ecuadorian Amazon," *Plant.*, 11, p. 1186. 2022. <https://doi.org/https://www.mdpi.com/2223-7747/11/9/1186>
- [32] C. W. Martin, "Heavy metal trends in floodplain sediments and valley fill, River Lahn, Germany," *Catena*, 39, pp. 53-68. 2000. [https://doi.org/10.1016/S0341-8162\(99\)00080-6](https://doi.org/10.1016/S0341-8162(99)00080-6)
- [33] S. Sauvé, W. Hendershot and H. E. Allen, "Solid-solution partitioning of metals in contaminated soils: Dependence on pH, total metal burden, and organic matter," *Environ Sci Technol.*, 34, pp. 1125-1131. 2000. <https://doi.org/10.1021/ES9907764>
- [34] M. E. B. Pineda and A. M. G. Rodríguez, "Metales pesados (Cd, Cr y Hg): su impacto en el ambiente y posibles estrategias biotecnológicas para su remediación," *I3+*, 2, pp. 82-112. 2015. <https://doi.org/10.24267/23462329.113>
- [35] J. Barthwal and P. K. Smitha, "Nair Heavy Metal Accumulation in Medicinal Plants Collected from Environmentally Different Sites," *Biomed Environ Sci.*, 21, pp. 319-324. 2008. [https://doi.org/https://doi.org/10.1016/S0895-3988\(08\)60049-5](https://doi.org/https://doi.org/10.1016/S0895-3988(08)60049-5)
- [36] C. Song, L. Lei and Q. Yang, "Pb, Cu botanogeochemical anomalies and toxic effects on plant cells in Pb-Zn (Sn) ore fields, Northeast Guangxi Autonomous Region, China," *Chinese J Geochemistry.*, 26, pp. 329-332. 2007. <https://doi.org/10.1007/s11631-007-0329-7>
- [37] E. Fernández-Ondoño, G. Bacchetta, A. M. Lallena, F. B. Navarro, I. Ortiz and M. N. Jiménez, "Use of BCR sequential extraction procedures for soils and plant metal transfer predictions in contaminated mine tailings in Sardinia," *J Geochemical Exploration*, 172, pp. 133-141. 2017. <https://doi.org/10.1016/j.gexplo.2016.09.013>
- [38] O. Akintola and I. A. Bodele, "Distribution and accumulation of heavy metals in Red Cedar (*Cedrela odorata*) wood seedling grown in dumpsite soil," *J Appl Sci Environ Manag.*, 23, p. 811. 2019. <https://doi.org/10.4314/jasem.v23i5.6>
- [39] J. Marrugo-Negrete, S. Marrugo-Madrid, J. Pinedo-Hernández, J. Durango-Hernández and S. Díez, "Screening of native plant species for phytoremediation potential at a Hg-contaminated mining site," *Sci Total Environ* 542, pp. 809-816. 2016. <https://doi.org/10.1016/j.scitotenv.2015.10.117>
- [40] R. A. Rivera-Rhon and E. Bravo-Grijalva, "Gobernanzas criminales y enclaves productivos de la minería ilegal en el Ecuador," *Rev Logos Cienc Tecnol.*, 15, pp. 49-69. 2023. <https://doi.org/10.22335/RLCT.V15I2.1734>
- [41] R. Estupiñán, P. Romero, M. García, D. Garcés and P.Valverde, "La minería en Ecuador. Pasado, presente y futuro," *Boletín Geológico y Min*, 132. 2021. <https://doi.org/10.21701/bolgeomin.132.4.010>